

QUINTESSENCE DRIVEN BARYOGENESIS

Diploma Thesis

by

Marc-Thomas Eisele

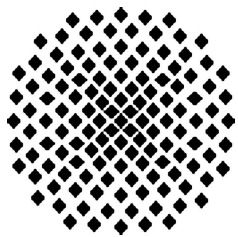
University of Stuttgart

May 2004

Thesis written at:

Technical University Munich
Physics Department T30d

Prof. Dr. Manfred Lindner



Meinen Eltern

*Two roads diverged in a wood, and I—
I took the one less traveled by,
And that has made all the difference.*

Robert Frost, The Road Not Taken

Contents

1	Introduction	1
1.1	Einleitung	3
1.2	Remarks	5
2	Introductory Cosmology	7
2.1	Robertson-Walker Metric and Expansion	7
2.2	Early Universe Thermodynamics	9
2.2.1	Particle and Energy Densities	9
2.2.2	Chemical Potentials	13
2.2.3	Entropy and Entropy Density	14
2.3	The Matter-Antimatter Asymmetry	15
3	Sphalerons	17
3.1	Anomalies	17
3.1.1	The Axial Anomaly	17
3.1.2	Anomalies in the Path-Integral Formalism	18
3.1.3	Anomalies and Topology	22
3.2	(B+L) Violation in the Standard Model	23
4	Quintessence	27
4.1	Acceleration of the Universe	27
4.2	Field-Theoretic Models for a Varying Λ -Term	27
4.3	Quintessence Potentials	28
4.3.1	Positive Power Potentials	28
4.3.2	Tracker Fields	29
4.3.3	Exponential Potentials	30
5	Baryogenesis Models	33
5.1	The Sakharov Conditions	33
5.2	A Simple Baryogenesis Model	34
5.3	Leptogenesis	36
5.4	Neutrino genesis	37
5.5	Interplay of Quintessence and Baryogenesis	41

6 Quintessence Driven Neutrinogenesis	45
6.1 The Model	46
6.1.1 Gauge Groups and Representations	46
6.1.2 Gauge Boson Masses	48
6.1.3 Fermion Masses	51
6.1.4 Yukawa Couplings	52
6.2 Neutrinogenesis, first try	53
6.2.1 Chemical Potentials	54
6.2.2 Initial Decay	55
6.2.3 Problems With Neutrinogenesis	57
6.3 Quintessence Driven Neutrinogenesis	60
6.3.1 The Uncoupled Quintessence Field	60
6.3.2 Varying Coupling Constants	61
6.3.3 The Effective Quintessence Potential	70
6.3.4 Further Issues and Comments	74
7 Summary and Conclusions	79
7.1 Zusammenfassung und Schlussfolgerungen	81
A Generators of SU(4)	83
B Calculated Yukawa Couplings	85
C Particle Freeze Out	87
D The Effect. Quintessence Potential II	89

Chapter 1

Introduction

Within the last fifty years, astroparticle physics has drawn more and more interest and attention within the scientific community. This is partially due to the fact that the universe provides us with a lot of data from processes whose energies are much higher than the scales ever to be reached by experiments executed on the surface of our earth. Therefore astroparticle physics can be used to study physics at higher energy scales and to test theories that yield new effects at these scales. The processes with the highest energies took place during the very early stages of our universe, which makes this period especially interesting.

One of the processes that supposedly took place during this time will be focused on more closely in this thesis: The generally accepted fact that our universe mainly consists of matter and barely any antimatter has not necessarily always been true. Its possible transition from a state in which matter and antimatter were equally abundant to a state in which practically only matter is present is called **baryogenesis**. This process cannot be explained within the standard model of elementary particle physics and therefore opens the door for new theories. These theories have to stand the test of yielding various data gathered from experiments and must hereby reproduce the standard model of particle physics to a certain degree. On the other hand, they also should introduce new processes such as baryogenesis, with the parameters partially fixed by the just mentioned measurements.

However, these tests of a theory all rely on the assumption that the laws governing physics in the early universe were the same as the ones today. While this assumption might seem plausible and attractive, it is not guaranteed to be true. One scenario in which it might be falsified is one of time-varying parameters, in which, of course, the shape of the laws would not be any different but the quantitative results would. This time dependence does not need to be explicit, the parameters can for example depend on the vacuum expectation value (VEV) of a field, which varies as the universe expands.

The interplay of the two topics baryogenesis and time varying coupling constants seems to yield a whole new variety of possible baryogenesis scenarios, as ingredients that are needed to create an asymmetry between matter and antimatter in the early universe do not necessarily have to be visible in the

theory that describes physics today.

This thesis treats these topics. It takes a closer look at a baryogenesis scenario which is also called **neutrino genesis** and presents typical problems that occur when trying to realize its idea of hiding asymmetries in decoupled sectors without the ad-hoc introduction of new particles in the original model. A specific model is constructed and it is shown how its problems in creating a baryon-asymmetric universe can be circumvented by the introduction of effectively time-dependent coupling constants, due to a **quintessence** field. Of course, such couplings will also provide some difficulties, and their treatment will be the center of the last part of this thesis.

The structure of this thesis is the following:

As some basic knowledge about early universe cosmology is needed, a brief introduction into this topic is given in the second chapter mainly focussing on the so called **Robertson-Walker metric** and its connection to the thermodynamics of the the early universe.

Since several baryogenesis scenarios make use of non-perturbative (B+L)-violating processes within the standard model, that occur due to anomalies, some more details on this topic will be presented in chapter three.

Chapter four will reflect the general idea behind quintessence fields, which are a possible explanation for the present acceleration of our universe, and also present some specific classes of quintessence models.

The general conditions for a baryogenesis scenario, as well as the concepts of several specific models are presented in chapter five, where also an example for a possible interplay of quintessence and baryogenesis is given.

Chapter six mainly presents the work done in the course of this thesis. It starts with general considerations on the embedding of neutrino genesis in realistic theories and the problems that are most likely to occur. This is followed by the presentation of a more detailed Pati-Salam model and its specific problems to produce a baryon asymmetry via neutrino genesis. It is then shown, how a quintessence coupling of various constants might possibly solve these problems, while also some newly occurring problems are considered. In this course it is also found, how mass variations of several orders of magnitude due to a quintessence field might be realized. At the end of this chapter further issues and comments are presented, mainly dealing with assumptions made during the calculations and their influence on the results.

The last chapter includes a summary of this work and general conclusions are drawn, while some further information and details are presented in the appendix.

1.1 Einleitung

Innerhalb der letzten fünfzig Jahre hat die Astroteilchenphysik mehr und mehr Interesse und Aufmerksamkeit innerhalb der wissenschaftlichen Gemeinschaft auf sich gezogen. Dies ist teilweise darauf zurückzuführen, dass das Universum uns sehr viele Daten von Prozessen liefert, deren Energien bei weit höheren Skalen liegen als diejenigen, die jemals durch auf der Erdoberfläche ausgeführte Experimente erreicht werden können. Daher ergibt sich durch die Astroteilchenphysik die Möglichkeit Physik an höheren Energieskalen zu untersuchen und Theorien zu testen, die neue Effekte bei diesen Skalen voraussagen. Die Prozesse mit den höchsten Energien ereigneten sich während der sehr frühen Phasen unseres Universums, was diese Zeit besonders interessant macht.

Mit einem der Prozesse, die vermutlich in dieser Zeit stattgefunden haben, wird sich diese Arbeit genauer auseinandersetzen: Die allgemein akzeptierte Aussage, dass unser Universum hauptsächlich aus Materie und kaum aus Antimaterie besteht, muss nicht immer wahr gewesen sein. Den möglichen Übergang von einem Zustand, in dem Materie und Antimaterie zu gleichen Teilen vorhanden waren, in einen Zustand, in dem praktisch nur noch Materie vorhanden ist, nennt man **Baryogenese**. Dieser Prozess kann nicht innerhalb des Standardmodells der Elementarteilchenphysik erklärt werden, womit sich die Möglichkeit für neue für neue Theorien eröffnet. Diese Theorien müssen den Test bestehen verschiedene, aus Experimenten gewonnene Daten zu liefern und hiermit zu einem gewissen Grad das Standardmodell zu reproduzieren. Auf der anderen Seite sollten sie auch neue Prozesse wie Baryogenese ermöglichen, wobei die Parameter teilweise schon durch die eben erwähnten Messungen festgelegt sind.

Diese Tests einer Theorie beruhen jedoch alle auf der Vermutung, dass die Gesetze, die die Physik im frühen Universum bestimmt haben, damals und heute dieselben waren. Obwohl diese Vermutung plausibel und attraktiv erscheinen mag, gibt es keine Garantie für ihre Richtigkeit. Ein Szenario, in dem sie sich als falsch herausstellen könnte, ist eines mit sich zeitlich verändernden Parametern, in dem die Form der Gesetze natürlich nicht verschieden wäre, wohl aber die quantitativen Ergebnisse. Diese Zeitabhängigkeit muss nicht explizit sein; die Parameter können zum Beispiel vom Vakuumenerwartungswert (VEW) eines Feldes abhängen, der sich während der Expansion des Universums verändert.

Das Zusammenspiel der beiden Themen Baryogenese und zeitlich veränderlich Kopplungskonstanten scheint eine ganz neue Auswahl an Baryogeneseszenarien hervorzubringen, da Eigenschaften, die benötigt werden um eine Asymmetrie zwischen Materie und Antimaterie zu erschaffen nicht notwendigerweise in der Theorie sichtbar sein müssen, die die Physik von heute beschreibt.

Diese beiden Themen werden in dieser Arbeit behandelt. Wir beschäftigen uns näher mit einem Baryogeneseszenario, welches auch **Neutrino-genese** genannt wird. Typische Probleme werden präsentiert, die auftreten, wenn man versucht die Neutrino-geneseidee zu realisieren Asymmetrien in entkoppelten Sektoren zu verstecken, hierbei jedoch auf die ad-hoc Einföhrung neuer Teilchen wie im ursprünglichen Modell verzichten will. Ein spezielles Modell wird konstruiert, und es wird gezeigt, wie dessen Schwierigkeiten ein baryonasymmetrisches

Universum zu erschaffen umgangen werden können, indem man effektiv zeitabhängige Kopplungen einführt, die auf ein **Quintessenzfeld** zurückgeführt werden können. Natürlich bringen solche Kopplungen auch neue Probleme mit sich. Deren Behandlung bildet den zentralen Punkt des letzten Teils dieser Arbeit.

Der Aufbau der Arbeit ist folgendermaßen:

Da elementare Grundkenntnisse über Kosmologie im frühen Universum benötigt werden, wird im zweiten Kapitel eine kurze Einführung in dieses Kapitel gegeben, die sich hauptsächlich auf die sogenannte **Robertson-Walker-Metrik** und ihre Verbindung zur Thermodynamik im frühen Universum bezieht.

Da mehrere Baryogeneseszenarien von nicht-pertubativen (B+L)-verletzenden Prozessen innerhalb des Standardmodells Gebrauch machen, die aufgrund von Anomalien auftreten, werden einige Details zu diesem Thema in Kapitel drei präsentiert.

Kapitel vier wird die allgemeine Idee hinter Quintessenzfeldern reflektieren, die eine mögliche Erklärung für die gegenwärtige Beschleunigung unseres Universum liefern. Zusätzlich werden einige spezielle Klassen von Quintessenzmodellen präsentiert.

Sowohl die allgemeinen Bedingungen für ein Baryogeneseszenario als auch die Konzepte mehrerer spezieller Modelle werden in Kapitel fünf präsentiert, wobei auch ein Beispiel für ein mögliches Zusammenspiel von Quintessenz und Baryogenese gegeben wird.

Kapitel sechs zeigt hauptsächlich was im Zuge dieser Diplomarbeit entstand. Es beginnt mit allgemeinen Erwägungen über die Einbettung der Neutrinogenese in realistische Theorien und die am wahrscheinlichsten auftretenden Probleme. Hierauf folgt die Vorstellung eines detaillierteren Pati-Salam Modells und seiner speziellen Probleme durch Neutrinogenese eine Baryonasymmetrie zu erzeugen. Es wird dann gezeigt, wie eine Quintessenzkopplung verschiedener Konstanten diese Probleme möglicherweise lösen könnte, wobei auch neu auftretende Probleme betrachtet werden. Im Zuge dessen wird ebenfalls herausgefunden, wie Massenänderungen mehrerer Größenordnungen aufgrund eines Quintessenzfeldes realisiert werden könnten. Am Ende dieses Kapitels werden weitere Probleme und Kommentare präsentiert, die sich hauptsächlich mit Vermutungen beschäftigen, die während der Rechnungen gemacht wurden, und mit ihrem Einfluss auf die Ergebnisse.

Das letzte Kapitel beinhaltet eine Zusammenfassung dieser Arbeit und allgemeine Schlussfolgerungen, wohingegen in den Appendizes weitere Informationen und Details präsentiert werden.

1.2 Remarks

- Within the whole course of this thesis we will work in natural units

$$\hbar = c = k_B = 1.$$

- Temperatures and masses will be given in units of GeV.
- For the numerical calculations concerning the quintessence field the program **xppaut** has been used, while all plots were done with **Mathematica**.
- For help with the English language and for the German translation references [1, 18] were used.
- This thesis was written with the help of L^AT_EX.

Chapter 2

Introductory Cosmology

2.1 Robertson-Walker Metric and Expansion

For most of the formulas in this chapter we refer the reader to [19, 33].

On large scales, we find our universe to be impressively homogeneous and isotropic. If we postulate that its space-time metric also possesses these two properties, we find that it can always be brought to the form

$$ds^2 = dt^2 - R^2(t) \left(\frac{dr^2}{1 - kr^2} + r^2 d\theta^2 + r^2 \sin^2 \theta d\phi^2 \right), \quad (2.1)$$

which is called the **Robertson-Walker metric**. Here, (t, r, θ, Φ) are the coordinates, while $R(t)$ is called the cosmic scale factor, which can be time dependent. The metric can always be chosen such that the constant k either equals 1, 0, or -1, which refers to an open, a flat, and a closed universe respectively.

To determine the dynamical behaviour of $R(t)$, we also need the **Einstein equations**, which determine the dynamics of any system in general relativity:

$$R_{\mu\nu} - \frac{1}{2} \mathcal{R} g_{\mu\nu} = 8\pi G T_{\mu\nu} + \Lambda g_{\mu\nu}, \quad (2.2)$$

where $R_{\mu\nu}$ stands for the Ricci tensor (not to be confused with the scale factor $R(t)$), \mathcal{R} for the Ricci scalar, $G \equiv 1/m_{\text{Pl}}^2$ for the gravitational constant, $T_{\mu\nu}$ for the energy-momentum tensor of all fields of the system, and Λ for a possible cosmological constant.

Our postulates of spatial homogeneity and isotropy yield a simple form of the energy-momentum tensor, in which all non-diagonal entries are zero and all spatial components are equal. Therefore it has the form of that of a perfect fluid

$$T_{\nu}^{\mu} = \text{diag}(\rho, -p, -p, -p). \quad (2.3)$$

Here $\rho(t)$ represents the energy density, while $p(t)$ stands for the pressure. The principle of general covariance leads to the conserved currents

$$T^{\mu\nu}{}_{;\nu} = 0, \quad (2.4)$$

which, in our case, yields for $\mu = 0$

$$d(\rho R^3) = -p d(R^3). \quad (2.5)$$

Physically this just says that the loss of energy in a certain volume is equal to the work done by it, which is the change of volume times its pressure. In spite of the fact that this statement seems quite simple, it allows us to determine the qualitative behaviour of $R(t)$ in dependence of ρ and its composition.

For most energy forms there is a simple connection between the energy density and the corresponding pressure, which is of the form

$$p = \omega \rho, \quad (2.6)$$

where ω is independent of time. Now it is simple to solve the differential equation (2.5) and we get

$$\rho \propto R^{-3(1+\omega)}. \quad (2.7)$$

For the most common examples of energy forms this yields:

$$\begin{aligned} \text{non-relativistic matter} : p &= 0 \Rightarrow \rho \propto R^{-3}, \\ \text{radiation} : p &= \frac{1}{3}\rho \Rightarrow \rho \propto R^{-4}, \\ \text{vacuum energy} : p &= -\rho \Rightarrow \rho = \text{const.} \end{aligned}$$

In order to find the behaviour of $R(t)$ and $\rho(t)$ with respect to time, we need to determine $R_{\mu\nu}$ and \mathcal{R} from the metric and plug the results into the Einstein equations. Only the four diagonal elements of these yield equations differing from $0=0$, and only two of these are independent. As the two independent equations we choose

$$\frac{\dot{R}^2}{R^2} + \frac{k}{R^2} = \frac{8\pi G}{3}\rho, \quad (2.8)$$

which is called the **Friedmann equation**, and

$$\frac{\ddot{R}}{R} = -\frac{4\pi G}{3}(\rho + 3p). \quad (2.9)$$

Introducing the variables

$$\rho_C \equiv \frac{3H^2}{8\pi G} \quad \text{and} \quad \Omega \equiv \frac{\rho}{\rho_C}, \quad (2.10)$$

where ρ_C is called the critical density, we can transform the Friedmann equation to

$$\frac{k}{H^2 R^2} = \Omega - 1, \quad (2.11)$$

where $H \equiv \dot{R}/R$ is the Hubble ratio.

Given the fact that, especially during early stages of the universe, its energy density was very close (if not equal) to the critical density (which means $\Omega \approx 1$), we see that the error in most calculations should not be too big, if $k = 0$ is assumed.

With this assumption, eq.(2.7), and $\Delta t \equiv \int_{R_i}^{R(t)} \dot{R}'^{-1} dR'$, the Friedmann equation yields:

$$\begin{aligned} \Delta t &= \frac{2}{3(1+\omega)} H_0^{-1} \left[\left(\frac{R}{R_0} \right)^{\frac{3(1+\omega)}{2}} - \left(\frac{R_i}{R_0} \right)^{\frac{3(1+\omega)}{2}} \right] \quad \text{for } \omega \neq -1, \\ \Delta t &= H_0^{-1} \ln \left| \frac{R}{R_i} \right| \quad \text{for } \omega = -1, \end{aligned} \quad (2.12)$$

where the 0 subscript refers to today's value of the corresponding parameters.

With the assumption that the universe was radiation dominated through all of its early stages ($t_i = 0$, $R(t_i) = 0$), we find the formula

$$R \propto t^{\frac{1}{2}}, \quad (2.13)$$

which we will use later on.

From eq.(2.12), we can also see that in case of dominating vacuum energy ($\omega = -1$), the universe expands exponentially with respect to time.

2.2 Early Universe Thermodynamics

The universe of the cosmological standard model (CSM) can strictly never have been in thermal equilibrium. This is due to the fact that this model, which mainly bases on the Robertson-Walker metric, does not possess a time-like killing-vector. Still we can say that there were stages during which the universe has been in local thermal equilibrium (LTE), which can always be said if the reaction rates of all processes are faster than the rate of change of the cosmological circumstances. Thus, when speaking of equilibrium, we will think of LTE in the following parts of this thesis, if not specified differently.

2.2.1 Particle and Energy Densities

To determine the particle density n , energy density ρ , and the pressure p of a particle species in LTE, we have to evaluate the phase space integrals

$$n_{\text{eq}} = \frac{g}{(2\pi)^3} \int f(\vec{p}) d^3p, \quad (2.14a)$$

$$\rho_{\text{eq}} = \frac{g}{(2\pi)^3} \int E(\vec{p}) f(\vec{p}) d^3p, \quad (2.14b)$$

$$p_{\text{eq}} = \frac{g}{(2\pi)^3} \int \frac{|\vec{p}|^2}{3E} f(\vec{p}) d^3p, \quad (2.14c)$$

where g is the number of the degrees of freedom of the particle species, $E \equiv \sqrt{m^2 + p^2}$ is their energy, m is their mass, $f(\vec{p})$ is their total phase-space distribution, and the integrals are to be taken over all phase-space. For the phase-space distribution we have

$$f(\vec{p}) = \frac{1}{\exp((E - \mu)/T) \pm 1}, \quad (2.15)$$

where μ represents the chemical potential of the particle species, and the $+$ refers to fermions, while the $-$ refers to bosons.

For species with $f(\vec{p}) \ll 1$ for all \vec{p} , we can simplify things by using the Maxwell-Boltzmann distribution

$$f(\vec{p}) = \exp\left(-\frac{(E - \mu)}{T}\right). \quad (2.16)$$

In these cases we can compute eqs.(2.14) analytically [20]:
By making the substitutions $x \equiv m/T$ and $z \equiv E/T$ and integrating out the angular parts of \vec{p} eq.(2.14a) becomes

$$n_{\text{eq, MB}} = \frac{gT^3}{2\pi^2} \int_x^\infty z \sqrt{z^2 - x^2} e^{-(z-\mu/T)} dz. \quad (2.17)$$

This expression turns out to be

$$n_{\text{eq, MB}} = \frac{gT^3 e^{\mu/T}}{2\pi^2} x^2 K_2(x), \quad (2.18)$$

where $K_2(x)$ is a modified Bessel function.

In the limits of large x this leads to

$$n_{\text{eq, MB}} = g \left(\frac{mT^3}{2\pi} \right)^{\frac{3}{2}} e^{-(m-\mu)/T} \left[1 + \frac{15}{8x} + \frac{105}{128x^2} + \dots \right], \quad m \gg T, \quad (2.19)$$

while it yields

$$n_{\text{eq, MB}} = \frac{gT^3 e^{\mu/T}}{\pi^2} \left[1 - \frac{1}{4}x^2 - \dots \right], \quad m \ll T, \quad (2.20)$$

for small x .

We see that the particle density is (in leading order) independent of the mass of the particle in the extreme relativistic case, while its abundance is exponentially suppressed in the non-relativistic limit and $m > \mu$.

To calculate the mean energy and energy density, we first present the intermediate result for the mean time dilation

$$\begin{aligned} \left\langle \frac{m}{E} \right\rangle_{\text{MB}} &= \frac{\int_x^\infty x \sqrt{z^2 - x^2} e^{-z} dz}{\int_x^\infty z \sqrt{z^2 - x^2} e^{-z} dz} \\ &= \frac{K_1(x)}{K_2(x)}. \end{aligned} \quad (2.21)$$

In classical non-relativistic statistical mechanics the equipartition theorem states that the mean energy per quadratic degree of freedom is $\frac{1}{2}T$. By finding a corresponding relativistic quantity, we will finally be able to calculate the mean energy of a particle. This quantity turns out to be

$$Q \equiv p_i \frac{\partial E}{\partial p_i}, \quad (2.22)$$

where i is arbitrary but fixed. For its mean value we get

$$\langle Q \rangle_{\text{MB}} = \left\langle p_i \frac{\partial E}{\partial p_i} \right\rangle_{\text{MB}} = T, \quad (2.23)$$

after integrating by parts.

In the non-relativistic case we have $E = \sum p_i^2/(2m)$ and thus eq.(2.23) confirms the classical equipartition theorem. In the relativistic case, however, we have $Q = p_i^2/E$ and eq.(2.23) therefore gives

$$\left\langle \frac{\vec{p}^2}{E} \right\rangle_{\text{MB}} = \left\langle E - \frac{m^2}{E} \right\rangle_{\text{MB}} = 3T. \quad (2.24)$$

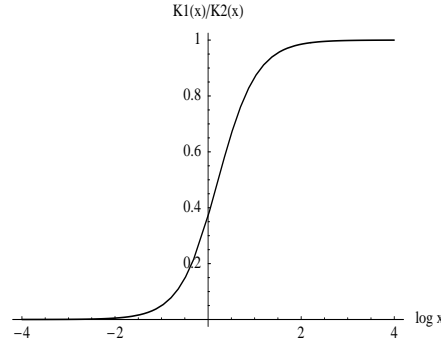


Figure 2.1: The behaviour of the quotient $K_1(x)/K_2(x)$ in dependence of the logarithm of x with x ranging from 10^{-4} to 10^4 .

Since we know the mean time dilation from eq.(2.21), we can now calculate the mean energy:

$$\langle E \rangle_{\text{MB}} = 3T + m \frac{K_1(x)}{K_2(x)}. \quad (2.25)$$

In fig.2.1 the behaviour of the quotient in the second term of the sum is shown, and we reach the intuitively clear solution that for $m \gg T$ the mean energy of a particle is more or less its rest energy, while for large temperatures $m \ll T$, the mass of the particle becomes irrelevant and its mean energy basically is $3T$.

To calculate the energy density ρ , all one has to do is to multiply the particle density with the mean energy, giving [20]

$$\begin{aligned} \rho_{\text{eq, MB}} &= n_{\text{eq, MB}} \cdot \langle E \rangle_{\text{MB}} \\ &= \frac{gT^4 e^{\mu/T}}{2\pi^2} [3x^2 K_2(x) + x^3 K_1(x)] \\ &\simeq gm \left(\frac{mT}{2\pi}\right)^{\frac{3}{2}} e^{-(m-\mu)/T} \left[1 + \frac{27}{8x} + \dots\right], \quad T \ll m, \\ &\simeq \frac{3gT^4 e^{\mu/T}}{\pi^2} \left[1 - \frac{1}{12}x^2 + \dots\right], \quad T \gg m. \end{aligned} \quad (2.26)$$

Using Fermi-Dirac or Bose-Einstein statistics, the expressions in eqs.(2.14) cannot be given in terms of special functions for all parameter values. However, approximation formulas can be given for most relevant parameter ranges [19]: In the relativistic limit ($T \gg m$, $T \gg \mu$), eqs.(2.14) yield

$$n_{\text{eq}} \simeq \begin{cases} \frac{\zeta(3)}{\pi^2} gT^3 & \text{for bosons} \\ \frac{3}{4} \frac{\zeta(3)}{\pi^2} gT^3 & \text{for fermions} \end{cases}, \quad (2.27a)$$

$$\rho_{\text{eq}} \simeq \begin{cases} \frac{\pi^2}{30} gT^4 & \text{for bosons} \\ \frac{7}{8} \frac{\pi^2}{30} gT^4 & \text{for fermions} \end{cases}, \quad (2.27b)$$

$$p_{\text{eq}} = \frac{\rho}{3}, \quad (2.27c)$$

where $\zeta(x)$ is the Riemann zeta function with $\zeta(3) \approx 1.202$.

For degenerate fermions we find

$$n_{\text{eq}} = \frac{1}{6\pi^2} g \mu^3, \quad (2.28a)$$

$$\rho_{\text{eq}} = \frac{1}{8\pi^2} g \mu^4, \quad (2.28b)$$

$$p_{\text{eq}} = \frac{\rho}{3}, \quad (2.28c)$$

while we get for fermions or bosons with $\mu < 0$ and $|\mu| < T$

$$n_{\text{eq}} = e^{\frac{\mu}{T}} \frac{g}{\pi^2} T^3, \quad (2.29a)$$

$$\rho_{\text{eq}} = e^{\frac{\mu}{T}} \frac{3g}{\pi^2} T^4, \quad (2.29b)$$

$$p_{\text{eq}} = \frac{\rho}{3}. \quad (2.29c)$$

We see that for all kinds of radiation we get $\omega = 1/3$, which we used extensively in the last section.

In the limit of non-relativistic temperatures ($T \ll m$) eqs.(2.14) lead to

$$n_{\text{eq}} = g \left(\frac{mT}{2\pi} \right)^{\frac{3}{2}} e^{-(m-\mu)/T}, \quad (2.30a)$$

$$\rho_{\text{eq}} = mn, \quad (2.30b)$$

$$p_{\text{eq}} = Tn, \quad (2.30c)$$

from which we can see that it was reasonable to assume $\omega = 0$ for non-relativistic matter, since $p \ll \rho$ in that case.

We can see that the total energy density and pressure of all fields in the universe

$$\rho_{\text{total}} = \sum_{i \in \text{all fields}} \rho_i \quad \text{and} \quad p_{\text{total}} = \sum_{i \in \text{all fields}} p_i \quad (2.31)$$

are mainly given by the relativistic fields, as long as they are not decoupled from the other ones. Therefore the total energy density and pressure are often given as [19]

$$\begin{aligned} \rho_R &= \frac{\pi^2}{30} g_* T^4, \\ p_R &= \frac{\pi^2}{90} g_* T^4 = \frac{\rho_R}{3}, \end{aligned} \quad (2.32)$$

where T is the photon temperature and g_* is the number of effectively massless degrees of freedom with

$$g_* \equiv \sum_{i \in \text{bosons}} g_i \left(\frac{T_i}{T} \right)^4 + \frac{7}{8} \sum_{i \in \text{fermions}} g_i \left(\frac{T_i}{T} \right)^4, \quad (2.33)$$

where the sums are only to be taken over the effectively massless particles.

Finally we plug eq.(2.32) into the Friedman equation (eq.(2.8)) with $k = 0$, which leads to

$$H \approx 1.66 \cdot g_*^{\frac{1}{2}} \frac{T^2}{m_{\text{Pl}}}. \quad (2.34)$$

In addition eq.(2.13) gives us a connection between the cosmic scale factor and time during the radiation dominated era, such that we can now write down the relation between time and temperature during this phase

$$t = 0.301 \cdot g_*^{-\frac{1}{2}} \frac{m_{\text{Pl}}}{T^2}. \quad (2.35)$$

2.2.2 Chemical Potentials

If temperature and rest energy of a particle species is fixed, its abundance is determined by its chemical potential. Therefore chemical potentials are especially important, when dealing with the different abundances of particles and their anti-particles, which is what every baryogenesis model is essentially about.

By saying that a certain process or particle reaction is in equilibrium, we mean that its reaction rate is much faster than the rate at which the cosmological circumstances change, for which the corresponding scale is given by the Hubble rate H . If this is the case, the system will reach an equilibrium state with respect to this process, where forward and backward reactions will occur at the same rate and the system will no longer go through any changes due to this reaction.

If a certain volume has reached an equilibrium state, its free energy F is at a minimum with respect to possible changes it could undergo due to any fast enough process (see e.g. [21]).

We now denote an arbitrary reaction in equilibrium by

$$\sum_{\alpha} c_{\alpha} \alpha \longrightarrow \sum_{\beta} c_{\beta} \beta, \quad (2.36)$$

where α and β run over the various particle species in the respective channels, while $c_{\alpha,\beta}$ represent the number of particles per species needed for one reaction. This can also be written in the form

$$\sum_{\xi \in (\{\alpha\} \cup \{\beta\})} c_{\xi} \gamma = 0, \quad (2.37)$$

with $c_{\xi} \equiv c_{\alpha}$ for $\xi = \alpha$ and $c_{\xi} \equiv -n_{\beta}$ for $\xi = \beta$.

If such a reaction takes place, F changes by

$$\begin{aligned} dF &= \sum_{\gamma} n_{\gamma} \frac{\partial F}{\partial N_{\gamma}} \\ &= \sum_{\gamma} n_{\gamma} \mu_{\gamma}, \end{aligned} \quad (2.38)$$

where μ_{γ} is the the chemical potential of the corresponding particle species. Since F is at a minimum with respect to all processes in equilibrium, we have the condition $dF = 0$, which leads to

$$\sum_{\gamma} n_{\gamma} \mu_{\gamma} = 0, \quad (2.39)$$

for any process in equilibrium.

This immediately results in the fact that the chemical potential of photons is zero

$$\mu_\gamma = 0, \quad (2.40)$$

as an arbitrary number of them can be emitted or absorbed in any reaction.

From this it can now be deduced that the chemical potential of a particle and its anti-particle only differ in the sign, as long as pair-annihilation is in equilibrium ($a + \bar{a} \leftrightarrow 2\gamma$)

$$\mu_a = -\mu_{\bar{a}}. \quad (2.41)$$

In this case the excess of a fermion species over its antiparticle can be calculated, and we find

$$\begin{aligned} n_+ - n_- &= \frac{gT^3}{2\pi^2} \int_x^\infty dz z \sqrt{z^2 - x^2} [(e^{z-\mu/T} + 1)^{-1} - (e^{z+\mu/T} + 1)^{-1}] \\ &= \frac{gT^3}{6\pi^2} \left[\pi^2 \frac{\mu}{T} + \left(\frac{\mu}{T} \right)^3 \right] \quad \text{for } T \gg m \\ &= 2g \left(\frac{mT}{2\pi} \right)^{\frac{3}{2}} \sinh \left(\frac{\mu}{T} \right) e^{-\frac{m}{T}} \quad \text{for } T \ll m, \end{aligned} \quad (2.42)$$

as both particles have the same mass.

2.2.3 Entropy and Entropy Density

If we apply the second law of thermodynamics to a comoving volume element, we find

$$TdS(V, T) = d(\rho(T)V) + p(T)dV = d((\rho + p)V) - Vdp, \quad (2.43)$$

where $V \equiv R^3$ is the physical volume of the comoving volume element, which has coordinate volume one, and dS is its change of entropy.

From the condition

$$\frac{\partial^2 S}{\partial T \partial V} = \frac{\partial^2 S}{\partial V \partial T} \quad (2.44)$$

we get

$$T \frac{dp}{dT} = \rho(T) + p(T). \quad (2.45)$$

The first law of thermodynamics (eq.(2.5)) can also be written as

$$V \frac{dp}{dt} = \frac{d}{dt} (V(\rho + p)), \quad (2.46)$$

which together with eq.(2.45) takes the form

$$\frac{d}{dT} \left[\frac{R^3}{T} (\rho(T) + p(T)) \right] = 0. \quad (2.47)$$

But using eq.(2.43) along with eq.(2.45), we find

$$dS = \left[\frac{R^3}{T} (\rho(T) + p(T)) \right], \quad (2.48)$$

which yields

$$\frac{dS}{dt} = 0, \quad (2.49)$$

stating that the entropy in a comoving volume does not change with time.

Eq.(2.48) also tells us that the entropy per unit volume $s \equiv S/V$ is

$$s = \frac{\rho(T) + p(T)}{T} + \text{possible additive constant}. \quad (2.50)$$

Using eqs.(2.32), we find

$$s = \frac{2\pi^2}{45} g_{*S} T^3, \quad (2.51)$$

with

$$g_{*S} \equiv \sum_{i \in \text{bosons}} g_i \left(\frac{T_i}{T} \right)^3 + \frac{7}{8} \sum_{i \in \text{fermions}} g_i \left(\frac{T_i}{T} \right)^3, \quad (2.52)$$

where the sum is again to be taken over all effectively massless particles.

Conservation of S yields $s \propto R^{-3}$, which changes at the same rate as the particle density of a species that has effectively been frozen out, since this means that its number per comoving volume is not changing.

Therefore a quantity like the baryon asymmetry n_B has to be compared to the entropy density

$$B \equiv \frac{n_B}{s} \equiv \frac{n_b - n_{\bar{b}}}{s} \quad (2.53)$$

or to the density of another effectively frozen particle species like the photon $\eta \equiv n_B/n_\gamma$ to yield a meaningful value.

Finally we find from the conservation of S and eq.(2.51) that $g_{*S} T^3 R^3$ is a conserved quantity, and in periods during which the number of effectively massless particles is not changing, we have the relation

$$T \propto \frac{1}{R}. \quad (2.54)$$

2.3 The Matter-Antimatter Asymmetry

The fact that there are almost only baryons and no anti-baryons in our universe is usually referred to as the **matter-antimatter asymmetry** or simply **baryon asymmetry**.

So far, no primordial antimatter has been observed. Antimatter is contained in cosmic rays (namely antiprotons) but the ratio $n_p/n_{\bar{p}} \approx 10^{-4}$ can be explained by secondary production of anti-protons arising from protons hitting interstellar matter, which leads to processes like $p + p \rightarrow 3p + \bar{p}$.

This still leaves the possible existence of huge amounts of antimatter far away from us, equalling out the surplus of matter in our galaxy, such that the total baryon asymmetry is zero. However, if such bunches of antimatter would exist, there would also be annihilation radiation sent out from the borders of areas with respective matter and antimatter domination. The failure to observe this radiation leads to the conclusion that such areas must be separated on scales of the size of at least $10^{14} M_\odot$. On the other hand, the size of B , which we

will get to in the course of this section, is of an order of magnitude that implies that the temperature of separation of matter and antimatter must have been at a value greater than 38 MeV. But at this time, the causally connected region contained only about $10^7 M_\odot$, such that causality forbids such a scenario.

Therefore it is reasonable to assume that we actually live in a baryon asymmetric universe.

A very precise estimate for B comes from the theory of big bang nucleosynthesis (BBN), where today's abundances of light nuclei (p, D, ^3H , ^4H , etc.) are predicted in dependence of the input parameter B . Comparing this with astro-physical observations yields [25]

$$B \approx (2 - 8) \times 10^{-11}. \quad (2.55)$$

Examples for processes yielding a universe with the measured matter-antimatter-asymmetry at cold temperatures, but starting out from a symmetric state at early times, will be given in a separate chapter.

Chapter 3

Sphalerons

A large fraction of baryogenesis scenarios also involves non-perturbative processes at a certain stage, alongside all the regular perturbative processes typical for all areas of particle physics. These processes arise from the topological structure of gauge field theories, and shall be considered more closely in this section, where we mainly follow [6, 17, 27, 29, 35].

3.1 Anomalies

While in classical physics there is a definite connection between symmetries and conserved quantities given by Noether's theorem, which states that every symmetry of the Lagrangian of a physical system directly leads to a conserved quantity, things get more complicated in quantum field theory, where quantum effects can destroy symmetries of the Lagrangian and therefore lead to violation of the conservation laws acquired from the classical treatment of the Lagrangian. This is usually the case in parity-violating theories.

3.1.1 The Axial Anomaly

The most common example for an anomaly is the **Adler-Bell-Jackiw anomaly** or simply **axial anomaly**:

A massless gauge theory (e.g. massless QED), is invariant under the chiral transformation

$$\Psi(x) \rightarrow e^{-i\omega\gamma_5}\Psi(x). \quad (3.1)$$

Noether's theorem now yields a conserved current, which is normally taken to be the chiral current

$$j_5^\mu \equiv \bar{\Psi}\gamma^\mu\gamma_5\Psi, \quad (3.2)$$

where classical treatment yields

$$\partial_\mu j_5^\mu = 0. \quad (3.3)$$

As stated before, in the quantum case things are a little different, which can be seen from the two diagrams in fig.3.1.

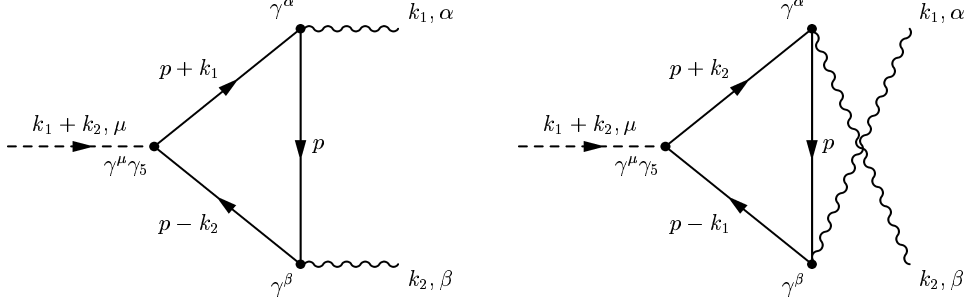


Figure 3.1: Two diagrams that lead to the Adler-Bell-Jackiw anomaly. In QED they give the lowest-order amplitude for an external source creating two photons. In the Weinberg-Salam model, it yields the lowest-order description of the process $Z \rightarrow 2\gamma$, when summed over all internal fermion loops. The last process is only a virtual process, as a spin one state cannot decay into two photons.

These two diagrams are divergent, so that they have to be regularized when calculating their value (see e.g. [17]). The problem when doing this is that one can only conserve the axial current by sacrificing the gauge symmetry, which in this case would mean violation of the Ward identity. Since the conservation of currents associated with the gauge symmetry is an experimental fact (at least in QED), one has to choose a regularisation scheme that violates eq.(3.3). Since it can be shown that the axial anomaly is only due to the one-loop feyman graphs of the processes described in fig.3.1, the quantitative calculation shows

$$(k_1 + k_2)^\mu T_{\alpha\beta\mu}(k_1, k_2) = \frac{i}{2\pi^2} k_1^\mu k_2^\nu \varepsilon_{\alpha\beta\mu\nu}, \quad (3.4)$$

where $T_{\alpha\beta\mu}(k_1, k_2)$ is the renormalized matrix-element for the two processes, and we stress again that we are in the limit of a gauge theory with zero fermion masses.

Fourier transformation of this expression and the insertion of the coupling constant (e.g. e in QED) yields the final result

$$\langle k_1, \alpha; k_2, \beta | \partial^\mu j_{5\mu}(0) | 0 \rangle = -\frac{e^2}{16\pi^2} \langle k_1, \alpha; k_2, \beta | \varepsilon^{\alpha\nu\beta\lambda} F_{\alpha\nu} F_{\beta\lambda}(0) | 0 \rangle, \quad (3.5)$$

where we can see that, even in the massless limit, the axial current is not conserved in this process and therefore in the whole theory.

3.1.2 Anomalies in the Path-Integral Formalism

The origin of anomalies in the path-integral formalism can help understanding their nature quite a bit. Since axial anomalies are not the only important ones, we will perform a more general treatment in this part of the section, and hereby mostly follow [35], where also the reference to the original paper is given.

In the canonical formalism the symmetry of a theory under a transformation of the fields $\Psi(x) \rightarrow U(x)\Psi(x)$ is usually shown by plugging the tranformed

fields into the Langrangian \mathcal{L} and showing that it is invariant under this transformation. In the path-integral formalism, however, we also have the fermionic measures, that additionally transform under U , which can be a transformation in Lorentz- as well as in flavor-space: ¹

$$d\Psi d\bar{\Psi} \rightarrow (\det \mathcal{U} \det \bar{\mathcal{U}})^{-1} d\Psi d\bar{\Psi}, \quad (3.6)$$

with

$$\mathcal{U}_{xn,ym} \equiv U(x)_{nm} \delta^4(x-y), \quad (3.7a)$$

$$\bar{\mathcal{U}}_{xn,ym} \equiv (\gamma^0 U(x)^\dagger \gamma^0)_{nm} \delta^4(x-y), \quad (3.7b)$$

where the indices n and m can run in Lorentz- and any flavor-space, depending on the symmetry. We see that, unless U contains a transformation in Lorentz-space, the two factors of γ^0 in eq.(3.7b), can be contracted and $\bar{\mathcal{U}}$ simply becomes the hermitian conjugate of \mathcal{U} .

In the case of U only operating in flavor-space, we can write it as

$$U(x) = \exp(i\alpha(x)t), \quad (3.8)$$

where t is an ordinary hermitian matrix, which also does not work on Lorentz-space. This leads to the fact that \mathcal{U} is either unitary or pseudounitary:

$$\bar{\mathcal{U}}\mathcal{U} = 1, \quad (3.9)$$

which both implies that the measure is invariant under the transformation we described. Therefore no anomalies will occur.

However, if U also contains a chiral transformation (compare eq.(3.1)) with

$$U(x) = \exp(i\gamma_5 \alpha(x)t), \quad (3.10)$$

where t again only acts on flavor-space, \mathcal{U} turns out to be pseudo-hermitian, with

$$\bar{\mathcal{U}} = \mathcal{U}. \quad (3.11)$$

Now the measure is not invariant under U ; instead, we have

$$d\Psi d\bar{\Psi} \rightarrow (\det \mathcal{U})^{-2} d\Psi d\bar{\Psi}. \quad (3.12)$$

Working only with infinitesimal transformations and using the formula $\det M = \exp(\text{tr}(\ln M))$, as well as $\ln(1+x) \rightarrow x$ for $x \rightarrow 0$, we can transform this expression to

$$d\Psi d\bar{\Psi} \rightarrow \exp \left[i \int d^4x \alpha(x) \mathcal{A}(x) \right] d\Psi d\bar{\Psi}, \quad (3.13)$$

where $\mathcal{A}(x)$ is called the anomaly function, given by

$$\mathcal{A}(x) \equiv -2 \text{tr}(\gamma_5 t) \delta^4(x-x). \quad (3.14)$$

¹In this part of the text we do not necessarily refer to what is also called generation-space by using the expression flavor-space, but to some general space in which our full Langrangian is embedded.

So far, $\mathcal{A}(x)$, has no physical meaning, since the trace over γ_5 will be zero, but we also have an infinite factor due to the δ -function in the equation. Therefore some method of regularization will have to be used.

Putting this aside for a moment, we see that besides the weight $\exp(i \int d^4x \mathcal{L})$, which is always present when integrating over the fields in the path-integral method, an additional factor has appeared due to eq.(3.13), such that instead of having a measure that transforms under U , we can also consider the measure to be fixed and the Lagrangian to be transforming under U as

$$\mathcal{L}(x) \rightarrow \mathcal{L}(x) + \alpha(x)\mathcal{A}(x), \quad (3.15)$$

if it was originally invariant under the corresponding transformation.

As stated before, $\mathcal{A}(x)$ can be regularized. This can be done in a gauge and Lorentz invariant manner [35] yielding

$$\mathcal{A}(x) = -\frac{1}{16\pi^2} \varepsilon_{\mu\nu\rho\sigma} F_{\alpha}^{\mu\nu}(x) F_{\beta}^{\rho\sigma}(x) \text{tr}(t_{\alpha} t_{\beta} t), \quad (3.16)$$

where $t_{\alpha,\beta}$ are generators of the gauge group, while the $F_{\alpha}^{\mu\nu}$ are the corresponding generators. If t is the unit matrix (referring to eq.(3.1)), the expression on the right-hand side of eq.(3.16) is called the **Chern-Pontryagin density**.

In the case of U being a symmetry of the system the action will be left invariant for constant α . Whereas, if $\alpha(x)$ is allowed to be space-time dependent, but going to zero at the integration borders, the change in the action will be [34]

$$\delta S = \int d^4x J_5^{\mu}(x) \partial_{\mu} \alpha(x), \quad (3.17)$$

with $J_5^{\mu}(x)$ being the classically conserved current, which is of course the chiral current if U is described by eq.(3.1).

Combining this with eq.(3.15), we see that the complete change of a path-integral is

$$\delta \int d\Psi d\bar{\Psi} e^{iS} = \int d\Psi d\bar{\Psi} \left[i \int d^4x \mathcal{A}(x) \alpha(x) + J_5^{\mu}(x) \partial_{\mu} \alpha(x) \right] e^{iS}, \quad (3.18)$$

for infinitesimal $\alpha(x)$.

But since U is just describing an infinitesimal change of variables for arbitrary $\alpha(x)$, it must not change the quantum averages of the fields, that obey the Euler-Lagrange equations. Therefore eq.(3.18) has to yield zero for both sides and arbitrary $\alpha(x)$. Integration by parts within the squared brackets thus yields

$$\langle \partial_{\mu} J_5^{\mu}(x) \rangle_A = \mathcal{A} = -\frac{1}{16\pi^2} \varepsilon_{\mu\nu\rho\sigma} F_{\alpha}^{\mu\nu}(x) F_{\beta}^{\rho\sigma}(x) \text{tr}(t_{\alpha} t_{\beta} t), \quad (3.19)$$

where the brackets $\langle \rangle_A$ represent the quantum average, and the equation is valid for arbitrary gauge fields.

In the special case of $t_{ij} = e^2 \delta_{ij}$ and the right normalization of the gauge generators this confirms our result in eq.(3.5).

Even though we find the axial current not to be conserved due to quantum effects, we can still find a conserved quantity:

Defining the **Chern-Simons class**

$$G^\mu \equiv 2\varepsilon^{\mu\nu\lambda\rho} \left[A_{\gamma\nu} \partial_\lambda A_{\gamma\rho} + \frac{1}{3} C_{\alpha\beta\gamma} A_{\alpha\nu} A_{\beta\lambda} A_{\gamma\rho} \right], \quad (3.20)$$

with $C_{\alpha\beta\gamma}$ being the structure constant of our gauge group, we get the identity

$$\partial_\mu G^\mu = \frac{1}{2} \varepsilon_{\mu\nu\rho\sigma} F_\alpha^{\mu\nu} F_\alpha^{\rho\sigma}. \quad (3.21)$$

Therefore we find the conservation of the current K^μ

$$\partial_\mu K^\mu = 0, \quad (3.22)$$

where

$$K^\mu \equiv \langle J_5^\mu \rangle_\mu + \frac{N}{8\pi^2} G^\mu, \quad (3.23)$$

and N is the norm of the gauge group generators. However we have to stress that this current is not gauge invariant.

For the sake of completeness we also want to mention the possible violation of gauge symmetries by anomalies. Besides the aesthetical problem that a gauge theory in which only the Lagrangian and not the actual physics have a certain symmetry and the hereby much more questionable motivation for the postulation of gauge symmetries, there are also real physical problems occurring in anomaly violated gauge theories. One of them being the fact that these theories will might generate divergent gauge boson mass terms through triangle diagrams [27].

In general, a theory can also be formulated by only using left-handed weyl spinors, which is usually the case in grand unified theories. In this case the anomalous current is given by

$$\langle \partial_\mu J_\alpha^\mu(x) \rangle = -\frac{1}{32\pi^2} D_{\alpha\beta\gamma} \varepsilon^{\kappa\nu\lambda\rho} F_{\kappa\nu}^\beta(x) F_{\lambda\rho}^\gamma(x), \quad (3.24)$$

where $D \equiv \frac{1}{2} \text{tr}(\{T_\alpha, T_\beta\} T_\gamma)$ and the T_i are the generators of the used representations of the gauge theory.

To prevent our gauge symmetries from being destroyed, the condition

$$D_{\alpha\beta\gamma} = 0 \quad (3.25)$$

needs to be fulfilled for all indices α, β, γ .

For the model presented in this thesis, it is enough to know that its gauge group is a subgroup of $SO(10)$, for which it has been shown that all its representations are anomaly free.

3.1.3 Anomalies and Topology

Important new insights can also be gained, when treating anomalies topologically. Some of them will be presented in this section, where we will simplify things by fixing our gauge group to be $SU(2)$ with coupling constant g , gauge fields A_μ , and field strength tensors $F_{\mu\nu}$.

Since we just saw that the axial current is not conserved, we now want to calculate the possible change of the axial charge $q_{\text{ax}}(t) \equiv \int d^3x \bar{\Psi} \gamma^0 \gamma_5 \Psi$ within time. Herefore we take a step back and consider vacuum transition amplitudes of gauge fields: In order for the action to be finite in any process, we get the condition

$$F^{\mu\nu} \xrightarrow{x \rightarrow \infty} \mathcal{O}(x^{-3}), \text{ with } x^2 = x_0^2 + \vec{x}^2, \quad (3.26)$$

which implies

$$A^\mu \xrightarrow{x \rightarrow \infty} -\frac{i}{g} U \partial^\mu U^{-1} + \mathcal{O}(x^{-2}), \quad (3.27)$$

with $U(x) \in SU(2)$, since the A^μ should except for the gauge freedom be completely determined by $F^{\mu\nu}$.

Now we define the four dimensional Volume in Minkowski space

$$V_4 \equiv \{(t, x) | t_i \leq t \leq t_f \wedge 0 < x < r\}, \quad (3.28)$$

which can be understood as a large four-dimensional cylinder, with top and bottom surfaces t_f and t_i , and consider the topological charge q_{top} , defined by

$$q_{\text{top}} \equiv \frac{g^2}{16\pi^2} \int_{V_4} d^4x \partial_\mu G^\mu, \quad (3.29)$$

where G^μ is the Chern-Simons class defined by eq.(3.20).

Gauss' theorem, which is also valid in Minkowski space, now gives

$$q_{\text{top}} = \frac{g^2}{16\pi^2} \int_{\partial V_4} dS_\mu G^\mu, \quad (3.30)$$

where dS_μ represents an element of the three-dimensional hyper-surface ∂V_4 .

When choosing r, t_i, t_f large enough, our fields will be of the form given in eq.(3.27), such that the vacuum will be totally determined by $U(x)$ with $x \in \partial V_4$, and we can regard q as the functional

$$q_{\text{top}}[U] = \frac{1}{24\pi^2} \int_{\partial V_4} dS_\mu \varepsilon^{\mu\alpha\beta\gamma} \text{tr} [U(\partial_\alpha U^{-1})U(\partial_\beta U^{-1})U(\partial_\gamma U^{-1})]. \quad (3.31)$$

Since ∂V_4 is isomorphic to the three dimensional spherical hyper-surface S_3 , we may also write

$$q_{\text{top}}[U] = \frac{1}{24\pi^2} \int_{S_3} dS_\mu \varepsilon^{\mu\alpha\beta\gamma} \text{tr} [U(\partial_\alpha U^{-1})U(\partial_\beta U^{-1})U(\partial_\gamma U^{-1})]. \quad (3.32)$$

Any arbitrary $U(x)$ is now a continous function with domain and range S_3 , which can therefore be categorized by homotopy classes, that differ from each

other in the winding number. It can further be shown that eq.(3.32) exactly yields this winding number.

Since q is gauge invariant, one can now choose a gauge (the temporal gauge), in which the only contribution comes from the top and the bottom of the cylinder:

$$q_{\text{top}} = \frac{g^2}{16\pi^2} \int_{\mathbb{R}^3} d^3x G^0 \Big|_{t_i}^{t_f}, \quad (3.33)$$

such that q_{top} can now be seen as the difference of two spatial winding numbers [35]; one of them at $t = t_i \approx -\infty$ and one of them at $t = t_f \approx \infty$. These spatial winding numbers can be changed by regauging, but their difference is gauge invariant. It can therefore be said that a topological charge different from zero is due to the transition between distinct vacua.

If we now look at eq.(3.23) and integrate both sides over V_4 in temporal gauge, we see that the change of the axial charge exactly equals the topological charge, such that the axial current is not conserved in the transition of the gauge fields between two topologically different vacua.²

3.2 (B+L) Violation in the Standard Model

The standard model Langrangian has global symmetries in addition to the postulated gauge symmetries. Two of them are the invariance under separate phase rotations of quarks and leptons:

$$\begin{aligned} U_q : q(x) &\rightarrow e^{i\omega/3} q(x) \quad , \quad l(x) \rightarrow l(x), \\ U_l : q(x) &\rightarrow q(x) \quad , \quad l(x) \rightarrow e^{i\lambda} l(x). \end{aligned} \quad (3.34)$$

Classically these symmetries would again yield conserved currents, namely

$$\begin{aligned} \partial_\mu J_B^\mu &\equiv \partial_\mu \sum_q \frac{1}{3} \bar{q} \gamma^\mu q = 0 \\ \text{and } \partial_\mu J_L^\mu &\equiv \partial_\mu \sum_l \bar{l} \gamma^\mu l = 0, \end{aligned} \quad (3.35)$$

hereby implying the conservation of baryon- and lepton-number.

However, the conservation of these currents is destroyed by anomalies: Decomposing the fermionic fields into left- and right-handed ones, we get (see eq.(3.5))

$$\begin{aligned} \partial_\mu \bar{f}_L \gamma^\mu f_L &= -c_L \frac{g^2}{32\pi^2} \varepsilon_{\mu\nu\rho\sigma} F^{a\mu\nu} F^{a\rho\sigma}, \\ \partial_\mu \bar{f}_R \gamma^\mu f_R &= +c_R \frac{g^2}{32\pi^2} \varepsilon_{\mu\nu\rho\sigma} F^{a\mu\nu} F^{a\rho\sigma}, \end{aligned} \quad (3.36)$$

where the $c_{L,R}$ depend on the different gauge groups, and the F -tensors can be the field-strength tensors of any gauge group within the standard model. But since left- and right-handed fermions belong to the same representations in $SU(3)_C$ and because there are no degenerate vacua in $U(1)_Y$, we only care about $SU(2)_L$ in the following.

²The coat of the cylinder does also not give a contribution for the fermionic fields, since they should fall off quickly for $|\vec{x}| \rightarrow \infty$ to have a finite amount of energy.

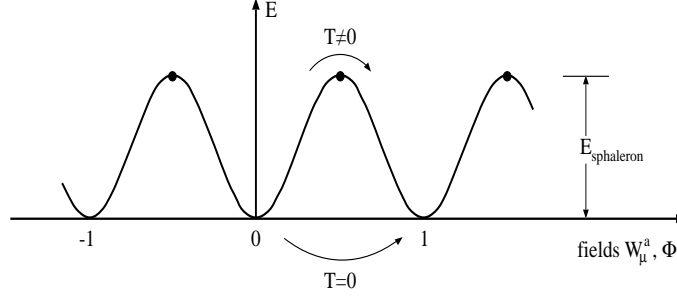


Figure 3.2: Qualitative slice through the different field constellations. One can see that to get from one vacuum states to another, the fields can either tunnel through the barrier, or thermal fluctuations can help the fields to transform continuously, if their temperature is different from 0. (Picture taken from [6])

Adding left- and right-handed currents up, we obtain

$$\partial_\mu J_B^\mu = \partial_\mu J_L^\mu = -\frac{3}{32\pi^2} g^2 \varepsilon_{\mu\nu\rho\sigma} F^{a\mu\nu} F^{a\rho\sigma}, \quad (3.37)$$

from which we can see that even though the baryonic and leptonic current are both violated, their difference is conserved:

$$\partial_\mu (J_B^\mu - J_L^\mu) \equiv \partial_\mu J_{B-L}^\mu = 0 \quad (3.38)$$

Using our knowledge from the last section, we know that these anomalies are due to topological transitions between different vacuum states, which are separated from each other by barriers of finite energy. If we integrate over V_4 again, we find [6]

$$\Delta \hat{B} = \Delta \hat{L} = 3q_{\text{top}}[U], \quad (3.39)$$

whereas a closer investigation of the global U(1)-symmetries yields [6]

$$\Delta \hat{B}/3 = \Delta \hat{L}_e = \Delta \hat{L}_\mu = \Delta \hat{L}_\tau = q_{\text{top}}[U]. \quad (3.40)$$

Since transitions between adjacent vacua are the most probable ones, we now want to find the transition amplitude between these states. To make things more illustrative, we consider the qualitative one-dimensional slice through the different field constellations and their energy in fig.3.2. We see that at $T = 0$ it would not be possible for classical fields to get from one vacuum state to another. For quantum fields, however, this is possible by the well-known tunneling effect. In this case the virtual transition between the different gauge-field configurations is called **Instanton**. Nevertheless, the probability for such a process is incredibly small. [29] e.g. finds the probability for a corresponding decay process to be of the order of 10^{-262} , which corresponds to a time scale of approximately 10^{218} years.

Yet, if the standard model is connected to a heat bath the situation changes since the fields now also have the possibility of transforming continuously. Such transitions between vacua are called **sphalerons**. This term was also used for

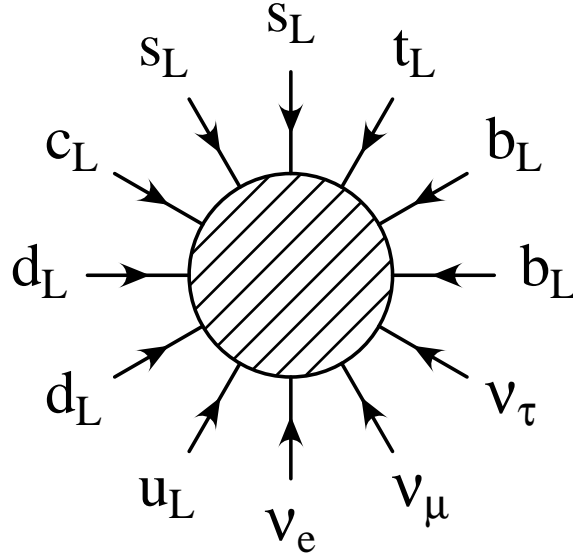


Figure 3.3: An example for a (B+L)-violating sphaleron process. (Picture taken from [6])

the field constellation right at the top of the energy barrier separating different vacua. Sphaleron processes are often illustrated by diagrams similar to Feynman diagrams and of which we present an example in fig.3.3 . It should be kept in mind however that these processes are non perturbative as opposed to Feynman diagrams.

The rate for such processes is difficult to compute and we will only present the result given in [6] for temperatures T at which these processes are in thermal equilibrium ($\Gamma \ll H$):

$$T_{EW} \sim 100\text{GeV} < T \lesssim 10^{12}\text{GeV} \quad (3.41)$$

This relation is the reason, why it was thought for a long time that any (B-L)-conserving baryon asymmetry would be washed out by sphaleron processes. However, we will get to know a counter example in the course of this thesis.

Chapter 4

Quintessence

For most of the information in this chapter the reader is referred to [30] and its references.

4.1 Acceleration of the Universe

Observations of high red-shift Type Ia supernovae (SNIa), which are used as standard candles in cosmology, seem to indicate that the expansion rate of our universe is increasing at present times and that the universe is therefore accelerating. Looking at eq.(2.9) we see that this has to be due to some new form of energy with negative pressure, if the results as well as the Robertson-Walker metric are valid. This new kind of energy is also referred to as **dark energy**. One possibility for such a behaviour is a positive Λ -term, which naturally possesses negative pressure, due to its accompaniment by the metric tensor (see eq.(2.2)), which has negative spatial eigenvalues. Another possibility is the appearance of additional classical fields, which we will look at later on. When combining the observations of the mentioned supernovae with the ones of the cosmic microwave background (CMB) a model with $\Omega_m + \Omega_\Lambda \simeq 1$ is suggested.

Also, the conservative limit for the amount of clustered matter yielded by dynamical estimates is $\Omega_m \lesssim 0.3$. The attempt to make a model with $\Omega_m \approx 1$ by the addition of cold dark matter failed to quantitatively explain the structure formation within our universe, whereas a model with $\Omega_m \approx 0.3$ as well as $\Omega_m \approx 0.7$ goes together remarkably well with a variety of observational data.

One reason why the possibility of a cosmological constant is less attractive to many people than the possibility of a dynamical Λ -term is its smallness. Since Ω_Λ and Ω_m are of the same order of magnitude today, they must have been at very different orders of magnitude in the early universe, if Λ remained constant. Reference [2] presents a ratio of 10^{-123} between the two densities at Planck time, which would require a dramatic amount of fine tuning.

4.2 Field-Theoretic Models for a Varying Λ -Term

Of the different classes of models to achieve a time-varying Λ -term a highly favored one is the field-theoretical ansatz, which is also quite successful in de-

scribing early universe inflation.

In this case an additional homogeneous scalar field Φ , which is often called **quintessence field**, is assumed together with some self-interacting potential,¹ such that we get the additional term

$$\begin{aligned}\mathcal{L}_\Phi &= \frac{1}{2}\partial^\mu\Phi\partial_\mu\Phi - V(\Phi) \\ &= \frac{1}{2}\dot{\Phi}^2 - V(\Phi)\end{aligned}\tag{4.1}$$

for the complete Lagrangian of the system.

This leads to the energy-momentum tensor

$$T_\Phi^{\mu\nu} = \partial^\mu\Phi\partial^\nu\Phi - V(\Phi),\tag{4.2}$$

hereby yielding

$$\begin{aligned}\rho_\Lambda &\equiv \rho_\Phi = \frac{1}{2}\dot{\Phi}^2 + V(\Phi) \\ p_\Lambda &\equiv p_\Phi = \frac{1}{2}\dot{\Phi}^2 - V(\Phi),\end{aligned}\tag{4.3}$$

from which we can see that for constant Φ we get a cosmological constant with $\omega \equiv \rho_\Lambda/p_\Lambda = -1$. Variation of the full Lagrangian now leads to the equations governing the evolution of the universe (with $k = 0$):

$$H^2 = \frac{8\pi G}{3}(\rho_m + \rho_\gamma + \rho_\Lambda)\tag{4.4a}$$

$$\dot{H} = -4\pi G(\rho_m + \frac{4}{3}\rho_\gamma + \rho_\Lambda + p_\Lambda)\tag{4.4b}$$

$$\ddot{\Phi} + 3H\dot{\Phi} + \frac{dV}{d\Phi} = 0\tag{4.4c}$$

In the work in the later parts of this thesis, we will work with the simplified version of these equations: When differentiating with respect to the cosmic scale factor R instead of time, the first two of these equations are sufficient to determine $\Phi(R)$ as we find ²

$$\frac{d\Phi}{dR} = Y/H,\tag{4.5a}$$

$$\frac{dY}{dR} = -3Y - \frac{dV(\Phi)}{d\Phi} \cdot \left(\frac{8\pi}{3}H\right)^{-1},\tag{4.5b}$$

with $Y \equiv \dot{\Phi}$ in orders of $M_{\text{Pl}}H_0$, Φ in orders of M_{Pl} , and V in orders of the critical energy density ρ_c .

4.3 Quintessence Potentials

4.3.1 Positive Power Potentials

One of the earlier models for an appropriate quintessence potential, was a potential of the form

$$V \propto \Phi^q, \quad q \geq 2.\tag{4.6}$$

¹By homogeneous it is meant that the field can be considered as spatially constant at least on a scale comparable to H^{-1} .

²The author is very grateful to Mathias Garny for pointing this out to him, as well as for providing him with some private notes on this topic.

If Φ fullfills the slow-roll condition $\dot{\Phi}^2 \ll V(\Phi)$, its equation of state ($p_\Lambda \approx -\rho_\Lambda$) will resemble that of a cosmological constant, which is a favoured value emerging from SNIa and CMB measurements as mentioned before. For the potential $V = \frac{1}{2}m^2\Phi^2$ this yields the constraint $(m/H_0)^2 \lesssim 1$ which leads to the extremely small mass of $m \lesssim 10^{-33}\text{eV}$.

It must also be pointed out that models with simple potentials like $V = \frac{1}{2}m^2\Phi^2$ run into similiar problems as the cosmological constant: Due to eq.(4.4) the system is enormously overdamped at times ranging from the Planck epoch $z \approx 10^{19}$ until $z \approx 2$ (z being the red shift), such that the energy density of the scalar field at early times, must have already been extremely small at early stages, which in return leads again to the already mentioned extreme fine tuning problem ([5, 30] and references).

4.3.2 Tracker Fields

The just mentioned problem of a possible cosmological constant or a positive power potential for the quintessence field, can be circumvented when using a potential of the type

$$V(\Phi) = \frac{M^{4+\alpha}}{\Phi^\alpha}. \quad (4.7)$$

To see why this model works better than the model before we assume the universe to expand according to a power law $R(t) \propto t^q$, which is true for radiation or matter dominated stages (see eq.(2.12)). Eg.(4.4) then yields

$$\ddot{\Phi} + 3\frac{q}{t}\dot{\Phi} - \frac{\alpha M^{4+\alpha}}{\Phi^{\alpha+1}}, \quad (4.8)$$

with the solution

$$\Phi \propto t^{\frac{2}{2+\alpha}}. \quad (4.9)$$

Carrying on with the calculation, we find

$$\frac{\rho_\Phi}{\rho_B} \propto t^{\frac{4}{2+\alpha}}, \quad (4.10)$$

such that for $\alpha \geq 0$, the energy densitiy of Φ will eventually get bigger than the background density ρ_B .

This can also be seen from the fact that ρ_Φ decreases as $1/R^{3(1+\omega_\Phi)}$ as can be seen from eq.(2.7), whereas $\rho_m \propto 1/R^3$ and $\rho_r \propto 1/R^4$. Which means that the background energy density will get smaller at a faster pace.

The fact that the energy density decreases faster than the density of the dark energy is of course also true for a cosmological constant or the positive power potential. The difference here is that the constraints for the parameters are much less rigid, since this class of potentials posseses what is called a **tracker** property, meaning that after the Hubble constant has reached a certain value, ρ_Φ and ρ_B will keep track of each other and ρ_B will only slowly get smaller than ρ_Φ . The model now even features the possibility of a dark energy, which starts out only few orders of magnitude smaller than the background energy density, but which will not be dominant until very recent times, therefore not interrupting

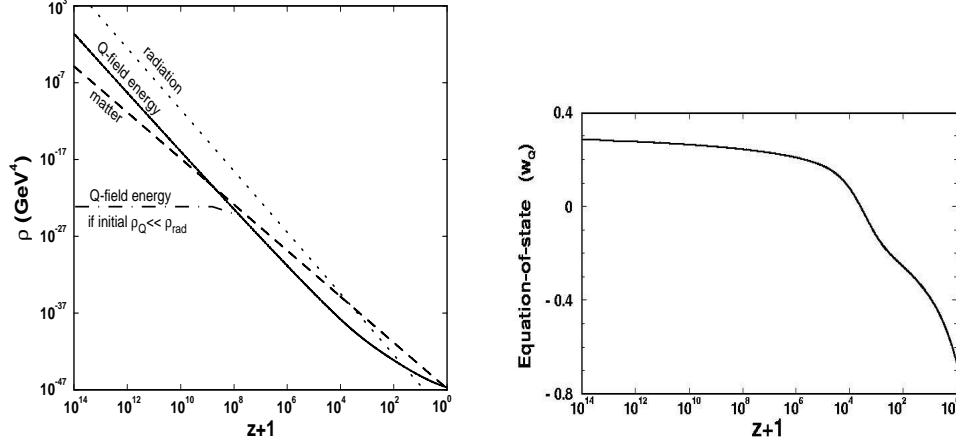


Figure 4.1: An example for the tracker property of a quintessence field is shown in the left graph. In this case the potential is $V(\Phi) = M^4[\exp(M_{\text{MB}}/Q) - 1]$. For the quintessence curve that starts out at a lower energy, one can see that its energy density remains more or less constant, until it is only a few orders of magnitude smaller than the background energy density. Then the tracking behaviour starts, and both densities decrease at a similar rate until finally ρ_Λ gets bigger. If both energy densities start out with approximately the same orders of magnitude, one can see that their ratio does not change very much. The behaviour of ω_Φ in this model is shown in the graph on the right-hand side. [36]

bounds from big bang nucleosynthesis (BBN). Hereby the fine tuning problem of the potentials before can be circumvented. An example for a model with similar behaviour is shown in fig.4.1 .

4.3.3 Exponential Potentials

Even though the potentials presented in the last paragraphs had appealing features, not everybody is fully pleased with them. This is due to the fact that observations favor an equation of state with $\omega_\Lambda \approx -1$ as stated before. Without fine tuning the potentials presented in the last section yield $\omega_\Lambda > -0.7$, which still is within the 2σ bounds of ref. [5], but not the favored value. We therefore take a look at one more class of potential quintessence models:

Solutions of quintessence models with potentials of the form

$$V \propto e^{\lambda\Phi/M_{\text{Pl}}} \quad (4.11)$$

yield a slightly different qualitative quintessence behaviour from the ones obtained from the potentials in the last section. They are called **attractor solutions**:

- In the case $\lambda^2 > 3(\omega_B + 1)$, where ω_B is the equation of state of the background energy, Ω_Λ takes on a constant value of $\Omega_\Lambda = 3(\omega_B + 1)/\lambda^2$ after an initial phase and the equation of state yields $\omega_\Lambda = \omega_B$.

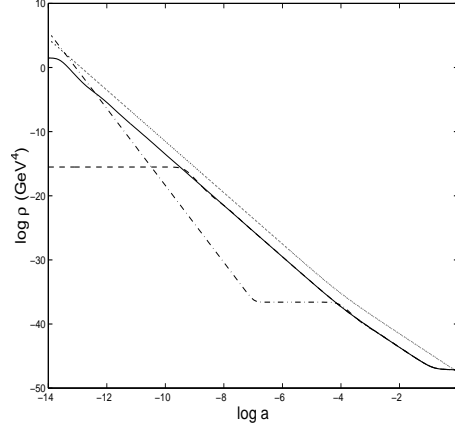


Figure 4.2: The behaviour of the energy density of a quintessence field for several initial conditions in case of a potential described by eq.(4.12) and parameters $\alpha = 20$, $\beta = 0.5$. The solid line shows the case of equipartition at the end of inflation. The dotted line represents ρ_B [5]

- In the case $\lambda^2 < 3(\omega_B + 1)$ the equation of state goes to $\omega_\Lambda = -1 + \lambda^2/3$ and we additionally find $\Omega_\Lambda = 1$.

Both cases are not satisfactory: While the second case does not yield a subdominant dark energy density during BBN, the first case will not lead to a dominating one today, since it is also constrained by BBN, and the ratio of the energy densities remains fixed in both cases.

The situation changes however when choosing a potential of the form

$$V = M^4 \left[\exp \left(\frac{\alpha \Phi}{M_{\text{Pl}}} \right) + \exp \left(\frac{\beta \Phi}{M_{\text{Pl}}} \right) \right], \quad (4.12)$$

with α leading to case one and β leading to case two, if they were used separately. This way, we can obtain a behaviour of the field that is subdominant during the phase of BBN, but also one that leads to a dark energy dominated universe today.

Another nice feature of these potentials is the enlarged range for acceptable initial conditions. Even though this range was also big for the models presented in the last section, it did not allow the dark energy density to start out bigger than the energy density of the other fields. Now we can also get appealing behaviour from fields with such initial conditions. A qualitative behaviour of such a case is shown in fig.4.2 .

Things get even nicer, when we choose β to be smaller than zero. In this case the potential will have a minimum, and the differential equation of Φ will be that of a damped oscillator. Thus, the field will actually become constant, and we achieve the desired equation of state $\omega_\Lambda = -1$ mentioned earlier. A possible shape of ω_Λ for positive and negative β is shown in fig.4.3 .

Finally we want to address the issue of fine tuning in such potentials as it is not clear why the factor M in eq.(4.12) should be of the order of approximately

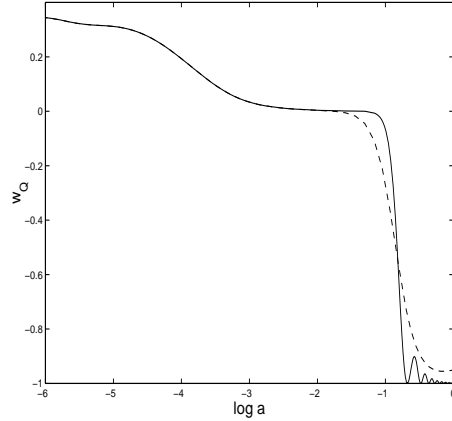


Figure 4.3: The evolution of the equation of state of the quintessence field at late times in the cases of $\alpha = 20, \beta = 0.5$ (dashed line) and $\alpha = 20, \beta = -20$ (dotted line). [5]

$10^{-31}M_{\text{Pl}}$ to achieve a value for ρ_Λ of the order of 10^{-47}GeV today. Luckily we do not have to introduce a new energy scale for this, if we assume the original potential to be of the form

$$V = M^4 \left[\exp \left(\frac{\alpha(\Phi - A)}{M_{\text{Pl}}} \right) + \exp \left(\frac{\beta(\Phi - B)}{M_{\text{Pl}}} \right) \right]. \quad (4.13)$$

In this case all the parameters can be much closer to the Planck scale and we still get the values needed to fit astrophysical observations. While it can still be said that this ansatz includes fine tuning, it at least allows the pre-factor to be small without the introduction of a new energy scale.

Chapter 5

Baryogenesis Models

5.1 The Sakharov Conditions

Even though the class of processes that can transform a symmetric universe into a baryon asymmetric one is quite big, they all have to fulfill certain conditions, called the **Sakharov conditions** [31], if their framework is a local quantum field theory:

- **Baryon number violation (B-violation):**

Obviously any theory starting from a B-symmetric state and ending up in an asymmetric state has to violate B at some point.

- **C- and CP-violation:**

If B changes its sign when acted on by some unitary operator \mathcal{O} , the baryon number of any eigenstate Ψ of \mathcal{O} is zero:

$$\begin{aligned}\langle \hat{B} \rangle &= \langle \Psi | \hat{B} | \Psi \rangle \\ &= \langle \Psi | \mathcal{O}^\dagger \hat{B} \mathcal{O} | \Psi \rangle \\ &= \langle \Psi | -\hat{B} | \Psi \rangle \\ &= 0.\end{aligned}\tag{5.1}$$

Since B does change its sign under C and CP and we believe the early universe has been C- and CP- symmetric and therefore an eigenstate of these operators, both of them need to be violated at some point to create a baryon asymmetry.

- **Departure from thermal equilibrium:**

In chemical equilibrium all chemical potentials referring to non-conserved quantum numbers have to be zero to minimize the free energy. Starting from a symmetric state in which $\mu_i = 0$ for any particle (see eq.(2.42)), we see that any change in B , would be due to a change of the chemical potential of a non-conserved quantum number. But since these have to be equal to zero in order to minimize the free energy, they will not change their value and keep B hereby fixed. Therefore baryon asymmetric states can only exist, if not all of the processes (i.e. mainly the B-violating processes) are in equilibrium.

particle		final state	branching ratio Γ	B
\bar{X}	\rightarrow	$q\bar{q}$	r_x	$2/3$
X	\rightarrow	$\bar{q}l$	$1 - r_x$	$-1/3$
$\bar{\bar{X}}$	\rightarrow	$\bar{q}q$	\bar{r}_x	$-2/3$
\bar{X}	\rightarrow	ql	$1 - \bar{r}_x$	$1/3$
Y	\rightarrow	$q\bar{q}$	r_y	$2/3$
Y	\rightarrow	$\bar{q}l$	$1 - r_y$	$-1/3$
\bar{Y}	\rightarrow	$\bar{q}q$	\bar{r}_y	$-2/3$
\bar{Y}	\rightarrow	ql	$1 - \bar{r}_y$	$1/3$

Table 5.1: The decay channels and rates, as well as the corresponding baryon number of the decay channel in the model specified in the text.

5.2 A Simple Baryogenesis Model

A simple toy-model leading to baryogenesis is presented in ref. [19]. Here two GUT-motivated heavy bosons are added to the standard model and couple to quarks and leptons in a CP-violating manner. This leads to the decay of the heavier bosons with the various branching ratios illustrated in table 5.1. Therefore the decay of a boson-antiboson pair gives the net baryon numbers $\varepsilon_{X,Y}$

$$\begin{aligned}\varepsilon_X &= \sum_i B_i \frac{\Gamma(X \rightarrow f_i) - \Gamma(\bar{X} \rightarrow \bar{f}_i)}{\Gamma_{X,\text{total}}}, \\ \varepsilon_Y &= \sum_i B_i \frac{\Gamma(Y \rightarrow f_i) - \Gamma(\bar{Y} \rightarrow \bar{f}_i)}{\Gamma_{Y,\text{total}}},\end{aligned}\tag{5.2}$$

where i runs over all decay channels.

The CP-violating couplings can be realized by the interaction term

$$\mathcal{L}_{\text{int}} = g_1 X f_2^\dagger f_1 + g_2 X f_4^\dagger f_3 + g_3 Y f_1^\dagger f_3 + g_4 X f_2^\dagger f_4 + \text{h.c.}\tag{5.3}$$

in the Lagrangian, where the f_i denote various fermionic states, and the g_i are complex Yukawa couplings. The one-loop corrections to the decay diagrams now yield CP-violating structures. Since these diagrams are similar to the ones presented in the model of this thesis, they are not shown here explicitly.

A departure from equilibrium can be achieved when the decay rate is much smaller than the Hubble rate (compare section 2.2.2):

Assume the bosons were in thermal equilibrium at some early time, corresponding to a high temperature. At these times, the equilibrium abundance of the bosons is approximately the same as the one of massless particles such as photons (see eq.(2.27)). Since the equilibrium particle density is proportional to T^3 , which is in return proportional to R^{-3} the abundance of the particles will remain in equilibrium, even if no reactions take place as long as they can be considered massless. At temperatures below their mass, their abundance should be exponentially suppressed. Which leads to the fact that they will be overabundant, if their decay rates are not fast enough.

The important rates are in this case the decay (Γ_D) and inverse decay processes (Γ_{ID}), as well as B-nonconserving $2 \leftrightarrow 2$ scattering processes (Γ_S) and pair annihilation (Γ_{Ann}). The rate for pair annihilation is proportional to n_X and therefore "self-quenching". The important processes for keeping the particles in thermal equilibrium are therefore given by the first three ratios. Reference [19] gives the following approximate values for them:

$$\begin{aligned}\Gamma_D &\simeq \alpha m_X \begin{cases} m_X/T & , \quad T \geq m_X \\ 1 & , \quad T \leq m_X \end{cases} \\ \Gamma_{ID} &\simeq \Gamma_D \begin{cases} 1 & , \quad T \geq m_X \\ (\frac{m_X}{T})^{3/2} \exp(-\frac{m_X}{T}) & , \quad T \leq m_X \end{cases} \\ \Gamma_S &\simeq n\sigma \simeq \frac{\alpha^2 T^5}{(T^2 + m_X^2)^2},\end{aligned}\tag{5.4}$$

where $\alpha \sim g^2/(4\pi)$ is a measure of the coupling strength and the formulas for Y are of the same shape. The additional factor of m_X/T in the first equation comes from the fact that most particles are at relativistic energies, and therefore their decay time is dilated. The suppression factor in the second equation roots from the suppressed abundance of particles having enough energy to generate a heavy boson.

We see that after the temperature has fallen below the rest energy of the bosons the decay processes are the most important ones. To see if they decay out of equilibrium, we introduce the quantity

$$K \equiv \left(\frac{\Gamma_D}{2H} \right)_{T=m_X} = \frac{\alpha m_{Pl}}{3.3 g_*^{1/2} m_X}.\tag{5.5}$$

Taking the limit in which the particles simply drift and eventually decay (called the **British limit**) we can easily calculate the created baryon asymmetry: The particles decay around $t \sim \Gamma_D^{-1}$ which can be transformed to the condition

$$T \sim K^{\frac{1}{2}} m_X,\tag{5.6}$$

with the help of eq.(2.35). At this time, they are overabundant by many orders of magnitude, such that we can say that all of the particles will decay. As each decay produces baryon number ε and since the abundance of heavy bosons is n_γ before they decay, the baryon asymmetry density n_B will be

$$n_B \sim \varepsilon_X n_X + \varepsilon_Y n_Y \sim (\varepsilon_X + \varepsilon_Y) n_\gamma.\tag{5.7}$$

With $s \sim g_* n_\gamma$ we can now calculate the baryon asymmetry to be

$$B \equiv \frac{n_B}{s} \sim \frac{\varepsilon}{g_*}.\tag{5.8}$$

With g_* of the order 10^2 to 10^3 we see that a small CP-violation is sufficient to account for $B \sim 10^{-11}$.

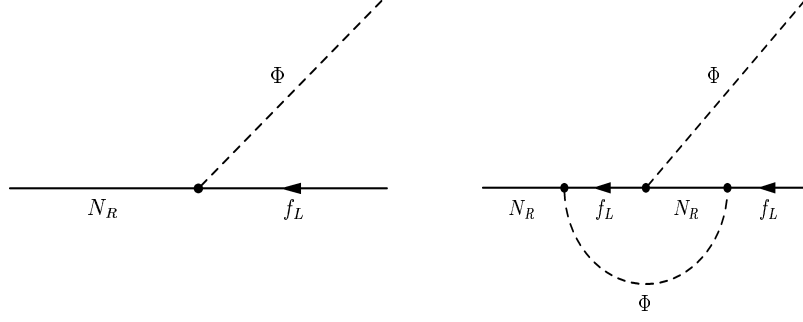


Figure 5.1: The two interfering diagrams leading to CP-violating decays of right-handed neutrinos used in the original leptogenesis paper [13]. In other leptogenesis scenarios additional diagrams were considered.

5.3 Leptogenesis

One of the most attractive baryogenesis scenarios is given by what is referred to as **leptogenesis**, which was first introduced in Reference [13]. Here, a heavy gauge singlet per generation N_R^i is added to the standard model, leading to the Lagrangian

$$\mathcal{L} = \mathcal{L}_{\text{SM}} + \bar{N}_R^i \not{\partial} N_R^i + M_i \bar{N}_R^{iC} N_R + g_{ij} \bar{N}_R^i l_L^j \Phi^\dagger + \text{h.c.}, \quad (5.9)$$

where \mathcal{L}_{SM} is the standard model Lagrangian, Φ is the standard model Higgs doublet, and l_L are the left-handed leptons. The nice feature is that these particles do not only get their motivation from leptogenesis. As we can see from the Lagrangian they also give masses to the neutrinos and can therefore be interpreted as the right-handed neutrino component. The M_i -terms imply a Majorana nature for neutrinos and yield a natural explanation for the small neutrino masses via the see-saw-mechanism in case of large M_i (e.g. [24]). Therefore these particles are not only introduced for the sake of baryogenesis, which makes this model attractive to a large fraction of the scientific community.

The Lagrangian yields the tree-level decays

$$N_R \rightarrow l_L + \bar{\Phi}, \quad (5.10a)$$

$$N_R \rightarrow \bar{l}_L + \Phi, \quad (5.10b)$$

which have different branching ratios due to interferences of diagrams like the ones shown in fig.5.1. Therefore the average decay of a right-handed neutrino produces a mean lepton number ε . Depending on the ratio K of the decay rate and the Hubble rate, the asymmetry might be partially washed out again (or even completely washed out if $K \gg 1$), and the lepton asymmetry L' is found to be

$$L' \equiv \frac{n_L - n_{\bar{L}}}{s} = \kappa' \frac{\varepsilon}{g_*}, \quad (5.11)$$

where κ' is the wash-out factor due to the processes considered so far.

Since all of this takes place at very high temperatures, the sphaleron processes are in thermal equilibrium (eq.(3.41)). Therefore a significant part of this lepton asymmetry is now converted to a baryon asymmetry, so that we finally get

$$L = \kappa \frac{\varepsilon}{g_*}, \quad (5.12)$$

$$B = -a(B - L) \simeq -aL, \quad (5.13)$$

where κ represents all wash-out effects including sphalerons and a is a constant. To give the reader a feeling for the size of a , we present its value in the model from section 5.5. There we get $a = \frac{28}{79}$ [7, 14].

To yield a baryon asymmetry of the observed order of magnitude references [8, 9] find the bounds

$$M_1 \leq 10^{10} \text{GeV and } \bar{m} \leq 0.2 \text{eV}, \quad (5.14)$$

with M_1 being the lightest Majorana mass of the right-handed neutrinos and \bar{m} being the mean of the light neutrino masses.

5.4 Neutrino genesis

The neutrino genesis scenario is a basis for this thesis and therefore we will consider it in some more detail than the other two scenarios. It was originally introduced in [11, 28].

While the leptogenesis scenario assumes neutrinos to be Majorana particles and therefore exploits the hereby following lepton-number violations, the neutrino genesis requires them to be Dirac particles and takes advantage of the small Yukawa couplings that follow from this assumption. These couplings can in fact be so small that the right-handed neutrinos (which are of course gauge singlets as in the Majorana case) will be totally decoupled from the other particles during relevant stages. Neutrino genesis uses this fact to hide an asymmetry in this sector while sphalerons are active. Hereby a baryogenesis scenario was introduced that was (B-L)-conserving at all stages, a feature not given by many theories, since sphalerons were thought to wash-out every (B+L)-asymmetry before electro-weak symmetry breaking.

To create an asymmetry in the right-handed neutrino sector, before hiding it there, two heavy scalar particles Φ, Ψ (with the same quantum numbers as the standard model Higgs doublet, but not developing a VEV) are added to the standard model Lagrangian in addition to the right-handed neutrinos ν_R . While the Majorana mass term was forbidden new Yukawa interactions were introduced:

$$\mathcal{L}'_{\text{Yuk}} = F(l_l \cdot \Phi) \nu_R^c + F'(l_l \cdot \Phi^c) e_R^c + G(l_l \cdot \Psi) \nu_R^c + G'(l_l \cdot \Psi^c) e_R^c + \text{h.c.}, \quad (5.15)$$

where F, F', G, G' are 3×3 -matrices in generation space.

These couplings lead to the decays

$$\left. \begin{array}{c} \Phi \\ \Psi \end{array} \right\} \rightarrow \left\{ \begin{array}{c} \bar{l} + \nu_R \\ l + \bar{e}_R \end{array} \right. \quad (5.16)$$

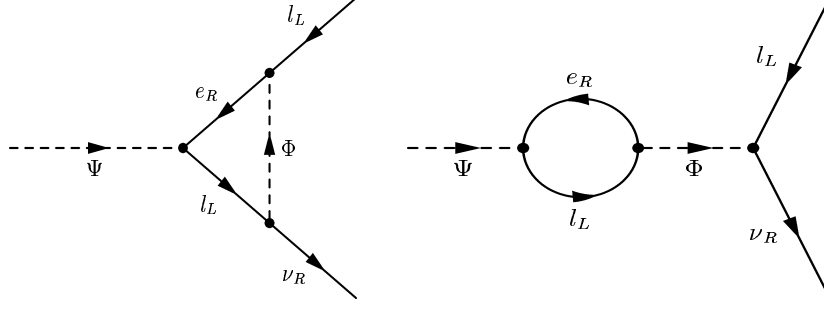


Figure 5.2: The two important one-loop diagrams that interfere with the tree-level decay diagram of Ψ . The diagrams interfering with the tree-level decay of Φ can be obtained by interchanging Φ and Ψ

and the corresponding charge conjugated processes.

Again the interference of the the tree level decay diagrams with higher order corrections, for which the most important diagrams are shown in fig.5.2, yields a CP-violating decay. The important part of the asymmetry is created in the right-handed neutrino sector and is calculated to be

$$\begin{aligned}
 \varepsilon_\Psi &= \frac{\Gamma(\Phi \rightarrow \bar{l}\nu) - \Gamma(\bar{\Phi} \rightarrow l\bar{\nu})}{\Gamma(\Phi \rightarrow l\nu) + \Gamma(\bar{\Phi} \rightarrow l\bar{\nu})} \\
 &= \frac{\text{Im} \left(\text{tr}[G^\dagger F' G'^\dagger F] \right)}{16\pi \left(\text{tr}[G^\dagger G] + \text{tr}[G'^\dagger G'] \right)} \cdot \left[1 - \frac{M_\Phi^2}{M_\Psi^2} \ln \left(1 + \frac{M_\Psi^2}{M_\Phi^2} \right) \right] \\
 &\quad - \frac{\text{Im} \left(\text{tr}[G^\dagger F] + [G' F'^\dagger] \right)}{16\pi \left(\text{tr}[G^\dagger G] + \text{tr}[G'^\dagger G'] \right)} \cdot \left[\frac{M_\Psi^2}{M_\Psi^2 - M_\Phi^2} \right],
 \end{aligned} \tag{5.17}$$

where $M_{\Psi,\Phi}$ are the masses of the scalars, and the simplifying condition $(M_\Phi - M_\Psi)^2 \gg (\Gamma_\Phi - \Gamma_\Psi)^2$ is assumed. The corresponding value for ε_Φ can be obtained when making the interchanges $\Psi \leftrightarrow \Phi$ and $G \leftrightarrow F$. We get the formula for the asymmetry Y_ν in the right-handed neutrino sector by similar argumentation to the one leading to eq.(5.8) and find

$$Y_\nu \equiv \frac{n_\nu}{s} \sim \frac{\varepsilon_\Phi + \varepsilon_\Psi}{g_*}, \tag{5.18}$$

in the case of out-of equilibrium decay. This in return is ensured by the condition

$$K_\Psi \equiv \frac{\Gamma(\Phi)}{2H(M_\Phi)} \leq 1, \tag{5.19}$$

and the same condition for K_Φ , which is analogously defined.

With the simplifying assumptions

$$\begin{aligned}
 M_\Phi &\sim M_\Psi \sim \mathcal{O}(M), \\
 \text{tr}[F^\dagger F] &\sim \text{tr}[F'^\dagger F'] \sim \text{tr}[G^\dagger G] \sim \text{tr}[G'^\dagger G'] \sim \text{tr}[G^\dagger F] \sim \text{tr}[G'^\dagger F'] \sim \mathcal{O}(\lambda^2), \\
 \text{Im} \left(\text{tr}[G^\dagger F' G'^\dagger F] \right) &\sim \mathcal{O}(\lambda^4),
 \end{aligned} \tag{5.20}$$

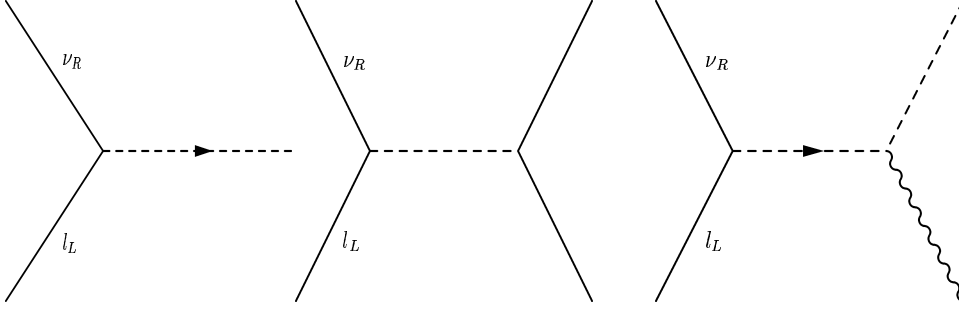


Figure 5.3: The diagrams responsible for the equilibration of the right-handed neutrinos. The dashed lines represent the standard model Higgs doublet, while solid lines represent fermions and wavy lines gauge bosons.

one obtains the conditions

$$\varepsilon \sim \frac{\lambda^2}{16\pi}, \quad \frac{\lambda^2 M_{\text{Pl}}}{g_*^{1/2} M} \lesssim 1. \quad (5.21)$$

If a lepton asymmetry is stored in the right-handed neutrino sector, sphalerons will partially transform the corresponding asymmetry in the left-handed sector into a baryon asymmetry. This can be seen in an analysis of chemical potentials, which has also been used in sections 5.3 and 6.2.1. Quantitatively one gets

$$n_B = -\frac{28}{79} n_{\nu_R}. \quad (5.22)$$

Therefore the observed baryon asymmetry can be obtained if $\lambda \sim 10^{-3}$ and $M \geq 10^{12} \text{ GeV}$.

To keep the right-handed neutrinos from equilibrating, the processes shown in fig.5.3 must be effectively inactive during the era of sphalerons activity. With all Yukawa and gauge couplings of the order one or smaller, their reaction rate at temperatures above the critical temperature T_c is estimated to be roughly

$$\Gamma \lesssim h_i^2 T, \quad (5.23)$$

with h_i being the Yukawa coupling of the neutrinos responsible for their mass m_{ν_i} and i being a generation index.

This rate has to be smaller than the Hubble rate in order to be frozen out. With the estimate $H \sim T^2/M_{\text{Pl}}$, this yields

$$h_i \leq \sqrt{\frac{T_c}{M_{\text{Pl}}}} \sim 10^{-8} \text{ or } m_{\nu_i} \sim h_i T_c \leq 1 \text{ keV} \quad (5.24)$$

A more detailed analysis using Boltzmann equations [28] even yields $m_{\nu_i} \leq 10 \text{ keV}$, which is easily fulfilled by all experimental bounds.

Therefore the smallness of the neutrino masses enables them to hide an asymmetry in their sector and keep it from being washed out by sphalerons. The principle is also illustrated in fig.5.4 .

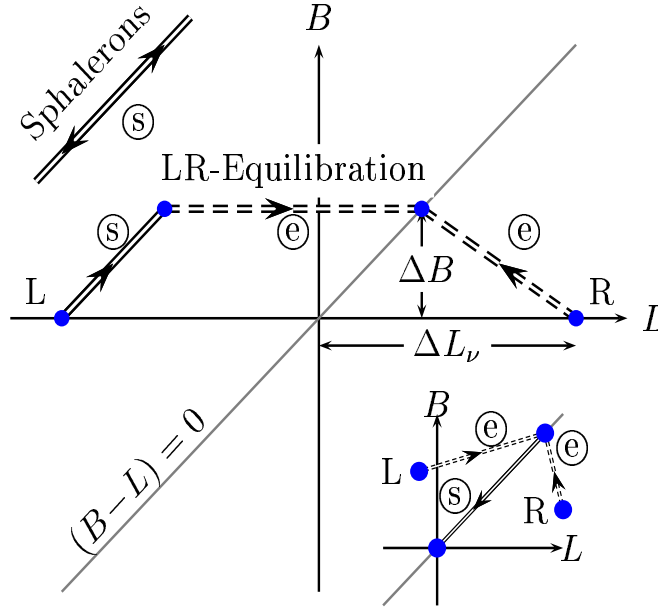


Figure 5.4: This graph illustrates the principle of neutrino genesis: An initial decay produces a positive lepton asymmetry in the right-handed neutrino-sector and a negative one in the left-handed sector, hereby conserving $(B-L)$. The asymmetry in the right-handed sector remains uncoupled, while sphalerons partially transform the negative lepton asymmetry into a positive baryon asymmetry. After electro-weak symmetry has been broken and sphaleron activities stopped, left-right equilibration can take place, yielding positive baryon and lepton asymmetries. The little picture illustrates the simple washout of a $(B+L)$ -asymmetry that cannot partially be hidden. [11]

5.5 Interplay of Quintessence and Baryogenesis

Before presenting the model developed for this thesis, we want to take a look at an example for an interplay of quintessence and baryogenesis. The information within this section is mainly drawn from [7] and its references.

Even though leptogenesis is an attractive option for the creation of a baryon asymmetry in the early universe there are still some subtle points worth mentioning in this context.

If the universe went through a time of inflation, which would be an explanation for the estimated age, flatness, isotropy and homogeneity of our universe, and a hereby followed period of reheating, a reheating temperature of the order of magnitude of the right-handed neutrinos would be needed to populate these states, whose decay yields the lepton asymmetry. As we already saw in section 5.3 the mass of these particles has to be at least 10^{10}GeV , which hereby sets the scale for the reheating temperature T_R . Unfortunately, this provides a problem in super-symmetric theories, since the (non-)abundance of gravitinos yields the bound $T_R \leq 10^8 \text{ to } 10^{10}\text{GeV}$. As we can see, these bounds are only marginally compatible. Also, the possibility of degenerate small neutrino masses is strongly disfavored in the regular leptogenesis scenario, while there are cosmological studies that prefer degenerate neutrinos with masses of 0.2eV .

Before explaining the mechanism used in reference [7] to solve these problems, let us look at leptogenesis more quantitatively than we did before. In the case of minimal thermal leptogenesis and a hierarchical neutrino spectrum ($m_3 \approx \sqrt{\Delta m_{\text{atm}}^2} \approx 0.05\text{eV} \gg \sqrt{\Delta m_{\text{sol}}^2} \approx 0.008\text{eV} \gg m_1$), an upper bound for the maximal CP-asymmetry ε is given by

$$|\varepsilon| \lesssim \frac{3}{8\pi} \frac{M_1 \sqrt{\Delta m_{\text{atm}}^2}}{v^2}, \quad (5.25)$$

where Δm_{atm}^2 is the atmospheric mass difference and $v = 246\text{GeV}$ the VEV of the standard model Higgs doublet.

In the case of degenerate neutrinos ($m_1 \approx m_2 \approx m_3 \approx \bar{m}/\sqrt{3} \gg \sqrt{\Delta m_{\text{atm}}^2}$) we find

$$|\varepsilon| \lesssim \frac{3\sqrt{3}}{8\pi} \frac{M_1 \sqrt{\Delta m_{\text{atm}}^2}}{v^2 \bar{m}}, \quad (5.26)$$

with \bar{m} being the quadratic mean of the light neutrino masses.

The final baryon asymmetry can then be calculated with the help of two coupled Boltzmann equations, yielding a result that only depends on four input parameters: The mass of the lightest right-handed neutrino M_1 , the effective light neutrino mass \tilde{m} , the quadratic mean of the light neutrino masses \bar{m} , and the maximal CP asymmetry ε given by eqs.(5.25) and (5.26). The important information is that the wash-out of the asymmetry suppresses the resulting asymmetry exponentially, as soon as $M_1 \bar{m}^2$ becomes sizeable. Therefore the bounds on the masses in minimal thermal leptogenesis are mainly due to the fact that we need a large enough CP-asymmetry ($\Rightarrow M \gtrsim 10^{10}\text{GeV}$) and a small washout ($\Rightarrow \bar{m} \lesssim 0.2\text{eV}$), which are exactly the bounds leading to the problems that were mentioned above. One can also see that the degenerate

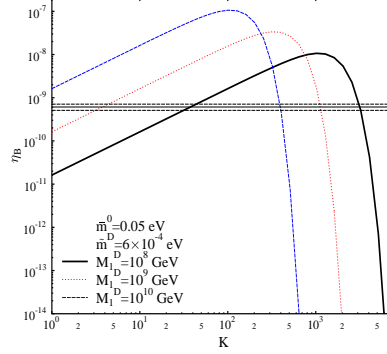


Figure 5.5: This graph shows the dependence of the final baryon asymmetry η_B on the parameter K as specified in the text. M_1^D has been fixed at several values, while \bar{m}^0 was assigned to be 0.05eV, and the effective neutrino mass \bar{m} has been fixed at 6×10^{-4} eV. The three horizontal lines form the boundary of the observed value of η_B . [7]

neutrino case is disfavored, since the corresponding ε is much smaller than the one in the hierarchical case.

The method used in reference [7] to soften these bounds is to make the heavy mass parameter of the right-handed neutrinos dependent on a quintessence field Q , such that it will have two different values at the time of their decay and today:

$$M_1^0 = M_1^D \cdot K(Q^D), \quad (5.27)$$

where $K(Q)$ is some function of Q to be specified later.

This variation of M_1 also leads to a dependence of \bar{m} on Q due to the see-saw mechanism:

$$\bar{m} \propto \frac{1}{M_1} \implies \bar{m} \rightarrow \bar{m} \cdot K(Q) \quad (5.28)$$

Since Δm_{atm}^2 also varies the way \bar{m} does, we get the following implications:

- In the hierarchical case, we can now fix M_1^D at a value below 10^{10} GeV and still get a large enough ε , since this is now proportional to $K(Q)$:

$$|\varepsilon| \lesssim \frac{3}{8\pi} \frac{M_1^D \sqrt{\Delta m_{\text{atm}}^2}}{v^2} \cdot K(Q^D) \quad (5.29)$$

Therefore the needed reheating temperature can be several orders of magnitude smaller as in the uncoupled model. A graph showing the final matter-antimatter asymmetry in dependence of K with M_1^D fixed at several values can be found in fig.5.5 .

- In the degenerate case a fixed M_1^D leads to a dependence $\varepsilon \propto K(Q)^{-1}$. Therefore K needs to be smaller during the era of decay. A graph similar to the one in the hierarchical case is shown in fig.5.6 . We see that now the Mass M_1^D has to be much higher than in the hierachical case,

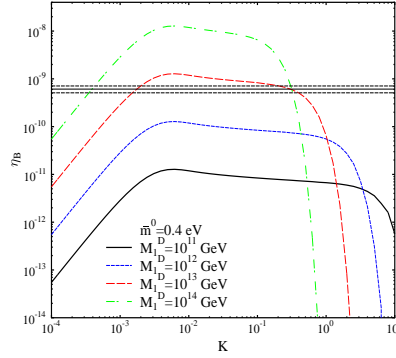


Figure 5.6: The final baryon asymmetry in the case of degenerate neutrinos and in dependence of the parameter K for different parameter values. [7]

which leads to the fact that we are still left with the mentioned gravitino problem. On the other hand, without varying masses a baryon asymmetry of the required magnitude could not be achieved at all with the chosen parameters, and hence some progress still is still achieved.

What is left to show is that such a coupling is actually possible and that the coupling does not disturb the behaviour of the quintessence field. In this model a quintessence potential of the form

$$V(Q) \equiv V_0(e^{\lambda Q} + e^{-\lambda Q}) \quad (5.30)$$

was chosen (compare section 4.3.3), with $\lambda = 100M_{\text{Pl}}^{-1}$ and the initial conditions $Q_i = 1.374M_{\text{Pl}}$ and $\omega_i = 0$.

The ratio $K(Q)$ is given by

$$K(Q) \equiv \exp\left(\beta \frac{Q}{M_{\text{Pl}}}\right). \quad (5.31)$$

Also, an additional effective quintessence potential $V_I(Q)$ is given by the mass couplings $M_i(Q)$

$$V_I(Q) \equiv \sum_i \int \frac{d^3k}{(2\pi)^3} \sqrt{k^2 + M_i^2(Q)} f_i(k), \quad (5.32)$$

where the index i runs over the three different reight-handed neutrinos and $f_i(k)$ is the corresponding distribution function.

In the case of a Maxwell-Boltzmann distribution this expression yields (see eq.(2.26))

$$\begin{aligned} V_I(Q) &= \sum_i n_i \langle E \rangle \\ &= \frac{1}{\pi^2} \sum_{i=1}^3 3M_i^2(Q) T^2 K_2\left(\frac{M_i(Q)}{T}\right) + M_i^3(Q) T K_1\left(\frac{M_i(Q)}{T}\right). \end{aligned} \quad (5.33)$$

Now the authors let the numerics for the quintessence field run with the modified potential and find that it does not change its behaviour (to a significant degree), hereby supposedly justifying their model. Yet, this method has some subtleties, and we will get a little more into this when treating the effective quintessence potential in the model developed in context with this thesis.

For the moment, we just want to point out that quintessence dependent couplings of what would otherwise be constants of our theory, can be able to solve problems in baryogenesis. This due to the fact that bounds on several parameters given by recent measurements have not necessarily been valid at early stages when baryogenesis takes place in most models.

Chapter 6

Quintessence Driven Neutrinoogenesis

A less attractive feature of the original neutrinoogenesis model was the postulation of two additional scalar bosons, that only suited the purpose of igniting the baryogenesis process. Therefore one could make the neutrinoogenesis process more appealing, if one succeeds in embedding it into a theory that naturally yields particles with the necessary features. The most important of these features might be the complex couplings to different sectors of the particle spectrum, which is necessary to yield CP-violating decays, combined with the effective decoupling of these decay channels during relevant stages.

On the other hand, it is desirable not to give up the attractive features that are already present in the original scenario. One of them is the fact that it yields a possible baryogenesis process in a (B-L)-conserving theory. This characteristic, which we consider a key difference to the leptogenesis scenario, shall not be given up. In the remaining parts of this section, we will show how this and some other reasonable assumptions about our model will greatly reduce the class of candidates for initially decaying particles. Therefore, we will subsequently look at the different types of particles:

- **Fermions:**

In opposition to the original leptogenesis scenario, it seems unlikely that fermions can also play the role of the initially decaying particles in a neutrinoogenesis scenario which is embedded into an appealing extension of the standard model.

In the (B-L)-conserving case, left-right symmetric models, Pati-Salam-, $SU(5)$ -, and $SO(10)$ -models will usually just contain the standard model fermions and right-handed neutrinos. Since Majorana mass terms are forbidden, none of them is likely to decay out of equilibrium before electroweak symmetry breaking. Thus the possibly created asymmetry cannot be transformed by sphalerons, which rules them out as suitable candidates.

Models basing on the gauge group E_6 , contain additional fermions. However, if these fermions have masses of the order of the GUT breaking scale, their decay will most likely take place before the breaking of $SU(2)_R$,

which is a subgroup of E_6 . In this case any (B-L)-conserving asymmetry should be washed out by left- and(!) right-handed sphalerons.

All these arguments indicate (though not prove) that fermions might not be suitable candidates for starting a neutrino genesis scenario. Hence, we will not consider them for this role in the rest of this thesis.

- **Gauge Bosons:**

Gauge bosons also do not seem to be suitable candidates, since all of the coupling constants connected to them are real, and therefore it is unlikely that a suitable CP-violation will occur.

- **Higgs Bosons:**

After excluding fermions and vector bosons we are back with scalar bosons, also used in the original neutrino genesis toy model. Since we do not want to introduce new scalars for the sake of neutrino genesis, we have to take a look at the scalar bosons already present. We can either consider Higgs bosons that were introduced to break a gauge symmetry and do not couple to fermions as the initially decaying particles or we can consider Higgs particles that yield masses for fermions at lower temperatures in addition to breaking a symmetry.

In the first case complex and therefore CP-violating couplings connected to these bosons could only occur in the Higgs sector itself. This case would, however, most likely only lead to possible asymmetries in this sector, as it might be hardly possible to transfer this asymmetry to the fermion sector, since each scalar that couples to fermions will create a particle and an antiparticle. It is also not easy to imagine a transfer of this asymmetry via the gauge sector.

Therefore the only candidates left are mass generating scalar bosons.

Even though these arguments seem to quailfy mass generating Higgs scalars as the most promising candidates for starting a neutrino genesis processes by their decay, this scenario will also yield serious problems, as we will see in the course of this thesis. However, since we will be able to solve these problems with some additional assumptions, we first want to introduce a model, which was constructed in the course of this thesis, and which includes two different Higgs representations for generation of the fermion mass spectrum. Hereby the ad-hoc introduction of new particles in the original neutrino genesis scenario becomes obsolete.

6.1 The Model

6.1.1 Gauge Groups and Representations

In this section the model with which we will be working with in the remaining parts of this thesis is presented. As its gauge group we choose

$$SU(2)_L \otimes SU(2)_R \otimes SU(4)_{PS} \otimes D, \quad (6.1)$$

where D stands for the discrete D-Parity representing the interchange between R and L .¹ This gauge group is also called the **Pati-Salam** gauge group [26]. It will be successively broken down, hereby following the pattern

$$\begin{aligned} &\longrightarrow SU(2)_L \otimes SU(2)_R \otimes U(1)_{B-L} \otimes SU(3)_C \otimes D \\ &\longrightarrow SU(2)_L \otimes U(1)_Y \otimes SU(3)_C \\ &\longrightarrow U(1)_Q \otimes SU(3)_C. \end{aligned}$$

The fermion sector consists of two multiplets per generation. The left-handed fermions are the constituents of the representation $f_L = (2, 1, 4)$ and the right-handed fermions are represented by the $f_R = (1, 2, 4)$.² These two representations interchange under D . To make things more illustrative and in order to see which component of f corresponds to which standard model particle, we write

$$f_{L/R} = \begin{pmatrix} \begin{pmatrix} \nu_e \\ e^- \end{pmatrix} \\ \begin{pmatrix} u^r \\ d^r \end{pmatrix} \\ \begin{pmatrix} u^g \\ d^g \end{pmatrix} \\ \begin{pmatrix} u^b \\ d^b \end{pmatrix} \end{pmatrix}_{L/R} \quad (6.2)$$

for the first generation and the generalization to the other two generations should be clear.

It is now easy to illustrate the action of the different gauge group generators on f_L and f_R : The specific $SU(2)$ generators act on all the small brackets simultaneously, whereas the $SU(4)$ generators interchange the small brackets, but do not change their inner ($SU(2)$ -)structure. The generators for the two $SU(2)$ groups are given by the well-known pauli-matrices $\tau^i/2$ and the generators of the fundamental group of $SU(4)$ used in this model are given in appendix A and are referred to by T_{PS}^i , where i runs from 1 to 15.

The Higgs sector has to provide us with particle representations that either break down the gauge groups, following the pattern given in this section, or that generate fermion masses, with parts of them starting the baryogenesis process as discussed in the previous section.

For the first symmetry breaking we will use a scalar boson which we will call Ξ_{PS} and which transforms as $(1, 1, 15)$. The component Ξ_{PS}^1 has to develop a VEV to yield the achieved breaking pattern. After calculating the adjoint representation, one finds that this VEV leaves the generators T_{PS}^1 to T_{PS}^3 and T_{PS}^{10} to T_{PS}^{15} unbroken, whereas it breaks all the other generators of $SU(4)_{PS}$. In regular scenarios this VEV is usually chosen to be of the order 10^{14} to 10^{16}

¹This symmetry also ensures that the coupling constants of $SU(2)_L$ and $SU(2)_R$ are equal in the unbroken state, therefore leaving us with only 2 different coupling constants: $g_L = g_R \equiv g$ and g_{PS} .

²These two representations could easily result from a (16) of $SO(10)$, which breaks down to $(2, 1, 4) + (1, 2, \bar{4})$, therefore evening the way towards a grand unifying theory.

GeV or a little lower.³ After the breaking T_{PS}^1 represents $U(1)_{(B-L)}$ (up to some constant factor), whereas the other unbroken generators of $SU(4)_{PS}$ form $SU(3)_C$.

For the breaking of $SU(2)_R$ and D , we will employ the two representations $\Xi_R = (1, 2, 4)$ and $\Xi_L = (2, 1, 4)$, which interchange under D , but where only Ξ_R will develop a VEV, which will be in the $\Xi_{R,1}^1$ component.⁴ It is not hard to see that this VEV is left invariant by $Y \equiv I_{R,3} + (B - L)$, with $I_{R,3}$ being the third component of the right-handed isospin, as well as by $SU(3)_C$ specified above. Left-right symmetry breaking scales are usually of the order of 10^{12} GeV or less.

Finally, since all the particles of one generation are combined in only two representations, we need two different Higgs representations to generate their various masses. At least one of the VEVs needs to couple differently to leptons and quarks. This will become clearer, when we explicitly calculate the fermion masses in section 6.1.3. We choose $\Psi = (2, 2, 1)$ and $\Phi = (2, 2, 15)$ with the VEVs at Ψ_{11} and Φ_{11}^1 , respectively. This leaves us with the unbroken groups are $SU(3)_C$ and $U(1)_Q$ with $Q \equiv I_{L,3} + I_{R,3} + (B - L)$.

6.1.2 Gauge Boson Masses

Having specified the gauge group and the various particle representations, we now want to calculate their masses in dependence of the various parameters of our theory. The gauge-boson masses are generated by the kinetic terms of the Higgs-fields in the Lagrangian:

$$\begin{aligned} \mathcal{L}_{\text{Higgs, kin}} = & (D_\mu \Xi_{PS})^\dagger (D^\mu \Xi_{PS}) + (D_\mu \Xi_R)^\dagger (D^\mu \Xi_R) + (D_\mu \Xi_L)^\dagger (D^\mu \Xi_L) \\ & + (D_\mu \Phi)^\dagger (D^\mu \Phi) + (D_\mu \Psi)^\dagger (D^\mu \Psi) \end{aligned} \quad (6.3)$$

By inserting the VEVs and writing down all terms that include two gauge-boson fields (or one gauge-boson field twice), we get the mass matrices for all gauge bosons. We will do this explicitly for Φ , and just present the final terms stemming from the other fields:

The covariant derivative of Φ is

$$D_\mu \Phi = (\partial_\mu - \underbrace{igW_{L,\mu}^a \frac{\tau_L^a}{2}}_{\equiv \alpha} - \underbrace{igW_{R,\mu}^a \frac{\tau_R^a}{2}}_{\equiv \beta} - \underbrace{ig_{PS}W_{PS,\mu}^a T^a}_{\equiv \gamma}) \Phi, \quad (6.4)$$

which leads to the terms

$$\langle \alpha \rangle = \langle igW_{L,\mu}^a \frac{\tau_L^a}{2} \Phi \rangle = i\frac{g}{2} \begin{pmatrix} \langle \Phi \rangle W_{L,\mu}^3 & 0 \\ \sqrt{2} \langle \Phi \rangle W_{L,\mu}^- & 0 \end{pmatrix} \otimes \begin{pmatrix} 1 \\ 0 \\ 0 \\ \vdots \end{pmatrix}, \quad (6.5)$$

³In contrast to the breaking of left-right symmetry, the exact value of this symmetry breaking temperature cannot be chosen arbitrarily, since it includes a unification of constants.

⁴Upper indices always refer to $SU(4)_{PS}$, whereas the lower indices refer to the two $SU(2)$ gauge groups. If not specified it should be clear, which of the two is meant in each case. If there are two indices the first one refers to $SU(2)_L$.

with $W_L^\pm = \frac{W_L^1 \mp i W_L^2}{\sqrt{2}}$,

$$\langle \beta \rangle = \langle i g W_{R,\mu}^a \frac{\tau_R^a}{2} \Phi \rangle = i \frac{g}{2} \begin{pmatrix} -\langle \Phi \rangle W_{R,\mu}^3 & -\sqrt{2} \langle \Phi \rangle W_{R,\mu}^+ \\ 0 & 0 \end{pmatrix} \otimes \begin{pmatrix} 1 \\ 0 \\ 0 \\ \vdots \end{pmatrix}, \quad (6.6)$$

with W_R^\pm defined analogously to W_L^\pm , and

$$\langle \gamma \rangle = \langle i g_{PS} W_{PS}^a T_{adj}^a \Phi \rangle = \sqrt{\frac{2}{3}} g_{PS} \langle \Phi \rangle \begin{pmatrix} 1 & 0 \\ 0 & 0 \end{pmatrix} \otimes \begin{pmatrix} 0 \\ 0 \\ 0 \\ W^5 \\ -W^4 \\ W^7 \\ -W^6 \\ W^9 \\ -W^8 \\ 0 \\ 0 \\ 0 \\ 0 \\ 0 \\ 0 \\ 0 \end{pmatrix}. \quad (6.7)$$

With respect to 6.3 the following terms will contribute to the gauge boson masses:

$$\alpha^\dagger \alpha + \alpha^\dagger \beta + \alpha^\dagger \gamma + \beta^\dagger \alpha + \beta^\dagger \beta + \beta^\dagger \gamma + \gamma^\dagger \gamma + \gamma^\dagger \beta$$

Hence, plugging in the obtained results we find the terms

$$\begin{aligned} & \frac{g^2}{4} |\langle \Phi \rangle|^2 (|W_L^3|^2 + 2|W_L^+|^2) - \frac{g^2}{2} |\langle \Phi \rangle|^2 W_L^3 W_R^3 + \frac{g^2}{4} |\langle \Phi \rangle|^2 (|W_R^3|^2 + 2|W_R^+|^2) \\ & + \frac{4}{3} g_{PS}^2 |\langle \Phi \rangle|^2 (|W_{PS}^{1,-}|^2 + |W_{PS}^{2,-}|^2 + |W_{PS}^{3,-}|^2), \end{aligned} \quad (6.8)$$

where $W_{PS}^{1,\pm\frac{4}{3}} \equiv \frac{W_{PS}^4 \mp i W_{PS}^5}{\sqrt{2}}$, $W_{PS}^{2,\pm\frac{4}{3}} \equiv \frac{W_{PS}^6 \mp i W_{PS}^7}{\sqrt{2}}$, $W_{PS}^{3,\pm\frac{4}{3}} \equiv \frac{W_{PS}^8 \mp i W_{PS}^9}{\sqrt{2}}$.

Doing similar calculations for the other fields, we end up with the following masses and mass matrices for the gauge bosons.

Charged Sector

In the charged sector we do not get any mixing terms with the VEVs specified earlier. Therefore the results are particularly simple and we get

- two singly charged left-handed bosons W_L^\pm with mass $\frac{g^2}{2} (|\langle \Phi \rangle|^2 + |\langle \Psi \rangle|^2)$,
- two singly charged right-handed bosons W_R^\pm with mass $\frac{g^2}{2} (|\langle \Phi \rangle|^2 + |\langle \Psi \rangle|^2 + |\langle \Xi_R \rangle|^2)$,
- six bosons $W_{PS}^{1,\pm\frac{4}{3}}$, $W_{PS}^{2,\pm\frac{4}{3}}$, $W_{PS}^{3,\pm\frac{4}{3}}$ with charges $\pm\frac{4}{3}$ and mass $g_{PS}^2 (\frac{4}{3} |\langle \Phi \rangle|^2 + \frac{4}{3} |\langle \Psi \rangle|^2 + \frac{1}{2} |\langle \Xi_R \rangle|^2)$.

Neutral Sector

Since $SU(3)_C$ has not been broken, our theory still contains eight massless gluons, which are in this case denoted by W_{PS}^2 , W_{PS}^3 , W_{PS}^{10} , W_{PS}^{11} , W_{PS}^{12} , W_{PS}^{13} , W_{PS}^{14} , and W_{PS}^{15} .

The other three neutral particles W_L^3 , W_R^3 , and W_{PS}^1 are no mass eigenstates. Instead we find the following mass matrix:

	W_L^3	W_R^3	W_{PS}^1
W_L^3	$\frac{g^2}{2}(\langle\Phi\rangle ^2 + \langle\Psi\rangle ^2)$	$-\frac{g^2}{2}(\langle\Phi\rangle ^2 + \langle\Psi\rangle ^2)$	0
W_R^3	$-\frac{g^2}{2}(\langle\Phi\rangle ^2 + \langle\Psi\rangle ^2)$	$\frac{g^2}{2}(\langle\Phi\rangle ^2 + \langle\Psi\rangle ^2 + \langle\Xi_R\rangle ^2)$	$-\sqrt{\frac{3}{8}}gg_{PS} \langle\Xi_R\rangle ^2$
W_{PS}^1	0	$-\sqrt{\frac{3}{8}}gg_{PS} \langle\Xi_R\rangle ^2$	$\frac{3g_{PS}^2}{4} \langle\Xi_R\rangle ^2$

For further treatment it is convenient to define e and θ_W by ⁵

$$\sin \theta_W = \frac{e}{g} \quad \text{and} \quad \sqrt{\cos(2\theta_W)} = \sqrt{\frac{2}{3}} \frac{e}{g_{PS}}, \quad (6.9)$$

and to work in the basis

$$\begin{aligned} A &\equiv \sin \theta_W (W_L^3 + W_R^3) + \sqrt{\cos(2\theta_W)} W_{PS}^1 \\ Z &\equiv \cos \theta_W W_L^3 - \sin \theta_W \tan \theta_W W_R^3 - \tan \theta_W \sqrt{\cos(2\theta_W)} W_{PS}^1 \\ Z' &\equiv \frac{\sqrt{\cos(2\theta_W)}}{\cos \theta_W} W_R^3 - \tan \theta_W W_{PS}^1, \end{aligned} \quad (6.10)$$

where A is the eigenvector of the neutral mass matrix with eigenvalue zero and therefore represents the photon. The other two states are only approximately eigenvectors of the mass matrix (small mixing angle) but were defined to give the neutral current interaction within the Lagrangian the form

$$\mathcal{L}_{nc} = eJ_{em}^\mu A_\mu + \frac{g}{\cos \theta_W} \left[K_L^\mu Z_\mu + \frac{1}{\sqrt{\cos(2\theta_W)}} (\sin^2 \theta_W K_L^\mu + \cos^2 \theta_W K_R^\mu) Z'_\mu \right], \quad (6.11)$$

which is similar to the SM interaction

$$\mathcal{L}_{nc} = eJ_{em}^\mu A_\mu + \frac{g}{\cos \theta_W} K_L^\mu Z_\mu,$$

and where in both cases $K_{L/R}^\mu \equiv \sum_f \bar{f} \gamma^\mu [I_{L/R,3} P_{L/R} - Q \sin^2 \theta_W] f$ and $J_{em}^\mu \equiv \sum_f \bar{f} \gamma^\mu Q f$, with the latter one being the electromagnetic current.

The modification of \mathcal{L}_{nc} will yield constraints for the additional gauge bosons and hereby for the breaking scales of some of our gauge symmetries; but before we take a brief look at them we return to the neutral mass-mixing matrix.

⁵The following paragraphs are very similar to a treatment of left-right symmetric models in reference [24]

After the basis transformation to (6.10) we get the new mass-mixing

	Z	Z'
Z	$\frac{g^2}{2} \frac{(\langle\Phi\rangle ^2 + \langle\Psi\rangle ^2)}{\cos^2 \theta_W}$	$\frac{-g^2}{2} \frac{\sqrt{\cos(2\theta_W)}}{\cos^2 \theta_W} (\langle\Phi\rangle ^2 + \langle\Psi\rangle ^2)$
Z'	$\frac{-g^2}{2} \frac{\sqrt{\cos(2\theta_W)}}{\cos^2 \theta_W} (\langle\Phi\rangle ^2 + \langle\Psi\rangle ^2)$	$\frac{g^2}{2} \left[\frac{\cos(2\theta_W)}{\cos^2 \theta_W} (\langle\Phi\rangle ^2 + \langle\Psi\rangle ^2) + \frac{\cos^2 \theta_W}{\cos(2\theta_W)} \langle\Xi_R\rangle ^2 \right]$

So, for $|\langle\Xi_R\rangle|^2 \gg |\langle\Phi\rangle|^2 + |\langle\Psi\rangle|^2$, we get the mass eigenstates

$$\begin{aligned} Z_1 &\equiv Z \cos \xi + Z' \sin \xi \\ Z_2 &\equiv -Z \sin \xi + Z' \cos \xi \end{aligned} \quad (6.12)$$

with

$$|\tan(2\xi)| \approx 2 \frac{\cos^{\frac{3}{2}}(2\theta_W)}{\cos^4 \theta_W} \frac{|\langle\Phi\rangle|^2 + |\langle\Psi\rangle|^2}{|\langle\Xi_R\rangle|^2} \quad (6.13)$$

and the eigenvalues

$$\begin{aligned} M_Z^2 &\approx M_{Z_1}^2 \approx \frac{g^2}{2 \cos^2 \theta_W} (|\langle\Phi\rangle|^2 + |\langle\Psi\rangle|^2) \\ M_{Z'}^2 &\approx M_{Z_2}^2 \approx \frac{g^2}{2} \frac{\cos^2 \theta_W}{\cos(2\theta_W)} |\langle\Xi_R\rangle|^2 \end{aligned} \quad (6.14)$$

It is therefore clear that the values of our model in the gauge sector easily go together with all results from the experiments done so far, if we choose the VEVs of Ξ_{PS} and Ξ_R high enough. [24] postulates for L-R-symmetry breaking values in the TeV range. Since we will need the breaking of $SU(4)_{PS}$ to take place at temperatures higher than 10^{15}GeV and the breaking of $SU(2)_R$ not much below (if at all), constraints coming from the results in this section should be obeyed easily. ⁶

6.1.3 Fermion Masses

For the moment, we will restrict our equations to one generation of particles. In this case mass terms in our model will have to be of the form

$$m_{ij} \bar{f}_{R,i} f_{L,j} + \text{h.c.} \quad .$$

Since direct mass terms are forbidden by gauge invariance, we need to generate the masses via the Higgs mechanism. For the cartesian product of the 4 and the $\bar{4}$ of $SU(4)$ we get [32]:

$$\bar{4} \otimes 4 = 1 \oplus 15$$

Therefore the two obvious choices for fermion mass generating Higgs representations are $(2, 2, 1)$ and $(2, 2, 15)$, which we called Ψ and Φ , respectively. ⁷ The

⁶With the time-variation of constants, which is introduced later, these bounds could of course be weakened again.

⁷To be more exact one should either write $(2, \bar{2}, 1)$ and $(2, \bar{2}, 15)$ or include several σ_2 -matrices in the Yukawa couplings. But as 2 and $\bar{2}$ are isomorphic in $SU(2)$ people tend to omit the bar as well as the σ_2 -matrices, which we will also do in this thesis.

resulting Yukawa terms are therefore

$$\begin{aligned} \mathcal{L}_{\text{Yuk}} = & g_{\Psi} \bar{f}_{R,i} \Psi_{ij} f_{L,j} + g_{\tilde{\Psi}} \bar{f}_{R,i} \tilde{\Psi}_{ij} f_{L,j} \\ & + g_{\Phi} \bar{f}_{R,i} T_{PS}^a \Phi_{ij}^a f_{L,j} + g_{\tilde{\Phi}} \bar{f}_{R,i} T_{PS}^a \tilde{\Phi}_{ij}^a f_{L,j} + \text{h.c.}, \end{aligned} \quad (6.15)$$

where $\tilde{\Psi} \equiv \sigma_2 \Psi \sigma_2$ and $\tilde{\Phi}^a \equiv \sigma_2 \Phi^a \sigma_2$ are the charge conjugates of the original scalar particles.

By letting the Higgs bosons develop the VEVs specified before, we get find

$$\begin{aligned} \langle \mathcal{L}_{\text{Yuk}} \rangle = & g_{\Psi} |\langle \Psi \rangle| (|\nu_e|^2 + |u^r|^2 + |u^g|^2 + |u^b|^2) \\ & + g_{\tilde{\Psi}} |\langle \Psi \rangle| (|e^-|^2 + |d^r|^2 + |d^g|^2 + |d^b|^2) \\ & + g_{\Phi} \sqrt{\frac{3}{8}} |\langle \Phi \rangle| (-|\nu_e|^2 + \frac{1}{3}|u^r|^2 + \frac{1}{3}|u^g|^2 + \frac{1}{3}|u^b|^2) \\ & + g_{\tilde{\Phi}} \sqrt{\frac{3}{8}} |\langle \Phi \rangle| (-|e^-|^2 + \frac{1}{3}|d^r|^2 + \frac{1}{3}|d^g|^2 + \frac{1}{3}|d^b|^2) + \text{h.c.} \end{aligned} \quad (6.16)$$

Here one can see why two different Higgs representations are necessary: We now have four different variables to yield four different masses. If only one of these representations, or two identical ones, were used the ratio of the two quarks would be connected to the ratio of the two leptons. So if we do not want to rely on radiative corrections to achieve different fermion masses, we need to introduce two mass generating Higgs representations in this model to meet the experimental data. Since these particles are the ones that are also supposed to start neutrinogenesis, the ad-hoc introduction of new particles for this purpose has disappeared.

6.1.4 Yukawa Couplings

In order to get a feeling for the orders of magnitude of the different Yukawa couplings in this model, we will plug in numbers that will return the measured values for the fermion masses. It is emphasized that the chosen parameters are not necessarily the ones that have to be measured in order to confirm this model, but are rather some more or less natural choices giving us what we need in order to go on with our calculation.

With this in mind, we fix the values for $|\langle \Psi \rangle|$ and $|\langle \Phi \rangle|$ to be of the same size, which seems to be a rather natural choice. From section 6.1.2 we know that the sum of their squares is connected to the light gauge boson masses. This leaves us with

$$|\langle \Psi \rangle| = |\langle \Phi \rangle| \approx \frac{246 \text{ GeV}}{\sqrt{2}}. \quad (6.17)$$

Plugging in values for the various fermion masses and their mixings, eq.(6.16) now yields a system of linear equations from which the various Yukawa couplings can be determined. However, doing this without any treatment of the data would lead to a real system of equations with real Yukawa couplings as solutions. This would lead to CP-conserving decays and baryogenesis could not take place. Therefore we make the additional assumption that the lepton masses have relative phase compared to the quark masses. This assumption leads to complex Yukawa couplings. And even though the imaginary mass of

the leptons can be made real, by a specific tranformation, the Yukawa couplings will keep relative phases, which is crucial for CP-violating decays, as we will see later.⁸ All of this finally leads to

$$\begin{aligned}
g_\Psi &\approx \begin{pmatrix} 0.000012931+i1.49555\cdot 10^{-13} & 0.+i1.41379\cdot 10^{-13} & 0.+i8.97701\cdot 10^{-14} \\ 0.+i1.41379\cdot 10^{-13} & 0.00431034+i1.55089\cdot 10^{-13} & 0.+i1.32411\cdot 10^{-13} \\ 0.+i8.97701\cdot 10^{-14} & 0.+i1.32411\cdot 10^{-13} & 0.775862+i1.59342\cdot 10^{-13} \end{pmatrix}, \\
g_{\tilde{\Psi}} &\approx \begin{pmatrix} 0.000049233+i7.34195\cdot 10^{-7} & 0.0000997324-i9.66723\cdot 10^{-7} & 0.0000684053-i0.00002755 \\ 0.0000997324+i9.66723\cdot 10^{-7} & 0.00043173+i0.000152299 & 0.000633093+i1.02064\cdot 10^{-8} \\ 0.0000684053+i0.00002755 & 0.000633093-i1.02064\cdot 10^{-8} & 0.0176412+i0.00255316 \end{pmatrix}, \\
g_\Phi &\approx \begin{pmatrix} 0.0000211163-i7.32665\cdot 10^{-13} & -i6.92614\cdot 10^{-13} & -i4.39782\cdot 10^{-13} \\ -i6.92614\cdot 10^{-13} & 0.00703876-i7.59778\cdot 10^{-13} & i6.48678\cdot 10^{-13} \\ -i4.39782\cdot 10^{-13} & i6.48678\cdot 10^{-13} & 1.26698-i7.80613\cdot 10^{-13} \end{pmatrix}, \\
g_{\tilde{\Phi}} &\approx \begin{pmatrix} 0.0000803971-i3.59681\cdot 10^{-6} & 0.000162862-i1.57865\cdot 10^{-6} & 0.000111705-i0.0000449889 \\ 0.000162862+i1.57865\cdot 10^{-6} & 0.000705012-i0.000746109 & 0.00103384+i1.6667\cdot 10^{-8} \\ 0.000111705+i0.0000449889 & 0.00103384-i1.6667\cdot 10^{-8} & 0.0288079-i0.0125079 \end{pmatrix},
\end{aligned} \tag{6.18}$$

where the approximated values for femion masses and mixings are given in B for reasons of reproduction.⁹

Of course, one has to admit that the neutrino masses in this model arise from some fine tuning, since the same Yukawa couplings that give rise to the top-quark mass, when being added with some positive pre-factors, are also responsible for parts of the neutrino mass matrix, when being subtracted from each other. However, even though this is a rather unattractive feature, it does not affect the possible validity of this model.

6.2 Neutrino genesis, first try

Now that we have specified the model and its parameters, we want to see if it can provide us with a baryogenesis scenario. As mentioned before, we will run into several severe problems on our way, but we will find a way to handle the occuring problems in the latter parts of this thesis and the original results will still be needed. Therefore, we will still do the calculations in detail.

Taking a look at eq.(6.18), we already see a huge difference to the original scenario: The original neutrino genesis scenario worked because of the small Yukawa couplings of Dirac neutrinos. It enabled the right handed neutrinos to stay decoupled from the other particles and therefore hide an asymmetry in their sector. Since the small neutrino masses are now due to the fact that they are determined by the difference of two much bigger Yukawa couplings,

⁸The fact that all our fermions are part of only two multiplets per generation, whereas one has five of these in the standard model, also means that additional mixings could occur (e.g. in the charged lepton sector). Why these mixings are not observed goes beyond the scope of this thesis. Here we just accept the fact that they are not and chose our parameters in a way that yields realistic results.

⁹Since we only want to estimate orders of magnitude, it is not necessary to be highly precise at this point.

the coupling of the neutrinos is now of the same order of magnitude as for the other fermions. Besides, if their couplings actually were a lot smaller than the couplings of the other fermions, only a very small fraction of the Higgs bosons would decay in a channel containing neutrinos.

Therefore, it seems that our only hope for neutrino genesis to work in this model is, if the left- and the right-handed fermion sector stay completely decoupled during the era of sphaleron activity. This way, an asymmetry could be stored in the right-handed fermion sector, while the opposite asymmetry in the left-handed sector would be partially transformed.

6.2.1 Chemical Potentials

As we saw in eq.(2.42) the excess of a particle species over the corresponding antiparticle is dependent on the chemical potential. In the case of $\mu, m \ll T$, they are even proportional. Since the baryon excess we want to generate is of the order 10^{-10} , this approximation should be well justified for all particles.

We now use the method of chemical potentials similar to [12,16,28] in order to determine the final amount of baryon asymmetry. To make the upcoming calculations simple we will introduce some notation exclusively for this section. We will combine all the particles of generation a with weak isospin $\frac{1}{2}$ (left- or right-handed) to the vector $\vec{f}_{L/R}^a$ and all the particles with weak isospin of $-\frac{1}{2}$ to the vector $\vec{f}_{L/R}'^a$, such that

$$\vec{f}_L^1 = \begin{pmatrix} \nu_e \\ u^r \\ u^g \\ u^b \end{pmatrix}_L, \quad \vec{f}_L'^1 = \begin{pmatrix} e^- \\ d^r \\ d^g \\ d^b \end{pmatrix}_L,$$

with obvious definitions for the other two generations and opposite handedness. With this notation the important processes in equilibrium will be:

$$f_{L,i}^a + W_L^- \longleftrightarrow f_{L,i}'^a,$$

which lead to the following equations for the chemical potentials:

$$\mu_{f_{L,i}^a} + \mu_{W_L^-} = \mu_{f_{L,i}'^a} \quad (6.19)$$

At times before electro-weak symmetry breaking we have $I_L^3 = 0$ and therefore $\mu_{W_L^-} = 0$, which leads to

$$\mu_{f_{L,i}^a} = \mu_{f_{L,i}'^a}. \quad (6.20)$$

From sphaleronic processes we also have the condition

$$\sum_{a,i} \mu_{f_{L,i}^a} + \mu_{f_{L,i}'^a} = 0. \quad (6.21)$$

Since the right-handed sector is completely decoupled from this, the chemical potentials of all right-handed particles are fixed. We now define the input

parameter A arising from the specific decays used in the model, that cannot be changed by the processes in equilibrium:

$$A \equiv \sum_{a,i} \mu_{f_{R,i}^a} + \mu_{f'_{R,i}^a} \quad (6.22)$$

As in [28], we now calculate the chemical potential for $(B - L)$ and set it afterwards equal to zero, since our model is $(B - L)$ -conserving. In doing so we will get the final baryon-asymmetry in dependence of our input-parameter A :

$$\begin{aligned} \mu_{B-L} &= \mu_B - \mu_L \\ &= \mu_B - \sum_{a=1}^3 (\mu_{e_L^a} + \mu_{e_R^a} + \mu_{\nu_L^a} + \mu_{\nu_R^a}) \\ &\stackrel{(6.21)}{=} \mu_B - \sum_{a=1}^3 (\mu_{e_R^a} + \mu_{\nu_R^a} - \sum_{i=2}^4 (\mu_{f_{L,i}^a} + \mu_{f'_{L,i}^a})) \\ &= \mu_B - \sum_{a=1}^3 (\mu_{e_R^a} + \mu_{\nu_R^a}) + 3\mu_B - \sum_{a=1}^3 \sum_{i=2}^4 (\mu_{f_{R,i}^a} + \mu_{f'_{R,i}^a}) \\ &= 4\mu_B - A \end{aligned}$$

Hence,

$$\mu_B = \frac{1}{4}A = \frac{1}{4} \sum_{a,i} \mu_{f_{R,i}^a} + \mu_{f'_{R,i}^a}. \quad (6.23)$$

With the thoughts from the beginning of this section we therefore find

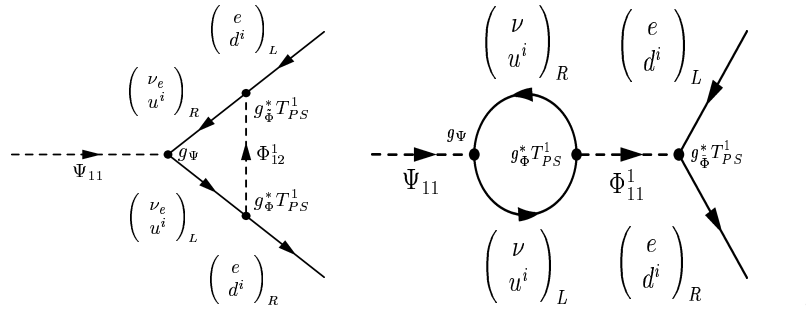
$$\boxed{n_B = \frac{1}{4}n_R} \quad , \quad (6.24)$$

where n_R is for the density of all right-handed fermions per comoving volume.

6.2.2 Initial Decay

Now that we have seen to what degree a left-right asymmetry would be transformed to a matter-antimatter asymmetry, we will calculate the resulting left-right asymmetry due to the possible out-of-equilibrium decay of our Higgs scalars.

From the Feynman-rules which originate from (6.15) we can draw many diagrams which represent a CP-violating decay, such as



where the first one is a vertex correction, while the second one is a correction to the self-energy of the scalar.

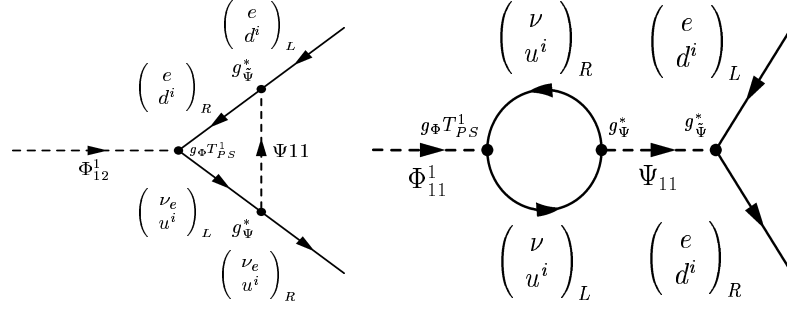


Figure 6.1: The corresponding diagrams to the examples in the text. In both cases the three loose ends have been fixed in a vertex, while the vertex that could be seen as the origin of the virtual scalar in the original diagram has been undone.

By connecting the loose ends of these graphs and undoing one of the vertices, each of these diagrams immediately induces a corresponding diagram, in which the two scalars change the roles of decaying and mediating particle. For the just presented examples the corresponding diagrams are shown in fig.6.1.

Since there are many processes similar to the just presented ones in our model, we will take one step back here, and present some general results obtained from graphs with similar structure as the ones we just introduced.

In graphs like the first one of the presented examples, where some heavy scalar S decays to some fermionic channel X by exchanging a virtual scalar S' , and where the fermions can be considered as massless, the difference in the decay rates of $\Gamma(S \rightarrow X)$ and $\Gamma(\tilde{S} \rightarrow \tilde{X})$ stems from the interference terms between this graph and the tree-level graph and can be calculated to be [19, 28]

$$\Delta_1(r) = \frac{m_S}{32\pi^2} \text{Im} \left\{ \text{tr}(g_{\tilde{\Psi}} g_{\Phi}^{\dagger} g_{\Psi} g_{\tilde{\Phi}}^{\dagger}) \right\} [1 - r^{-2} \ln(1 + r^2)], \quad (6.25)$$

with $m_{S/S'}$ being the mass of S , S' respectively and $r \equiv m_S/m_{S'}$. The nomenclature for the Yukawa couplings is the same as in the presented example for such a process at the beginning of this section. The trace in this expression was originally meant for the different generations, but in our case it has also to be taken in $SU(4)$ -flavor space.

In graphs like the second one in the presented example, which yields a correction to electron self-energy, the corresponding difference turns out to be [22, 28]

$$\Delta_2(r) = -\frac{m_S}{32\pi^2} \text{Im} \left\{ \text{tr}(g_{\tilde{\Psi}} g_{\tilde{\Phi}}^{\dagger}) \text{tr}(g_{\Psi} g_{\Phi}^{\dagger}) \right\} \left[\frac{1}{1 - r^{-2}} \right], \quad (6.26)$$

if $(m_S - m_{S'})^2 \gg (\Gamma_S - \Gamma_{S'})^2$ has been assumed, with $\Gamma_{S/S'}$ being the total decay rates.¹⁰ Since we also take the trace in $SU(4)$ -flavor space again, we find that the net contribution of the self-energy correction diagrams adds up

¹⁰Eqns. (6.25) and (6.26) show that one indeed needs two different Higgs representations, since even though there can be several Higgses in one representation, both eqns. would turn out to be zero, as $\text{Im}(g_x g_x^*) = 0$.

to a CP-violation of zero, as it is proportional to the trace of the product of a unit-matrix (coming from Ψ) and a generator of $SU(4)_{PS}$ (due to Φ) which is traceless by definition.

All the the relevant diagrams for the decays of the various Ψ -particles are listed in fig. 6.2. These diagrams and the corresponding processes for decaying Φ s, which create an asymmetry with opposite sign, lead to the net asymmetry ε' produced per decay

$$\begin{aligned}
\varepsilon' &= \sum_{\text{decay channels}} \frac{\Delta_1(r)}{\Gamma_S} - \frac{\Delta_1(r^{-1})}{\Gamma_{S'}} \\
&= 8 \times 15 \times \left(\frac{\frac{1}{32\pi^2} \frac{1}{2} \text{Im} \left[\text{tr}(g_{\Psi} g_{\Phi}^{\dagger} g_{\Psi} g_{\Phi}^{\dagger}) + \text{tr}(g_{\Psi} g_{\Phi}^{\dagger} g_{\Psi} g_{\Phi}^{\dagger}) \right] (1 - r^{-2} \ln(1 + r^2))}{\frac{1}{4\pi} (\text{tr}(g_{\Psi}^{\dagger} g_{\Psi}) + \text{tr}(g_{\Psi}^{\dagger} g_{\Psi}))} \right. \\
&\quad \left. - \frac{\frac{1}{32\pi^2} \frac{1}{2} \text{Im} \left[\text{tr}(g_{\Psi} g_{\Phi}^{\dagger} g_{\Psi} g_{\Phi}^{\dagger}) + \text{tr}(g_{\Psi} g_{\Phi}^{\dagger} g_{\Psi} g_{\Phi}^{\dagger}) \right] (1 - r^2 \ln(1 + r^{-2}))}{\frac{1}{4\pi} \frac{1}{2} (\text{tr}(g_{\Phi}^{\dagger} g_{\Phi}) + \text{tr}(g_{\Phi}^{\dagger} g_{\Phi}))} \right) \\
&= \frac{1}{\pi} \text{Im} \left[\text{tr}(g_{\Psi} g_{\Phi}^{\dagger} g_{\Psi} g_{\Phi}^{\dagger}) + \text{tr}(g_{\Psi} g_{\Phi}^{\dagger} g_{\Psi} g_{\Phi}^{\dagger}) \right] \\
&\quad \cdot \left(\frac{\frac{1}{2} (1 - r^{-2} \ln(1 + r^2))}{\text{tr}(g_{\Psi}^{\dagger} g_{\Psi}) + \text{tr}(g_{\Psi}^{\dagger} g_{\Psi})} - \frac{1 - r^2 \ln(1 + r^{-2})}{\text{tr}(g_{\Phi}^{\dagger} g_{\Phi}) + \text{tr}(g_{\Phi}^{\dagger} g_{\Phi})} \right) \\
&\stackrel{(6.18)}{=} \frac{8.67 \times 10^{-3}}{\pi} \left[0.83 \cdot (1 - r^{-2} \ln(1 + r^2)) - 0.62 \cdot (1 - r^2 \ln(1 + r^{-2})) \right], \tag{6.27}
\end{aligned}$$

with $r \equiv m_{\Psi}/m_{\Phi}$ again being the ratio of the masses of the two scalars. The several factors of $1/2$ come from the normalization of the $SU(4)$ generators. As a result of equation (6.24) only one fourth of this will remain as a baryon asymmetry.

$$\varepsilon = \frac{1}{4} \varepsilon'. \tag{6.28}$$

This finally yields the baryon-asymmetry per comoving volume

$$B \stackrel{[19]}{\approx} \frac{\varepsilon}{g_*} \approx 1.6 \times 10^{-6} \left[(1 - r^{-2} \ln(1 + r^2)) - 0.75 \cdot (1 - r^2 \ln(1 + r^{-2})) \right], \tag{6.29}$$

where we assumed $g^* \approx 350$.

The final baryon asymmetry in a model with the specified Higgs scalars and Yukawa couplings is therefore given by $B(r)$, if the out-of-equilibrium decay of the particles is followed by sphaleron wash-out. The behaviour of $B(r)$ is shown in fig.6.3 .

6.2.3 Problems With Neutrinogenesis

After these introductory calculations, we now have to present the problems that seem to rule out the possibility of baryogenesis in the introduced model.

The first problem we want to mention is the fact that our decaying Higgs scalars also develop a VEV. The temperature when this happens is usually of the order their masses, which is the same scale, when they should start to freeze out. In the case of out-of-equilibrium decay, the particles will therefore most likely decay after electro-weak symmetry breaking, and therefore no sphaleron

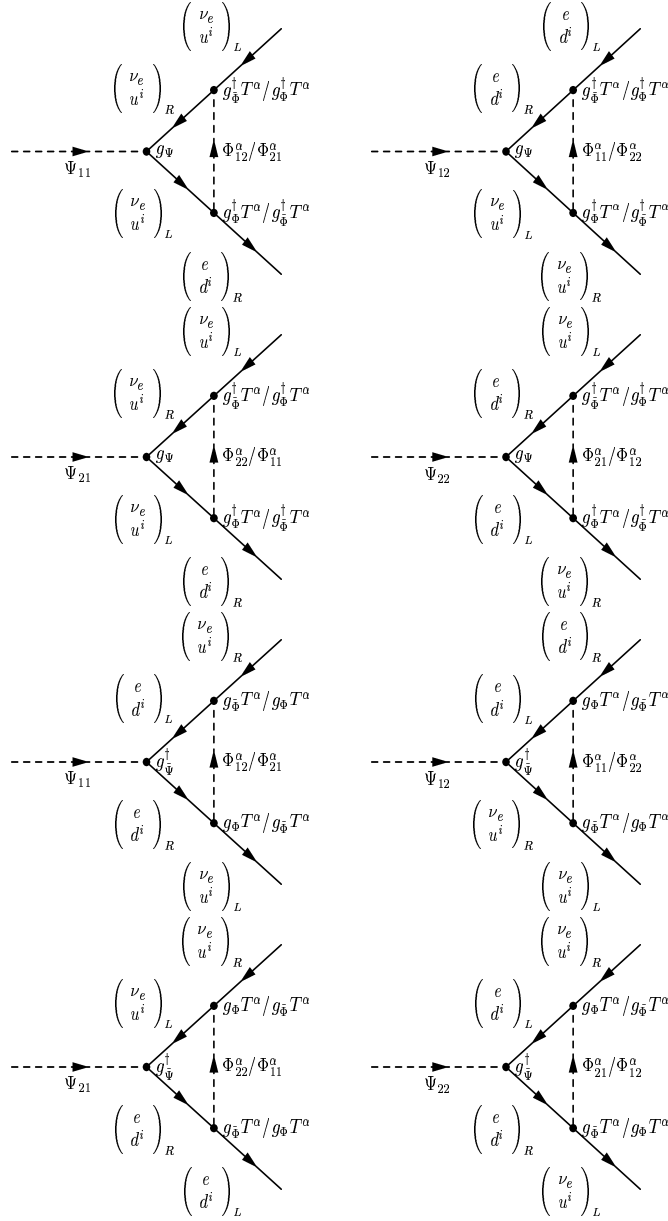


Figure 6.2: The different CP-violating decay modes of the various Ψ s with omitted generation indices on the fermions. Each graph stands for two different decays, where the first decay mode always gives a contribution of $\text{Im}(\text{tr}(g_{\bar{\Psi}} g_{\Phi}^{\dagger} g_{\Psi} g_{\Phi}^{\dagger}))$, whereas the second gives $\text{Im}(\text{tr}(g_{\bar{\Psi}} g_{\Phi}^{\dagger} g_{\Psi} g_{\Phi}^{\dagger}))$ in eq.(6.25). For the lower half of the graphs this is not so obvious. Here it is due to the fact that for each diagram all the couplings have to be complex conjugated relative to the corresponding graph in the upper half. The resulting minus sign is compensated by the fact that these diagrams create an asymmetry of opposite sign.

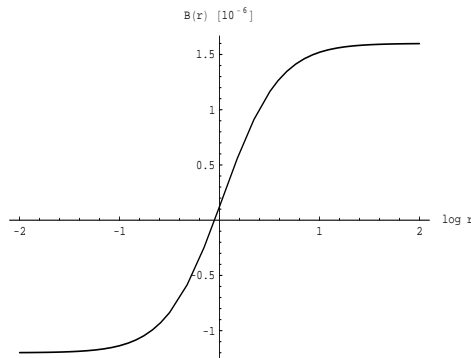


Figure 6.3: The produced baryon asymmetry B in orders of 10^{-6} depending on the logarithmic ratio of the masses of the decaying scalars r .

processes will be active to transform the asymmetry in the left handed sector. In this case left-right equilibration would erase every created asymmetry between the sectors.

Even if the out-of-equilibrium decay process would somehow take place before the the end of sphalerons activities there are still problems left. One of them stems from eq.(6.29), from which we can see that in case of masses of the same order of magnitude for Ψ and Φ the final baryon asymmetry will be of the order of 10^{-7} . Comparing this result with the measured value of $B \approx (2 - 8) \times 10^{-11}$ (see eq.(2.55)), we find that we are approximately four orders of magnitude away from reality. The obvious way to fix this issue would be to finetune r . For $r = 0.891983$ our values are in the right ballpark. Unfortunately, this requires a funetuning of the order of 10^{-6} , which does not make this option very attractive.

A further and more important problem arises from the out-of-equilibrium condition for the decay. Since we need the particles to decay when they are highly overabundant, their decay rate needs to be much smaller than the Hubble rate at $T \approx m_{\Psi, \Phi}$, which is the time they would start decaying if they were in equilibrium. The total decay rate of the scalars is given by

$$\Gamma_{\Phi} = m_{\Phi} \frac{\text{tr}(g_{\Phi}^{\dagger} g_{\Phi}) + \text{tr}(g_{\tilde{\Phi}}^{\dagger} g_{\tilde{\Phi}})}{4\pi} \equiv m_{\Phi} \alpha_{\Phi} \quad (6.30)$$

and the analogous equation for Γ_{Ψ} , which we both already used in the calculations in section 6.2.2. Thus our out-of-equilibrium condition is

$$K_{\Phi/\Psi} \equiv \frac{\Gamma_{\Phi/\Psi}}{2H(m_{\Phi/\Psi})} = \frac{\alpha_{\Phi/\Psi}}{\sqrt{g_*}} \frac{M_{\text{Pl}}}{m_{\Phi/\Psi}} \leq 1. \quad (6.31)$$

With the parameters we fixed so far, we find

$$\begin{aligned} \alpha_{\Phi/\Psi} &: \mathcal{O}(10^{-1}), \\ \sqrt{g_*} &: \mathcal{O}(10^1). \end{aligned} \quad (6.32)$$

With $M_{\text{Pl}} = \mathcal{O}(10^{19})\text{GeV}$ this would lead to the condition $m_{\Phi/\Psi} \geq 10^{17}\text{GeV}$, which implies masses even bigger than the GUT-breaking scale of 10^{16}GeV and is not very appropriate for a particle within a Pati-Salam-model. What makes it even worse is that these particles break the electro-weak symmetry in our model. Therefore their VEVs or at least an upper limit for them, can be determined by measuring the mass of the electro-weak gauge bosons (see section 6.1.2 and 6.1.3). These conditions combined lead to a difference of 10^{15}GeV between the mass of our scalars and their VEVs. As the VEV of a scalar particle is essentially determined by the ratio of its mass μ and the square-root of the coupling constant λ of its Φ^4 coupling term, this would require λ to be of the order of 10^{30} . It is obvious that, with such a huge value for the coupling constant, perturbation theory would not be justified, which in return yields the possible invalidity of our results.

6.3 Quintessence Driven Neutrino genesis

At first sight the pure amount of inconsistencies and problems for a neutrino-genesis process within the presented model seems to rule out this possibility completely. Yet, the fact that all these problems are due to inconsistencies in the numbers and the chronological order of processes instead of being due to the absence of essential ingredients in the model, allows us to circumvent all of them by making an additional assumption, which has already been introduced in section 5.5. If we couple some of the constants in our model to a quintessence field, they will effectively be varying with time. By choosing appropriate couplings we will be able to change the order of magnitude of the quantities which yield the problems for neutrino-genesis and hereby get rid of them. With couplings that yield a change of constants over several orders of magnitude, we will even be able to change the chronological order of processes, as we will be shown later. If we now look at the problems presented in the last chapter, it is obvious that the masses of the Higgs scalars Φ and Ψ as well as their Yukawa couplings will be among the varied constants. The possible necessity to also vary gauge coupling constants will be explained later.

6.3.1 The Uncoupled Quintessence Field

Before specifying the dependence of the various couplings on the quintessence field, we will fix the bare model of the field itself and choose a potential similar to the one used in [7]¹¹

$$V = V_0(e^{\lambda Q} + e^{-\lambda Q}). \quad (6.33)$$

For suitable parameters this potential leads to a model that has the appealing tracker property and all the other characteristics we need. We put $\lambda = 100/M_{\text{Pl}}$ and $V_0 = 0.375\rho_c$, where ρ_c is the critical density, such that for a field with $Q = 0$ and $\dot{Q} = 0$ we get a cosmological constant with an energy density of $0.75\rho_c$. The development of Q and ω with these parameters and the initial

¹¹In contrast to the introductory chapter on quintessence, we will refer to our quintessence field by the symbol Q .

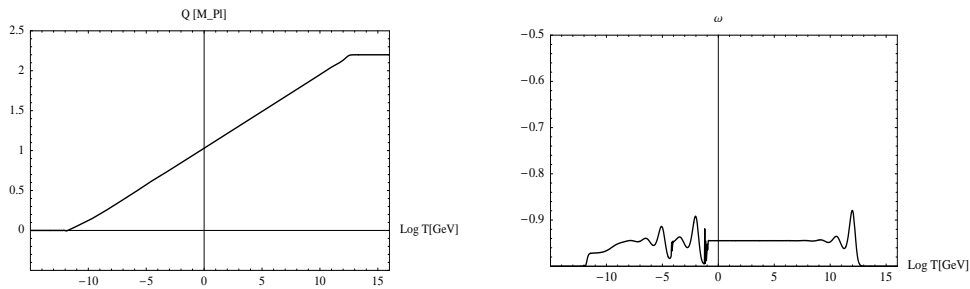


Figure 6.4: The dependence of the quintessence field (in units of M_{Pl}) and ω on the decadic logarithm of the temperature in units of GeV in the uncoupled case.

conditions $Q(T \approx 10^{16} \text{ GeV}) = 2.2 M_{\text{Pl}}$ and $\omega(T \approx 10^{16} \text{ GeV}) = -1$ is shown in fig.6.4, where we used the differential equations presented in eqs.(4.5) to calculate their behaviour. In fig.6.5 we can see the behaviour of the various energy forms in dependence of time, which will help us later on, when we will approximate their relative orders of magnitude. In the calculations for these figures as well as in all other numerical calculations the standard model particle content was assumed and several functions were only approximated, if not specified otherwise. However most of their features should not be lost when switching to our model since we are rather concerned with orders of magnitude.

6.3.2 Varying Coupling Constants

This section will treat the idea of quintessence coupled constants in more detail. However, before we do this in a quantitative way, we will take a closer look at the possible qualitative behaviours of the various constants with time that might yield baryogenesis.

To have the scalars Φ and Ψ decay out of equilibrium, we take a look at eq.(6.31) and see that they need to be very heavy during this stage, while we still need them to be small today. Of course we could also achieve a smaller $K_{\Phi/\Psi}$ by reducing the size of the Yukawa couplings, but the bounds within which we can vary them during the time of decay, are mainly set by eq.(6.29), where we can see that the final brayon asymmetry will be too small if we choose to reduce the Yukawa couplings by too many orders of magnitude. With Higgs masses at 10^{15} GeV and above the out-of-equilibrium condition should be fulfilled if we simultaneously reduce the Yukawa couplings in a way that will be specified later.

But heavy masses at early times and lighter masses today is not the only condition we need to imply on Φ and Ψ . As we need an era of sphaleron activity after their decay, the behaviour of their masses on their way down the energy scale is also constrained. Basically, there are two possibilities for the qualitative behaviour of these masses or rather their corresponding μ -parameters which are both presented in fig.6.6 .¹²

¹²By the term μ -parameter we refer to the parameters within the Higgs potential which

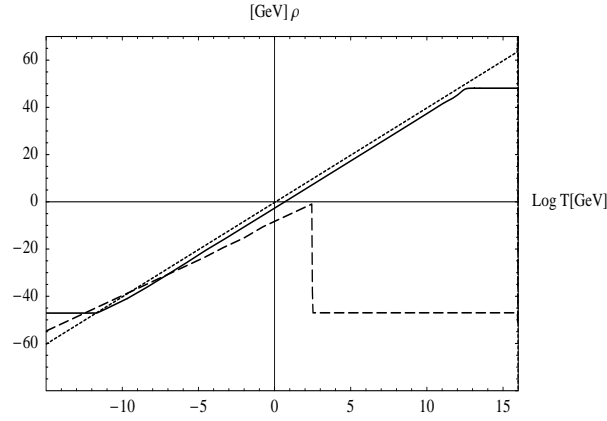


Figure 6.5: The approximate behaviour of the various energy densities. The solid line is the energy density of the quintessence field, while the shortly dashed one represents the radiation energy density. The line with the long dashes stands for the energy density due to matter, and is only to be considered after electro-weak symmetry breaking.

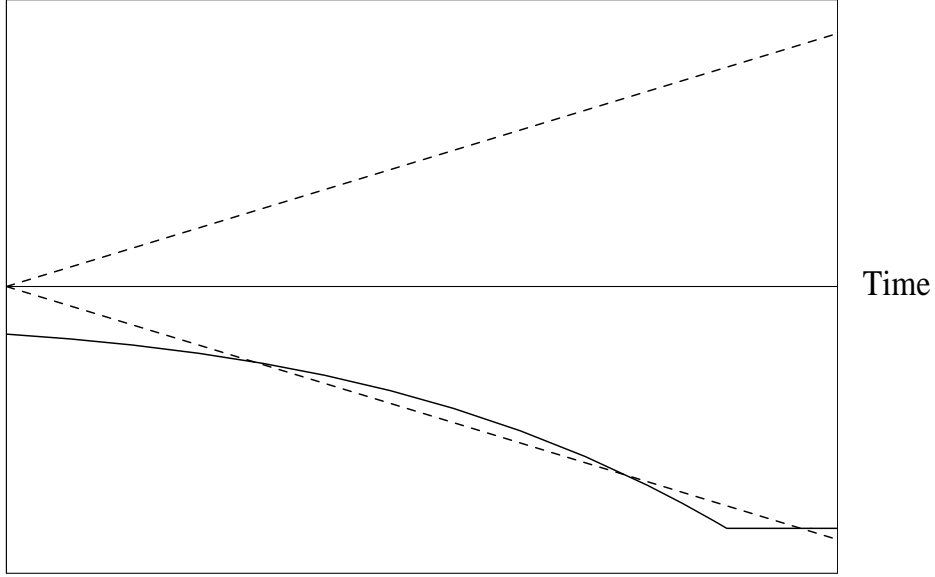
The first possibility features a constant negative sign of the μ -parameter. If this is the case, the Higgs bosons will have a VEV during their stage of decay, and therefore the mass-curve of each of these scalars will have to cross the temperature-curve two more times, such that there is a period with restored $SU(2)_L$ -symmetry after their decay, during which sphalerons are in thermal equilibrium once more and can partially transform the left-handed asymmetry.¹³

The second possibility uses the fact that the mass of a Higgs scalar is mainly determined by the absolute amount of the μ -parameters and not by its sign. Therefore we can also think of a Higgs particle with positive μ during the decay stage. This implies that the field does not have a VEV during this time, which also means unbroken electro-weak symmetry and sphaleron activities. At later stages the μ parameter needs to have a negative sign, of course, such that

are responsible for the mass of the corresponding boson. While the mass of a particle is always a positive quantity, this parameter can also be negative, as we can see for example in the standard model Higgs mechanism. Still, the mass and the absolute amount of the corresponding μ -parameter are usually of the same order of magnitude (except around the critical temperature), no matter if we are in the broken or unbroken phase. Since orders of magnitude will be all we need in the remaining calculations, we will therefore treat them as identical quantities.

¹³The transformation of the asymmetry however might not be completely described by the formalism in section 6.2.1, since now, there was a period with broken $SU(2)_L$ before the sphaleron washout. This means that the weak isospin does not have to be the same as in the beginning of the universe. Therefore the calculations after this point might be a little different. Yet, it is still likely that the order of the final baryon asymmetry will not differ dramatically from our result in section 6.2.1, and a baryogenesis of the right order of magnitude might still be able to take place. Independent of this, the calculation is still completely valid for the second possibility, which is the one will work with in the remainder of this thesis.

Energy



Energy

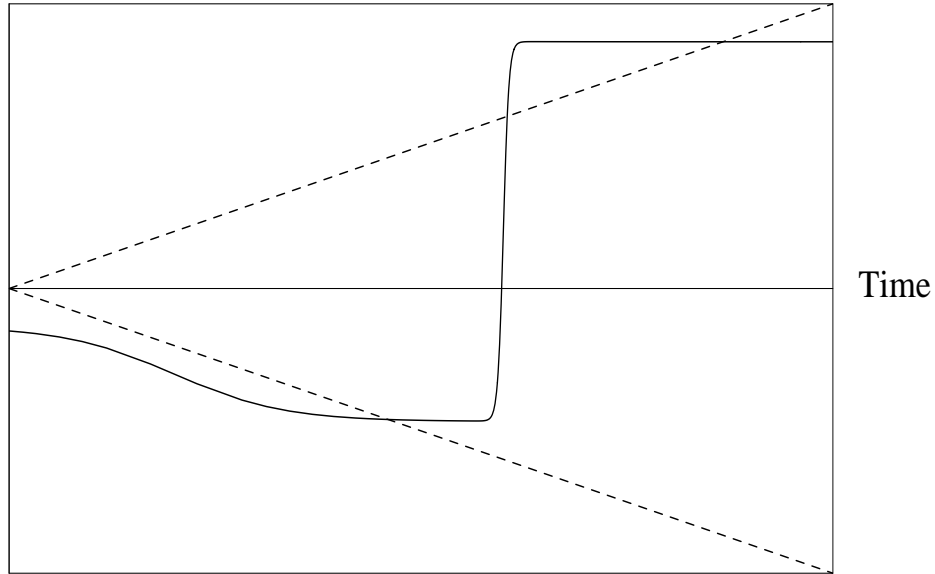


Figure 6.6: The two different ways for a time dependent μ -parameter that possibly render baryogenesis. In both graphs, the solid line shows the behaviour of μ , while the dashed lines represent the temperature as well as the negative temperature. In the first graph μ is always negative, such that after the decay of the particles its modulus has to fall below the temperature once more to enable sphalerons to be active again. In the second graph μ switches signs. Therefore electro-weak symmetry is not broken during the first decay stage of the scalars, and sphalerons can transform the left-handed asymmetry immediately.

the corresponding particles develop VEVs and the fermions and gauge bosons become massive.

As we already noted, the heavy masses of Φ and Ψ at early times enable them to decay out of equilibrium, and keep the left- and right-handed fermion sectors from equilibrating. But since their masses get lower as temperature falls, left-right-equilibration might take place during later stages. In order to not let this happen too early (namely while sphalerons are active), the Yukawa couplings also need to be effectively time-dependent. We will treat this problem on a more quantitative level later on, but we already note that they need to be several orders of magnitude smaller than the values we calculated in 6.1.3 .

We also want to note that varying the Yukawa couplings can also make the fine tuning of the masses of Φ and Ψ obsolete, which was required to obtain a baryon asymmetry of the right size in eq.(6.29); in addition it enables us to lower the mass bounds of the Higgs bosons during their era of decay by several orders of magnitude such that we might at least stay below the GUT-scale during all periods of baryogenesis in this model.

Mass Variation:

To be able to treat the idea of quintessence coupled constants in our model on a more quantitative level, we now give explicit formulae for the quintessence couplings. Of course, these couplings are not the only ones that might yield a matter-antimatter asymmetry in the end. However, the couplings cannot be chosen completely arbitrary as they should not destroy the original behaviour of the quintessence field.

To keep the notation simple, we will only refer to the variation

$$\mu \rightarrow \mu(Q), \quad (6.34)$$

hereby meaning the variation of all mass parameters in the Higgs potential of Φ and Ψ in a way analogous to the presented one.

Of the two different behaviours of μ described above and in fig.6.6 the second one seems to have the more appealing features. The biggest one of them being the just mentioned important characteristic that the addition to the effective quintessence potential stemming from this mass variation $m_{\Phi/\Psi}(Q)$ will not have a big effect on the behaviour of Q itself, whereas a behaviour as the first one in fig.6.6 can easily destroy the original behaviour of the quintessence field, and therefore its own behaviour in time will also not be the desired one.

Choosing the second type of behaviour for μ we also have the advantage of having our particles decay in the unbroken phase. Therefore the calculations done so far are much more exact: The calculations with the chemical potentials might not be completely correct, if a phase of broken electro-weak symmetry preceeds the era of sphaleron activity, as we might not be able to imply $I_L^3 = 0$ during the time of sphaleron activity. Also, the fact that the Higgs bosons would decay in their broken phase would have an impact on the validity of the calculations leading to eq.(6.29), since there will most likely be some mixing of Ψ - and Φ -components in this case. Therefore the propagators in the feynman diagrams of fig.6.2 would not represent mass eigenstates, and we would have to

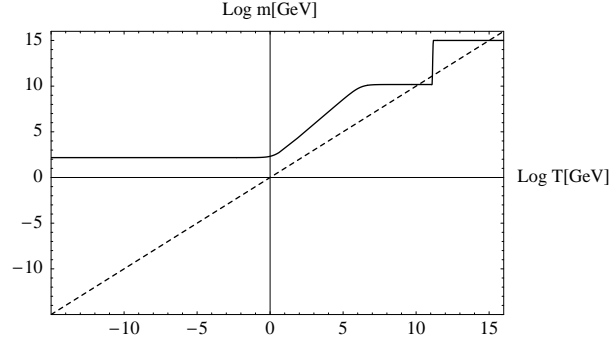


Figure 6.7: The effective temperature dependence of the Higgs mass, driven by the quintessence model specified in the text. The dashed line represents the temperature T , such that it is easy to see when the rest energy of Ψ and Φ is bigger or smaller than T . μ changes sign after its rapid change at around $T = 10^{11}\text{GeV}$. The effect of this coupling on the quintessence field has not been considered, yet.

draw other diagrams depending on the specific Higgs potential. With all of this in mind, we choose the coupling

$$\mu \rightarrow \frac{\mu_1}{2} \left(\tanh(\omega_1(Q + Q_{off,1})) + 1 + \frac{2\mu_0}{\mu_1} \right) + \frac{\mu_3}{2} \left(\tanh(\omega_2(Q + Q_{off,2})) + 1 + \frac{2\mu_2}{\mu_3} \right), \quad (6.35)$$

where the value of μ is almost constant for several periods, while it can change very rapidly in others. With ω_i and $Q_{off,i}$ in the right range, μ_1 gives the mass of the scalar boson during the decay stage, while the parameters μ_0 and μ_3 fix the value of μ at an intermediate period, which ends after the end of sphaleron activity. Finally $|\mu_0 + \mu_2|$ yields the mass of the particle today. The parameters ω_i and $Q_{off,i}$ determine the pace and the time of the mass transitions, respectively. Later on it will become clear why such a kind of coupling should not destroy the original behaviour of the quintessence field as opposed to many others.

As in section 5.5 we do not have to worry about renormalizability, since the coupling terms are renormalizable in the quantum fields, while Q is a classical field and its Lagrangian does not have to be renormalized.

Finally we fix the parameter values at $\mu_1 = 10^{15}\text{GeV}$, $\mu_0 = -150 \times 10^8\text{GeV}$, $\mu_3 = \mu_0$, $\mu_2 = -\mu_1 - 150\text{GeV}$, $\omega_1 = \frac{1000}{M_{\text{Pl}}}$, $\omega_2 = \frac{17}{M_{\text{Pl}}}$, $Q_{off,1} = -2.06M_{\text{Pl}}$, and $Q_{off,2} = -1.6M_{\text{Pl}}$. A plot of $m(Q)$ with these parameters as well as the temperature curve is shown in fig.6.7.

Yukawa Coupling Variation

As stated before it is not enough to just vary the mass of the fermion mass generating Higgs scalars. An additional variation of the Yukawa couplings does

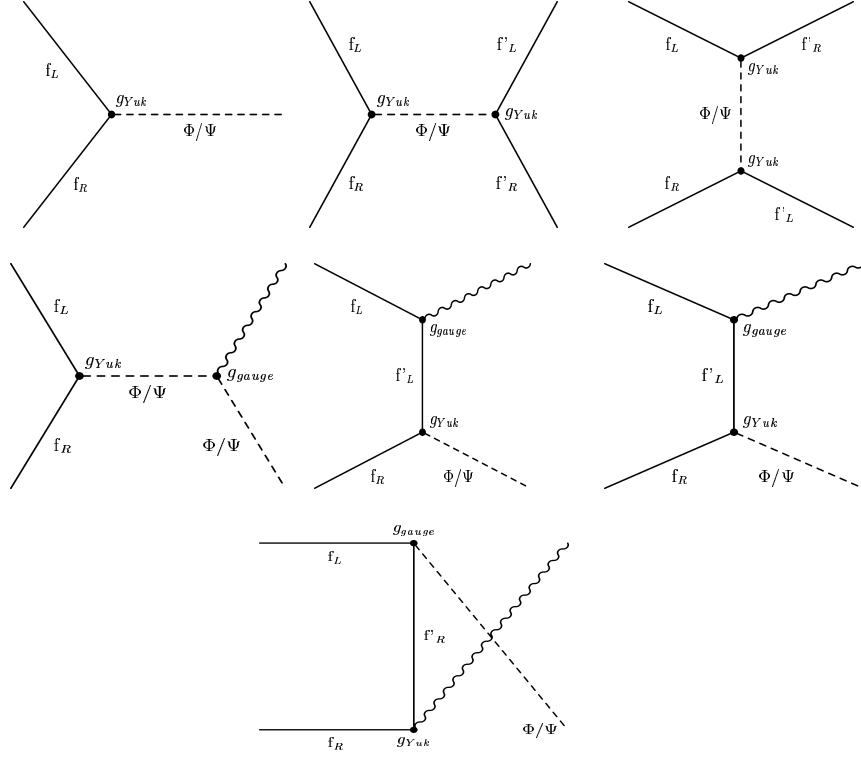


Figure 6.8: Relevant processes for left-right-equilibration. The solid lines represent fermions, the dashed ones the Higgs scalars, and the wavy lines represent gauge bosons. It should be noted that each diagram can represent several processes, since there are sixty different Φ particles and four different Ψ s.

not only enable us, to lower the masses of the Higgs bosons during the decay stage, it also seems to be required to prevent left-right-equilibration from taking place too early.

Generalizing the statements from [11, 28], we find that the dominant processes leading to left-right equilibration are shown in fig.6.8 . During stages of broken symmetry and during the decay stage, the rest energy of the left-right mediating scalars will be large compared to the temperature, and we estimate the reaction rates of the various processes in fig.6.8 to be given by (compare eq.(5.4) and [11, 19])

$$\begin{aligned}
 \Gamma_{\text{ID}} &\sim \frac{g_{Yuk}^2}{4\pi} m_{\Phi, \Psi} \left(\frac{m_{\Phi, \Psi}}{T} \right)^{\frac{3}{2}} \exp \left(-\frac{m_{\Phi, \Psi}}{T} \right), \\
 \Gamma_{2 \leftrightarrow 2} &\sim \frac{g_{Yuk}^2}{4\pi} \frac{g_{Yuk}^2}{4\pi} \frac{T^5}{m_{\Phi, \Psi}^4}, \\
 \Gamma_{\text{gauge}} &\sim \frac{g_{Yuk}^2}{4\pi} \frac{g_{\text{gauge}}^2}{4\pi} \frac{T^5}{m_{\Phi, \Psi}^4} \left(\frac{m_{\Phi, \Psi}}{T} \right)^{\frac{3}{2}} \exp \left(-\frac{m_{\Phi, \Psi}}{T} \right).
 \end{aligned} \tag{6.36}$$

Here g_{Yuk} represents a Yukawa coupling, and g_{gauge} stands for a gauge coupling. Γ_{ID} is the reaction rate of the inverse decay processes, while $\Gamma_{2 \leftrightarrow 2}$ denotes $2 \leftrightarrow 2$ scattering processes. Γ_{gauge} is an estimate for all the processes in fig.6.8 in

which a gauge boson is produced in addition to a Higgs boson. These processes can become important when one treats the problem more quantitatively with Boltzmann equations, which might be due to the fact that in this case the fermions do not need to have exactly the rest energy of the scalar. In the first and third ratio we see an additional suppression factor, since the fraction of initial particles with enough energy to produce a heavy scalar is suppressed by a Boltzmann factor. The second ratio describes a $2 \leftrightarrow 2$ scattering of massless fermions and therefore this factor does not appear.

In the period between electro-weak symmetry breaking and heavy particle decay the temperature is larger than the rest-energy of the Higgs scalars. Here we estimate (compare [11, 19]):

$$\begin{aligned}\Gamma_{\text{ID}} &\sim \frac{g_{Yuk}^2}{4\pi} \frac{m_{\Phi, \Psi}^2}{T}, \\ \Gamma_{2 \leftrightarrow 2} &\sim \frac{g_{Yuk}^2}{4\pi} \frac{g_{Yuk}^2}{4\pi} T, \\ \Gamma_{\text{gauge}} &\sim \frac{g_{Yuk}^2}{4\pi} \frac{g_{\text{gauge}}^2}{4\pi} T.\end{aligned}\tag{6.37}$$

Keeping these results in mind we now take a closer look at the constraints for the Yukawa couplings. For reasons of simplicity we will vary all Yukawa couplings in the same way, just as we did for the various μ -parameters of the Higgs bosons. This should make the notation $g \rightarrow g(Q)$ self-explanatory.

With the mass variation in eq.(6.35) we need g to be several orders of magnitude smaller than one in order to fulfill equations (6.29) and (6.32). In fact, with equal masses for all Φ and Ψ , we need g to be approximately of the order of 10^{-2} or g^2 to be of the order of 10^{-4} to get a baryon asymmetry of order 10^{-11} . This leads to a ratio K of the order of 10^{-2} , which in return ensures out-of-equilibrium decay.

To also ensure that left-right-equilibration does not take place too early, we have to take a closer look at the various interaction rates. In the drift-and-decay model the temperature at which our scalars finally start decaying is given by eq.(5.6), which in our case means $T \sim 10^{14}\text{GeV}$. By then the ratios leading to left-right-equilibration will all have become much smaller. Taking a look at eq.(6.36), we see that the ratio of each reaction rate and the Hubble rate has become smaller by a factor of the order 10^{-3} or even a higher exponent. Even when summed over all different Higgs channels (order 10^2 for the largest processes), the ratio is smaller than one. In addition to that, the reaction rates for all these particles are falling faster than the Hubble rate. As motivated in appendix C this should be sufficient to ensure that left-right equilibration does not take place, as long as the masses of Φ and Ψ remain of the order of 10^{15}GeV .

After the rapid change of the Higgs masses, the reaction rates we used for our estimations in the last paragraph are no longer valid. We now have to work with the formulas given in eq.(6.37). As one can see, all these rates are smaller than $\frac{\text{tr}(g_{Yuk}^\dagger g_{Yuk})}{4\pi} T$, which makes it enough to show that processes with this reaction rate are not relevant until sphaleron activity ends. At $T_1 \sim 10^{11}\text{GeV}$ the Higgs masses become smaller than the temperature. The relevant time

scale for reactions of the specified rate is $\Gamma^{-1} \sim 10^{-10}/\text{tr}(g^\dagger g)$ corresponding to a temperature of

$$T_2 \sim (K|_{T=T_1})^{\frac{1}{2}} T_1, \quad (6.38)$$

with

$$K|_{T=T_1} = \frac{\Gamma_D}{2H} \Big|_{T=T_1} \approx \frac{\text{tr}(g_{Yuk}^\dagger g_{Yuk})}{4\pi} \frac{M_{\text{Pl}}}{g_*^{1/2} T_1}. \quad (6.39)$$

Since the sphaleron era ends at approximately 10^{10}GeV in our model, T_2 has to be smaller than this value to keep left-right-equilibration from taking place too early. This leads to the condition $(K|_{T=T_1})^{1/2} \ll 10^{-1}$, which in return means $g \ll 10^{-3}$ until electro-weak symmetry is broken. Since we have many diagrams that can yield left-right equilibration (the number of relevant ones is probably of the order 10^2 at most of the order 10^3) the condition should be sharpened. g gets also constrained more strongly if we set $T_1 \sim 10^{11}$, which means that we use the time when μ starts changing instead of the time when its rest-energy is approximately equal to the temperature. When we consider all these points to be surely on the safe side, we find the condition $g \ll 10^{-5}$.

Now that we have quantified our constraints, we give an explicit example for a quintessence coupling of the Yukawa couplings by

$$g \rightarrow \frac{g_1}{2} \left(\tanh(\omega_g(Q + Q_{\text{off},g}) + 1 + \frac{2g_2}{g_1}) + 1 \right) + \frac{150\text{GeV}}{\mu(Q)}, \quad (6.40)$$

with $g_1 = 0.01$, $g_2 = 5 \times 10^{-7}$, $\omega_g = 1000$, $Q_{\text{off},g} = -2.14$, and $\mu(Q)$ as specified before. With this coupling g fulfills all our conditions. The behaviour of $g(Q)$ and $\mu(Q)$ with respect to the temperature is shown in fig.6.9. We will assume that these couplings do only have a negligible influence on the behaviour of the quintessence field, and motivate this assumption in the next section. In this case, we see that all our chosen couplings seem to yield the desired behaviour in time, and therefore produce a baryon-asymmetry of the correct order of magnitude, given the fact that the assumptions and estimations made in the course of this thesis are justified.¹⁴

We also want to point out that in the likely case that the VEVs and the μ -parameters of Φ and Ψ are proportional, the fermion masses will not change after electro-weak symmetry-breaking, due to the fact that they are determined by the product of the Yukawa couplings and Higgs VEVs, which remains constant with the quintessence coupling we chose. The benefits of this will become clear when we will take a closer look at the effective quintessence field potential, and the influence of the quintessence-driven couplings on the behaviour of the quintessence field itself. At this point we note that at around $10^{12.5}\text{GeV}$, when the Yukawa couplings start changing, the decay time Γ_D^{-1} has passed 10^5 times, such that it is safe to assume that at this point the density of the heavy particles is of the order of their equilibrium density ($n \lesssim 10^{40} \times \exp(-10^{2.5})$, if chemical potentials can be neglected). We also note that at $T \sim 10^{11}\text{GeV}$, when the Higgs scalars have reached their intermediate masses, the age of the universe is

¹⁴Also, by looking at the numbers at e.g. $t \sim 1\text{GeV}$, we see, that left-right-equilibration has taken place at some point.

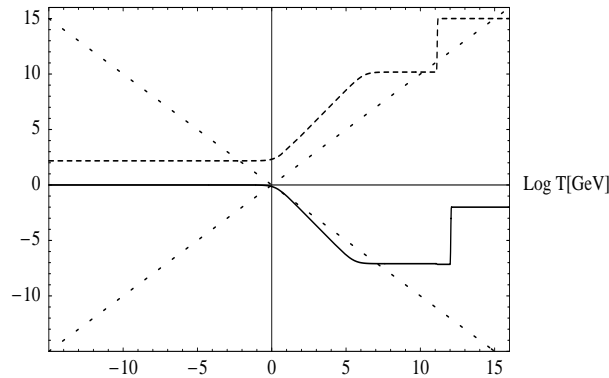


Figure 6.9: The temperature dependence of the Yukawa couplings g and the Higgs masses, driven by the quintessence model specified in the text. The solid line shows the logarithmic behaviour of g , while the dashed line represents the logarithm of the μ -parameters in GeV. The logarithmic temperature (in GeV) as well as its negative is represented by the dotted lines. Since the plots of μ and the Yukawa coupling are logarithmic, one can see that their product remains constant after electro-weak symmetry breaking from the fact that their incline only differs in sign during this stage.

smaller than $10^{-3}\Gamma_{ID+}^{-1}$. Where Γ_{ID+} represents the rate of all processes that produce a Φ or Ψ . This implies that, if no other processes are at work, by the time the Higgs scalars reach their intermediate masses, their abundance will still be suppressed by the exponential factor mentioned before.

A process that could also increase the abundance of Φ and Ψ is pair production by standard model gauge bosons. In order to keep the scalar particles from reaching abundances which are not exponentially suppressed after their initial period of decay, a quintessence dependence of the corresponding gauge coupling constants might also be needed. It should be obvious that this dependence can also be chosen in such a way that the masses of the gauge bosons do not change after symmetry breaking by using a coupling that yields today's values at $T \sim 1\text{GeV}$ while it changes proportionally to g_{Yuk} until its rapid change around $T = 10^{12}\text{GeV}$, if the mixing between right- and left-handed gauge bosons can be neglected, which can always be achieved by choosing the VEV of Ξ_R high enough. Before that the coupling constant for $SU(2)_L$ needs to be approximately of order one to yield unsuppressed sphaleron activity. We will not give explicit formulae here, since the couplings would be very similar to the already presented ones. It should be obvious that such couplings will not equilibrate Φ and Ψ during the time of rapid change of their masses, if we estimate the reaction rates in a similar way to eq.(6.37).¹⁵

¹⁵Note that this kind of coupling would violate D-Parity.

6.3.3 The Effective Quintessence Potential

When making mass-terms dependent on a quintessence field, this cannot be done in an arbitrary manner. If the mass of a particle depends on a quintessence field, the value of this field partially determines the energy of the system not only through its potential but also through these couplings, which leads to an effective quintessence potential term. It is important that the additional potential terms do not change the behaviour of the quintessence field, since otherwise the effective time-dependence of the coupling constants might be different. This section takes a closer look at these effective potentials and shows why the couplings we chose in our model are highly unlikely to destroy the original behaviour of the quintessence field.

The full Lagrangian of the system is now composed of the original Lagrangian of our model in section 6.1 and the quintessence part:

$$\mathcal{L} = \mathcal{L}_{kin} + \mathcal{L}_{Yuk} + \mathcal{L}_{Higgs} + \frac{1}{2}\partial^\mu Q \partial_\mu Q - V(Q), \quad (6.41)$$

where \mathcal{L}_{kin} represents the kinetic terms of the fermions and the gauge bosons, \mathcal{L}_{Yuk} stands for the Yukawa coupling terms, and \mathcal{L}_{Higgs} stands for the kinetic terms of the Higgs bosons as well as the Higgs potential. Q represents the quintessence field with its potential $V(Q)$, that was specified in eq.(6.33).

In the uncoupled case minimization of the action with respect to Q and the scale parameter R leads to the usual equations of motion shown in eq.(4.4). In the coupled case, $V(Q)$ is no longer the only term depending on Q since now also \mathcal{L}_{Yuk} and \mathcal{L}_{Higgs} have a Q dependence. To keep the form of eqs.(4.4), we define the effective quintessence potential [7]

$$\begin{aligned} V_{eff}(Q) &\equiv V(Q) + V_I(Q) \\ &\equiv V(Q) + \sum_{\text{all particles}} n_i \langle E \rangle_i \\ &= V(Q) + \sum_{\text{all particles}} \int \frac{d^3k}{(2\pi)^3} \sqrt{k^2 + m_i(Q)^2} f_i(k), \end{aligned} \quad (6.42)$$

which replaces $V(Q)$ in eq.(4.4c). Here, n_i stands for the particle density of each species, while $\langle E \rangle_i$ represents their mean energy. Analogously, the parameters $m_i(Q)$ represent the corresponding particle masses, while the $f_i(k)$ represent their distribution functions.

For the masses of Φ and Ψ the Q -dependence is due to the varying μ -parameters, where we assume the respective moduli to be equal. The gauge boson masses of $SU(2)_L$ also depend on the μ -parameters after electro-weak symmetry-breaking, since they are proportional to the VEVs of Φ and Ψ as well as to the gauge coupling constant. We assume $SU(2)_R$ to be broken at a scale, such that the corresponding gauge bosons effectively do not change their masses, even if Φ and Ψ do.¹⁶ In addition to the dependence on the VEVs the fermion

¹⁶The early time at which neutrino genesis takes place in our model, requires the breaking scale of $SU(2)_R$ to be much higher than in regular models. In this case it might seem attractive to have $SU(2)_R$ broken by the same representation that breaks $SU(4)_{PS}$, for which a breaking scale of 10^{15}GeV to 10^{16} is still very high but more likely than for $SU(2)_R$. Another possibility might of course be a quintessence dependent g_R .

masses are also influenced by the variation of the Yukawa couplings. However, let us not forget that even though various parameters important for the fermion- and left-handed gauge boson-masses depend on Q , we chose the couplings in such a way that their masses should be independent of the quintessence field at all times.

The new terms in the effective potential can provide serious problems for the tracker property of Q . Since they represent the energy of all the particles in our model, their absolute value is usually bigger than the original $V(Q)$, which has been constructed in such a way that the energy density of the quintessence field is at most of the same order of magnitude as the energy density provided by radiation and matter through early stages of the universe. Therefore the dependence of the masses on Q should not be too drastic, if one wants to keep the additional terms from overpowering the original potential in terms of influencing the behaviour of Q . However, the restrictions on the quintessence dependence of such masses can be extremely weakend, if their abundance is suppressed, and we will make use of this fact later.

The additional terms usually have their largest influence on Q , when the particle masses are of the same order of magnitude as the temperature. This becomes apparent by looking at the formulas for the different energy densities. If the mass of a particle is much larger than the temperature, its energy density is exponentially suppressed; on the other hand, if the particle mass is much smaller than the temperature, the energy density is independent of the particle mass in leading order (see section 2.2.1). Therefore we have to be especially carefull when the line representing the rest energy of a particle crosses the temperature line in graphs such as in fig.6.7.

A very crude estimate of the influence of these couplings can be obtained by assuming a Maxwell-Boltzmann distribution of the specific particles and integrating eq.(6.42), which then yields (compare eq.(2.26))

$$V_{eff}(Q) = V(Q) + \sum_{\text{all particles}} \frac{1}{\pi^2} \left[3m_i(Q)^2 T^2 K_2 \left(\frac{m_i(Q)}{T} \right) + m_i(Q)^3 T K_1 \left(\frac{m_i(Q)}{T} \right) \right], \quad (6.43)$$

if the chemical potentials can be neglected.

If the numerics do not significantly change upon using this potential, one can be confident that the couplings will generally not have a big influence on the system. This method has been used in reference [7].

However, the limits of this method become obvious, when we consider totally decoupled particles. In this case the number of particles would not change, regardless of Q , and therefore one could not simply differentiate the above potential with respect to Q , as the chemical potential would also depend on Q to keep n independent of it. In appendix D we even motivate the assumption that n in eq.(6.42) should generally not be differentiated with respect to it, since only its rate of change does instantaneuosly depend on it. For now, we will only assume

$$\frac{dV_I(Q)}{dQ} = \frac{d}{dQ}(n\langle E \rangle) \approx n \frac{d\langle E \rangle}{dQ}, \quad (6.44)$$

if the reaction rates keeping certain particles in equilibrium are smaller than

the Hubble rate, which corresponds to the obvious picture that the particles will not be able to follow a rapid change of Q .

By looking at the orders of magnitude, we see that with this assumption, the contribution of $V_I(Q)$ should be totally negligible: The rapid change of μ is before $T = 10^{10}\text{GeV}$, which corresponds to a value of Q of approximately $1.9M_{\text{Pl}}$ or more. With these values, we get

$$\begin{aligned} \left. \frac{dV(Q)}{dQ} \right|_{T=10^{10}\text{GeV}} &= \frac{d}{dQ} \left(0.375\rho_c \left[\exp\left(\frac{100}{m_{\text{Pl}}}Q\right) + \exp\left(-\frac{100}{M_{\text{Pl}}}Q\right) \right] \right)_{T=10^{11}\text{GeV}} \\ &> \rho_c \frac{100}{M_{\text{Pl}}} \exp(190) \\ &\approx 10^{18}\text{GeV}^3, \end{aligned} \tag{6.45}$$

which now has to be compared to the contribution of $V_I(Q)$, where we assume that the average energy of the particles is always of the order of the initial mass ($\sim 10^{15}\text{GeV}$) or less (compare eq.(2.25)):

$$\begin{aligned} \left. \frac{dV_I(Q)}{dQ} \right|_{T=10^{11}\text{GeV}} &\approx n \frac{d\langle E \rangle}{dQ} \\ &\lesssim (10^{15}\text{GeV})^3 \exp(-10^{2.5}) \frac{dm(Q)}{dQ}, \end{aligned} \tag{6.46}$$

with n being estimated as at the end of the last section. With $m(Q)$ being specified by eq.(6.35), and with the intermediate result

$$\begin{aligned} \frac{d}{dQ} \left(\frac{\mu_1}{2} \left[\tanh(\omega_1(Q + Q_{\text{off},1})) + 1 + \frac{2\mu_0}{\mu_1} \right] \right) \\ = \frac{\mu_1}{2} \left[1 - \tanh^2(\omega_1(Q + Q_{\text{off},1})) \right] \omega_1 \\ \leq \mu_1 \omega_1 \end{aligned} \tag{6.47}$$

we finally get

$$\begin{aligned} \left. \frac{dV_I(Q)}{dQ} \right|_{T=10^{11}\text{GeV}} &\lesssim (10^{15})^3 \cdot \exp(-10^{2.5}) 10^{15} \cdot 10^{-16}\text{GeV}^3 \\ &\lesssim 10^{-92}\text{GeV}^3, \end{aligned} \tag{6.48}$$

if the chemical potential can be neglected, which we will assume in the rest of this section. ¹⁷

Comparing these two values, we see that it is more than plausible that these quintessence coupled constants will not have any important effect on its behaviour during this stage. We can see that as long as the particle abundance is suppressed by this large factor, and the particles are decoupled, the additional term to the potential should be negligible. As we stated before, we can assume the abundance of the particles to be suppressed around $T \sim 10^{12}\text{GeV}$. Before that, the abundance might not be suppressed to this degree, however, the factor $d\mu/dQ$ is of the order 10^{-43} or smaller at higher temperatures. Therefore the additional potential term is still much smaller than the original quintessence potential, even at 10^{15}GeV .

When the μ -parameters start changing for the second time, we see that they are always at least two orders of magnitude larger than the temperature. This

¹⁷This should be a reasonable assumption, since the chemical potentials are zero in equilibrium, while in the completely uncoupled case the suppression should be even stronger.

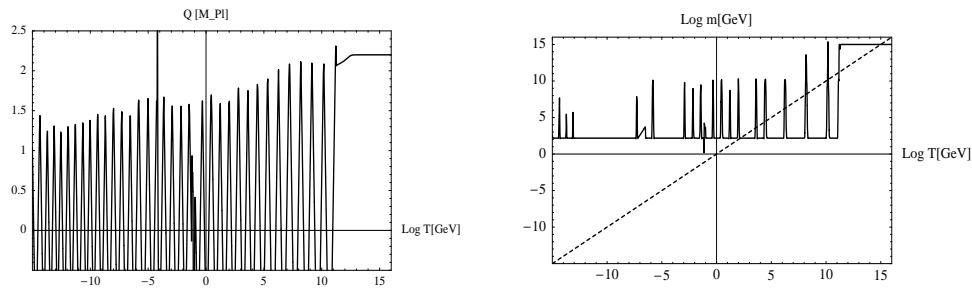


Figure 6.10: The behaviour of the quintessence field and the μ -parameter yielded by using the method from reference [7]. We see that their behaviour is very different from the uncoupled case

implies a suppression factor of at least 10^{-42} compared to the energy density of a massless particle. Since dm/dQ is at most of order $\mu_3 \cdot \omega_2 \sim 10^{-10}$, we can see that the effective potential term in this case is always much smaller than the original potential term, which should only be very few orders of magnitude smaller than the unsuppressed energy density of a massless particle (see fig. 6.5).

Alltogether it can now be seen that we chose our μ -parameters in such a way that they only vary, when the abundance of the corresponding particles is extremely suppressed. At all other times the parameters are practically constant. This way, the quintessence field behaves almost identically as in the uncoupled case. To show the necessity of our new approach to determine the effect of the couplings on the behaviour of the quintessence field, we consider fig. 6.10, where the former approach from reference [7] has been used. It can be seen that it seems to predict a behaviour of the quintessence field, which is highly different from the uncoupled case, and which is very unlikely to render baryogenesis.

For the fermion and gauge boson masses things are even easier. Until electroweak symmetry breaking they do not have any masses, and therefore the corresponding coupling constants can be varied arbitrarily.¹⁸ After symmetry breaking we chose these coupling constants in such a way that their variation should be completely annihilated by the variation of the VEVs, due to the fact that these should be proportional to the μ -parameters. Therefore the corresponding masses should not have a qualitative influence on the quintessence field.¹⁹

To check this second phase numerically and to show that the exponential suppression of the disturbances is big enough, we made use of the method

¹⁸If the Yukawa couplings or gauge coupling constants would vary in a way that would enable Φ and Ψ to equilibrate, their varying would, of course, have an influence on the energy of the system, however, dn/dQ should in this case still be zero (compare D).

¹⁹As we will partially see in the last part of this chapter, things might be a little more subtle, however, this argument works, as long as the fermion and gauge boson masses are determined by the product of the corresponding couplings and the μ -parameters to a sufficient degree, which we assume within this thesis.

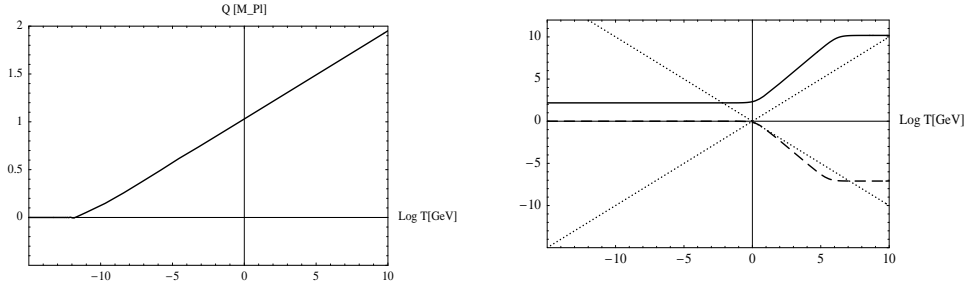


Figure 6.11: The behaviour of the quintessence field and the Q -dependent Higgs masses in the coupled case, where equilibrium distributions are assumed at temperatures lower than 10^{10}GeV . Fermion and gauge boson couplings have not been considered. Comparing the graphs with figures 6.9 and 6.4 we see that even with the assumption that the particles are in equilibrium, the quintessence behaviour does not change significantly.

from [7] and assumed equilibrium distributions for all Higgs particles (which might not true, but which should have the largest possible impact on the system) and therefore plug eq.(6.43) into our numerics instead of the bare potential term at temperatures lower than 10^{10}GeV . The result for 128 particles of masses $|\mu(Q)|$ is shown in figure 6.11, where we can see that the behaviour of Q has practically not changed (Φ : 60 particles + 60 antiparticles, Ψ : 4 particles + 4 antiparticles). It is not necessary to also put the fermion and gauge couplings explicitly into the numerics, as it is obvious that we can increase ω_g arbitrarily, which leads to the fact that the relation $g \propto (\mu)^{-1}$ holds up to any desired degree of accuracy, and we can therefore safely assume $dm_f/dQ = 0$. A similar relation should also hold for the gauge boson masses.

Putting everything from this section together, we see that the couplings we chose to achieve a baryon asymmetry are very likely to conserve the original quintessence field behaviour. From the specific couplings chosen in our model, it can also be seen how somewhat extreme couplings of mass-terms to a quintessence field can be realized: If processes that keep certain particles in equilibrium are frozen out, their mass generating couplings may vary dramatically, without having an influence on the quintessence field behaviour, if the particle abundance was initially exponentially suppressed.

6.3.4 Further Issues and Comments

Within the course of our calculations we neglected some rather subtle points that we will briefly cover here.

- **Thermal Running of Coupling Constants:**

Throughout most of this thesis, the fact that in quantum field theories coupling constants change with temperature has been completely neglected. If this is included, some new conditions arise. In cases without running effects which are not too big, it should still be possible for

any coupling constant g to achieve any reasonable effective behaviour $g(Q, T) = \alpha(T)$, where $\alpha(T)$ is some arbitrary function of the temperature: Calculate the behaviour of $g(g_0, T)$, where g is the renormalized Lagrangian with $g(T_0) = g_0$; if the running of g is not too big, there should always exist some g'_0 such that $g(g'_0, T) = \alpha(T)$. Since $Q : T \rightarrow Q(T)$ is bijective in the relevant temperature range, we can define the function $g_0 : Q \rightarrow g'_0$ such that the original behaviour of the coupling constants is achieved.

Yet, this cannot not necessarily be done during the phase of broken electro-weak symmetry. This is due to the fact that if our couplings are chosen in the way just described, we would find

$$\frac{d}{dT}(g\mu) = \frac{\partial(g\mu)}{\partial Q} \frac{dQ}{dT} + \frac{\partial(g\mu)}{\partial T} = 0, \quad (6.49)$$

with g, μ being the relevant quantities for the fermion and gauge boson masses, depending on the fact, if g represents a Yukawa or a gauge coupling. However, since the desired behaviour would rather be

$$\frac{\partial(g\mu)}{\partial Q} = 0, \quad (6.50)$$

in order for the fermion masses to be independent of the quintessence field, we might, at least in this temperature region, just stick with the couplings fixed in the previous sections. As long as the squares of the various gauge and Yukawa coupling constants increase by less than an order of magnitude in this region, this should not hurt our calculations. In the standard model this condition is fulfilled for the gauge coupling constants (see e.g. [23]), which is encouraging, though no proof for our model. If some or all coupling constants increase by more than an order of magnitude due to thermal effects, more detailed calculations might be necessary. For the Higgs masses, we want to stress that they should of course go to zero, when the μ parameters are of the order of the temperature, and hereby change by several orders of magnitude. However, at this time μ and all other couplings are very weakly depending of Q . If necessary, this dependence can be weakened even more, by increasing the corresponding ω -parameters in our couplings, such that this seems to be a minor issue. Still we want to mention that the various ω -parameters cannot be increased arbitrarily high and problems might occur due to this fact. During the time of rapid change, the coupling of μ can still be that of the bare coupling (eq.(6.35)), without our estimations changing dramatically.

- **Momentum Running of Coupling Constants:**

Besides the fact that coupling constants change with temperature, they also change with momentum. The fact that this has been neglected, when calculating expressions like eq.(2.14a) might yield additional constraints for this kind of running. However, this is usually neglected in the literature, and we also assume this effect to be negligible.

In this context it should also be mentioned that when using approximate fermion masses to determine the Yukawa couplings at the beginning of the last section, the running has also not been considered. However, if this would actually change any orders of magnitude, it should only be important during the initial decay phase. At that point, we could have varied the Yukawa couplings individually instead of all of them the same way. In this case the right order of magnitude for the produced asymmetry could still be generated.

- **Flavor Changing Neutral Currents:**

Models with several Higgs bosons for fermion mass generation yield flavor changing neutral currents (FCNCs) at tree level. The corresponding branching ratios must be very small in order to go together with measured data. Yet, since this thesis does not present a model with fixed Yukawa couplings and Higgs masses as the ones that were chosen were only needed to show that baryogenesis should be possible in models of this kind, the branching ratios for FCNCs have not been calculated for the presented model with the given parameters.

- **Left-Right Sphalerons:**

Looking at section 3.2 and especially eq.(3.36), we see that $SU(3)_C$ might also yield non-perturbative transitions, due to anomalies; with the difference that the anomalies of left- and right-handed currents are of the same size and only differ in sign. This could mean that non-perturbative transitions between left- and right-handed particles exist. If that was the case in the early universe, parts of our asymmetry might be washed out and only the asymmetry in the leptonic sector might be hidden. Yet, this is unlikely to change the order of magnitude of the created asymmetry, and even if it would, we could introduce a quintessence coupling of the corresponding gauge coupling constant, that would suppress these transitions. Since gluons are always massless, a subsequent increase of this constant should have no effect on the quintessence field.

- **Big Bang Nucleosynthesis:**

In order for our model not to interfere with nucleosynthesis the various μ -parameters and quintessence driven coupling constants need to reach their uncoupled values fast enough. At $T = 100\text{MeV}$ the graphs in fig.6.11 yield a value of less than 153GeV , while the Yukawa couplings have an additional multiplicative factor of ~ 0.98 , which means that all values only differ from their values today by less than approximately two percent, neglecting the running mentioned above. In case that this might still be too much, one has some freedom in varying several ω parameters in our couplings in a way that yields even better results. We also note that even though the parameters still change a little, all the fermion and gauge boson masses do not at these scales.

- **Further Higgs Parameters:**

Since the gauge coupling constants have been chosen to be very small at

the time of electro-weak symmetry breaking, other parameters in the Higgs potential might need considerable sizes to justify the assumption $T_c \approx \mu$, where T_c is the critical temperature. This seems to be implied by the formula for the critical Temperature in the Weinberg-Salam model (see e.g. [3]). Other constraints on the Higgs parameters might arise from the assumption $\langle \Phi \rangle, \langle \Psi \rangle \approx \mu$. However, it is assumed that these constraints go together fairly well.

Additional constraints might also be yielded by a possible proton decay mediated by the Higgs sector. Yet, this should have no effect on our baryogenesis scenario.

Chapter 7

Summary and Conclusions

While it seems to be probable that the universe went through a period of baryogenesis, the details might not be known for a long time, if ever. One possible scenario was presented in this thesis.

After introductions into several topics of cosmology and astroparticle physics, we considered various possibilities of embedding the original neutrino genesis scenario into models that could avoid the ad-hoc introduction of two new particle representations, that only served the purpose of rendering baryogenesis within this model but were not needed otherwise to explain observational data. With possible problems arising from various potential substitutes for these additional particles in mind, a specific model was introduced, which bases on the Pati-Salam gauge group $SU(2)_L \times SU(2)_R \times SU(4)_{PS}$. The particles that were supposed to start the baryogenesis process by decay were two fermion mass generating Higgs boson representations that both were needed to yield the measured spectrum of fermion masses and mixings.

After calculating the predictions for the various gauge boson masses in the limit of high breaking scales for $SU(2)_R$ and $SU(4)_{PS}$ and estimating the minimum breaking scales determined by these results, possible vacuum expectation values for the fermion mass generating Higgs representations were assumed, while also Yukawa couplings were fixed that yield the approximate fermion masses. These Yukawa couplings were also a source for the desired CP-violation. Several problems of this specific model for the creation of a matter-antimatter asymmetry were discussed and found to be potentially solved by time-varying coupling constants.

The effective time dependence of various coupling constants in the theory was achieved by making these couplings depend on the vacuum expectation value of a classical quintessence field, which is used in many cosmological scenarios to explain the size of the cosmological constant today. Various reaction rates were estimated, and the quintessence couplings were chosen in such a way that the constraints needed for baryogenesis, and based on the mentioned estimations, were obeyed by the coupling constants. The model was found to yield a baryon asymmetry of the correct order of magnitude, given the fact that the estimations and assumptions made during the course of the thesis were justified.

Finally the effect of these couplings on the behaviour of the quintessence

field was considered. Hereby the method used in another model [7] was shown to be limited, and an improved approach was introduced. Using this approach, the influence of the couplings was examined and found to be negligibly small in contrast to the result from the earlier method.

While these calculations were done for one specific model, the method used might be applicable to other models and shows a way of possibly realizing extreme couplings of mass terms to a quintessence field, by having the mass variation start at a point where the abundance of the corresponding particles is exponentially suppressed. A simultaneous suppression of the rates of reactions that could populate empty states of these particles seems to enable the mass term to be varied rapidly without having a qualitative effect on the behaviour of the quintessence field.

In summary, the baryon asymmetry in our universe and therefore its existence as we know it might be due to the effective time dependence of coupling constants. One possibility for this has been shown in this thesis, where the ad-hoc introduction of new particles in the original neutrino genesis scenario has been replaced by the introduction of varying coupling constants. In addition to this example and reference [7], the assumption of effectively time varying parameters might also help to save other baryogenesis scenarios from being in conflict with experimental data or being only marginally compatible with other bounds. An example for this could be electroweak baryogenesis in the standard model, where the λ -parameter of the Higgs potential might be varied in way that make electro-weak symmetry breaking a first order phase transition.

Also because of such interesting possibilities it is desirable that the nature of quintessence fields (if they exist) will be better understood. A goal in the further future might be to determine their interplay with the standard model particles on a fundamental level. In this case we might find real criteria to rule out certain quintessence dependings of coupling constants as well as criteria that possibly confirm the validity of others.

7.1 Zusammenfassung und Schlussfolgerungen

Während es scheint, dass das Universum durch eine Phase der Baryogenese ging, werden die Details für lange Zeit nicht bekannt sein, falls sie es überhaupt jemals sein werden.

Nach Einleitungen in mehrere Themen der Kosmologie und der Astroteilchenphysik, fingen wir an verschiedene Möglichkeiten zu erwägen das ursprüngliche Neutrinogenese-Szenario in realistischere Modelle einzubetten. Hierbei wurde versucht, auf die ad-hoc Einführung zweier neuer Teilchen Darstellungen zu verzichten, welche zwar Baryogenese innerhalb dieses Modells ermöglichen, ohne jedoch anderweitig benötigt zu werden um vorhandene Daten zu erklären. Im Bewusstsein möglicher Probleme, die von den verschiedenen möglichen Ersatzkandidaten für diese Teilchen ausgehen könnten, wurde ein spezielles Modell vorgestellt, welches auf der Pati-Salam Eichgruppe $SU(2)_L \times SU(2)_R \times SU(4)_{PS}$ basiert. Die Teilchen, denen es zugeordnet war den Baryogeneseprozess durch Zerfall zu starten, waren zwei, Fermionenmassen generierende Higgs-Boson Darstellungen, die beide benötigt wurden um das gemessene Spektrum der Fermionenmassen und -mischungen zu reproduzieren.

Nachdem die Voraussagen für die verschiedenen Eichbosonenmassen im Grenzwert hoher Brechungsskalen von $SU(2)_R$ und $SU(4)_{PS}$ berechnet und die dadurch bestimmten minimalen Brechungsskalen abgeschätzt worden waren, wurden mögliche Vakuumenerwartungswerte für die Fermionenmassen erzeugenden Higgs Darstellungen angenommen und Yukawakopplungen festgesetzt, die die ungefähren Fermionenmassen lieferten. Diese Yukawa Kopplungen waren auch die Quelle für die gewünschte CP-Verletzung. Mehrere Probleme dieses speziellen Modells eine Materie-Antimaterie Asymmetrie zu erzeugen wurden diskutiert und es wurde dargelegt, dass diese möglicherweise durch zeitlich veränderliche Kopplungskonstanten gelöst werden könnten.

Die effektive Zeitabhängigkeit verschiedener Kopplungskonstanten wurde dadurch erreicht, dass sie vom Vakuumenerwartungswert eines Quintessenzfeldes abhängig gemacht wurden, welches in vielen kosmologischen Szenarien dazu verwendet wird die heutige Größe der kosmologischen Konstanten zu erklären. Verschiedene Reaktionsraten wurden abgeschätzt, und die Quintessenzkopplungen wurden so gewählt, dass die Bedingungen eingehalten wurden, die für eine Baryogenese nötig waren, und die auf den erwähnten Abschätzungen beruhten. Es wurde erkannt, dass das Modell, eine Baryonasymmetrie der richtigen Größenordnung liefert, für den Fall, dass die im Rahmen der Arbeit gemachten Abschätzungen und Annahmen gerechtfertigt sind.

Schließlich wurde der Effekt dieser Kopplungen auf das Verhalten des Quintessenzfeldes betrachtet. Hierbei wurde gezeigt, dass die Methode, die in einem anderen Modell benutzt worden war, nur eingeschränkt anwendbar ist, und ein verfeinerter Ansatz wurde vorgestellt. Mit Hilfe dieses Ansatzes wurde der Einfluss der Kopplungen untersucht, und es wurde gezeigt, dass dieser vernachlässigbar klein sein sollte, im Gegensatz zum Ergebnis, der vorher erwähnten Methode.

Obwohl die Berechnungen für ein spezielles Modell vollzogen wurden, könnte die Methode auf andere Modelle anwendbar sein und zeigt eine Möglichkeit

extreme Kopplungen von Massentermen an ein Quintessenzfeld zu realisieren, indem die Massenveränderung zu einem Zeitpunkt beginnt, zu dem das Vorkommen des zugehörigen Teilchens exponentiell unterdrückt ist. Eine gleichzeitige Unterdrückung der Raten von Prozessen, die leere Zustände dieser Teilchen bevölkern könnten, scheint es dem Massenterm zu ermöglichen rapide variiert zu werden ohne einen qualitativen Effekt auf das Verhalten des Quintessenzfeldes zu haben.

Zusammenfassend kann man festhalten, dass die Baryonasymmetrie unseres Universums und damit seine Existenz, wie wir sie kennen, an der effektiven Zeitabhängigkeit von Kopplungskonstanten liegen könnte. Eine Möglichkeit hierfür wurde in dieser Diplomarbeit gezeigt, die die ad-hoc Einführung zusätzlicher Teilchen im ursprünglichen Neutrinogeneseszenario durch die Einführung sich verändernder Kopplungskonstanten ersetzt hat. Zusätzlich zu diesem Beispiel und Referenz [7], könnte die effektive Zeitabhängigkeit von Parametern es auch anderen Baryogeneseszenarien ermöglichen, nicht in Konflikt mit experimentellen Daten zu stehen oder nur geringfügig kompatibel mit anderen Schranken zu sein. Ein Beispiel hierfür könnte die elektro-schwache Baryogenese im Standardmodell sein, in der der λ -Parameter des Higgspotentials auf eine Weise variiert werden könnte, die die elektro-schwachen Symmetriebrechung zu einem Phasenübergang erster Ordnung machen könnte.

Auch wegen solch interessanter Möglichkeiten ist es wünschenswert, dass die Beschaffenheit von Quintessenzfeldern (falls sie existieren) besser verstanden wird. Ein Ziel in fernerer Zukunft könnte es sein, das Zusammenspiel mit den Teilchen des Standardmodells zu bestimmen. In diesem Fall könnten wir sowohl echte Kriterien finden, um bestimmte Quintessenzabhängigkeiten von Kopplungskonstanten auszuschliessen, als auch Kriterien, die möglicherweise die Richtigkeit anderer Kopplungen bestätigen.

Appendix A

Generators of SU(4)

We chose to work in the following basis of generators, which all have a norm of $1/2$:

$$\begin{aligned} T_{PS}^1 &= \sqrt{\frac{3}{8}} \begin{pmatrix} -1 & 0 & 0 & 0 \\ 0 & \frac{1}{3} & 0 & 0 \\ 0 & 0 & \frac{1}{3} & 0 \\ 0 & 0 & 0 & \frac{1}{3} \end{pmatrix} & T_{PS}^2 &= \sqrt{\frac{1}{12}} \begin{pmatrix} 0 & 0 & 0 & 0 \\ 0 & 1 & 0 & 0 \\ 0 & 0 & 1 & 0 \\ 0 & 0 & 0 & -2 \end{pmatrix} \\ T_{PS}^3 &= \frac{1}{2} \begin{pmatrix} 0 & 0 & 0 & 0 \\ 0 & 1 & 0 & 0 \\ 0 & 0 & -1 & 0 \\ 0 & 0 & 0 & 0 \end{pmatrix} & T_{PS}^4 &= \frac{1}{2} \begin{pmatrix} 0 & 1 & 0 & 0 \\ 1 & 0 & 0 & 0 \\ 0 & 0 & 0 & 0 \\ 0 & 0 & 0 & 0 \end{pmatrix} \\ T_{PS}^5 &= \frac{1}{2} \begin{pmatrix} 0 & -i & 0 & 0 \\ i & 0 & 0 & 0 \\ 0 & 0 & 0 & 0 \\ 0 & 0 & 0 & 0 \end{pmatrix} & T_{PS}^6 &= \frac{1}{2} \begin{pmatrix} 0 & 0 & 1 & 0 \\ 0 & 0 & 0 & 0 \\ 1 & 0 & 0 & 0 \\ 0 & 0 & 0 & 0 \end{pmatrix} \\ T_{PS}^7 &= \frac{1}{2} \begin{pmatrix} 0 & 0 & -i & 0 \\ 0 & 0 & 0 & 0 \\ i & 0 & 0 & 0 \\ 0 & 0 & 0 & 0 \end{pmatrix} & T_{PS}^8 &= \frac{1}{2} \begin{pmatrix} 0 & 0 & 0 & 1 \\ 0 & 0 & 0 & 0 \\ 0 & 0 & 0 & 0 \\ 1 & 0 & 0 & 0 \end{pmatrix} \\ T_{PS}^9 &= \frac{1}{2} \begin{pmatrix} 0 & 0 & 0 & -i \\ 0 & 0 & 0 & 0 \\ 0 & 0 & 0 & 0 \\ i & 0 & 0 & 0 \end{pmatrix} & T_{PS}^{10} &= \frac{1}{2} \begin{pmatrix} 0 & 0 & 0 & 0 \\ 0 & 0 & 1 & 0 \\ 0 & 1 & 0 & 0 \\ 0 & 0 & 0 & 0 \end{pmatrix} \end{aligned}$$

$$\begin{aligned}
T_{PS}^{11} &= \frac{1}{2} \begin{pmatrix} 0 & 0 & 0 & 0 \\ 0 & 0 & -i & 0 \\ 0 & i & 0 & 0 \\ 0 & 0 & 0 & 0 \end{pmatrix} & T_{PS}^{12} &= \frac{1}{2} \begin{pmatrix} 0 & 0 & 0 & 0 \\ 0 & 0 & 0 & 1 \\ 0 & 0 & 0 & 0 \\ 0 & 1 & 0 & 0 \end{pmatrix} \\
T_{PS}^{13} &= \frac{1}{2} \begin{pmatrix} 0 & 0 & 0 & 0 \\ 0 & 0 & 0 & -i \\ 0 & 0 & 0 & 0 \\ 0 & i & 0 & 0 \end{pmatrix} & T_{PS}^{14} &= \frac{1}{2} \begin{pmatrix} 0 & 0 & 0 & 0 \\ 0 & 0 & 0 & 0 \\ 0 & 0 & 0 & 1 \\ 0 & 0 & 1 & 0 \end{pmatrix} \\
T_{PS}^{15} &= \frac{1}{2} \begin{pmatrix} 0 & 0 & 0 & 0 \\ 0 & 0 & 0 & 0 \\ 0 & 0 & 0 & -i \\ 0 & 0 & i & 0 \end{pmatrix}
\end{aligned}$$

Appendix B

Calculated Yukawa Couplings

To enable the reader to reproduce the results obtained for our Yukawa couplings, we will explicitly give the values we used for the fermion masses and mixings.¹

Estimated masses and mixings:

$$\begin{array}{lll} \text{u: } m=3\text{MeV}, & \text{c: } m=1\text{GeV}, & \text{t: } m=180\text{GeV}, \\ \text{d: } m=7\text{MeV}, & \text{s: } m=100\text{MeV}, & \text{b: } m=4.1\text{GeV}, \\ \text{e: } m=0.511\text{MeV}, & \mu: m=106\text{MeV}, & \tau: m=1.777\text{GeV}, \\ \nu_e: m=0.1\text{eV}, & \nu_\mu: m=0.11\text{eV}, & \nu_\tau: m=0.11\text{eV}, \end{array}$$

$$\text{CKM-matrix: } \begin{pmatrix} 0.9745 & 0.217 & 0.0018 \exp(i\frac{2}{3}\pi) \\ 0.217 & 0.9737 & 0.036 \\ 0.004 \exp(i\frac{23}{180}\pi) & 0.035 & 0.9991 \end{pmatrix},$$

$$\text{MNS-matrix: } \begin{pmatrix} 0.83 & 0.56 & 0.00 \\ 0.40 & 0.59 & 0.71 \\ 0.40 & 0.59 & 0.71 \end{pmatrix}.$$

It is once more stressed that the exactness of these values is not important for the model introduced in this thesis, and the values are only presented to enable the reader to reproduce the calculated values.

¹The data that was simplified to the values presented was partially taken from [4, 10, 15, 24], while the author explicitly thanks Mark Rolinec and Felix Schwab for also providing him with some of the data.

Appendix C

Particle Freeze Out

Here we want to further motivate the statement from section 6.3.2 that an asymmetry x will not be washed out, if the rate for the wash-out processes Γ is smaller than the Hubble rate, while also decreasing at a faster rate:

It seems reasonable to assume that the differential equation for the washout of the asymmetry is given by

$$\frac{dx}{dt} = -\Gamma x, \quad (\text{C.1})$$

where Γ is not necessarily constant. The solution for this equation is given by

$$x(t) = x_0 \exp \left(- \int_{t_0}^t \Gamma(t') dt' \right) \quad (\text{C.2})$$

or

$$x(T) = x_0 \exp \left(- \int_{T_0}^T \Gamma(T') \frac{dt}{dT} dT \right). \quad (\text{C.3})$$

With help of eq.(2.35) and $K(T) \equiv \Gamma/(2H)$ this yields

$$x(T) = x_0 \exp \left(\int_{T_0}^T K(T') \frac{2}{T'} dT \right). \quad (\text{C.4})$$

For all the wash-out processes in our model the ratio K is decreasing proportional to T or faster; in the latter case it would obviously take even longer for the asymmetry to be washed-out. We therefore write $K = \alpha T/T_0$, with $2\alpha < 1$. Now, we find

$$\begin{aligned} x(T) &= x_0 \exp \left(\frac{2\alpha}{T_0} \int_{T_0}^T dT \right) \\ &= x_0 \exp \left(2\alpha \left[\frac{T}{T_0} - 1 \right] \right), \end{aligned} \quad (\text{C.5})$$

from which we see that no matter how deep the temperature falls, the asymmetry will never change its order of magnitude. Therefore we can say that processes of the above kind, will not be able to wash-out the corresponding asymmetry.

Appendix D

The Effective Quintessence Potential - a closer look

In section 6.3.3, we used a hand-waiving argument to make it plausible that the term dn/dQ can be neglected in equation (6.44) as the reaction is basically frozen out at this point. Yet, it seems that this should generally be true, which is due to the fact that an instantaneous and infinitesimal change of Q only changes dn/dt but not n , even though this has of course an effect on n in the long run.

The statement can be shown quantitatively, it is assumed that the differential equation for the behaviour of some particle species with density n , which is driven towards equilibrium density n_{eq} by reactions of combined rate Γ , is given by

$$\frac{dn}{dt} = -\Gamma(n - n_{eq}). \quad (\text{D.1})$$

We can now formally integrate both sides of these equations with respect to t and find

$$n = n_0 - \int_{t_0}^t \Gamma(Q(t')) [n(Q(t'), t') - n_{eq}(Q(t'))] dt', \quad (\text{D.2})$$

where $n(t_0) = n_0$. Differentiating this expression with respect to $Q(t)$ yields

$$\frac{dn}{dQ} = 0, \quad (\text{D.3})$$

as the right hand side only depends on $Q(t')$ with $t' < t$.

This way we again come to the conclusion that even though the behaviour of n is not independent of $Q(t)$, it always needs a finite time to react to instantaneous variations of Q , whereas the mean energy of each particle $\langle E \rangle$ changes instantaneously with Q , which leads to the fact that eq.(6.44) seems to be generally true.

Bibliography

- [1] Leo - link everything online. <http://dict.leo.org/>.
- [2] Ujjaini Alam, Varun Sahni, and A. A. Starobinsky. The case for dynamical dark energy revisited. 2004.
- [3] David Bailin and Alexander Love. *Introduction to Gauge Field Theory*. IOP, revised edition, 1993.
- [4] R. Michael Barnett et al. Review of particle physics. particle data group. *Phys. Rev.*, D54:1–720, 1996.
- [5] T. Barreiro, Edmund J. Copeland, and N. J. Nunes. Quintessence arising from exponential potentials. *Phys. Rev.*, D61:127301, 2000.
- [6] Werner Bernreuther. Cp violation and baryogenesis. *Lect. Notes Phys.*, 591:237–293, 2002.
- [7] Xiao-Jun Bi, Pei-hong Gu, Xiu-lian Wang, and Xin-min Zhang. Thermal leptogenesis in a model with mass varying neutrinos. 2003.
- [8] W. Buchmuller, P. Di Bari, and M. Plumacher. Cosmic microwave background, matter-antimatter asymmetry and neutrino masses. *Nucl. Phys.*, B643:367–390, 2002.
- [9] W. Buchmuller, P. Di Bari, and M. Plumacher. The neutrino mass window for baryogenesis. *Nucl. Phys.*, B665:445–468, 2003.
- [10] Andrzej J. Buras. Weak hamiltonian, cp violation and rare decays. 1998.
- [11] Karin Dick, Manfred Lindner, Michael Ratz, and David Wright. Leptogenesis with dirac neutrinos. *Phys. Rev. Lett.*, 84:4039–4042, 2000.
- [12] Herbert K. Dreiner and Graham G. Ross. Sphaleron erasure of primordial baryogenesis. *Nucl. Phys.*, B410:188–216, 1993.
- [13] M. Fukugita and T. Yanagida. Baryogenesis without grand unification. *Phys. Lett.*, B174:45, 1986.
- [14] G. F. Giudice, A. Notari, M. Raidal, A. Riotto, and A. Strumia. Towards a complete theory of thermal leptogenesis in the sm and mssm. *Nucl. Phys.*, B685:89–149, 2004.

- [15] K. Hagiwara and et al. Review of Particle Physics. *Physical Review D*, 66:010001+, 2002.
- [16] Jeffrey A. Harvey and Michael S. Turner. Cosmological baryon and lepton number in the presence of electroweak fermion number violation. *Phys. Rev.*, D42:3344–3349, 1990.
- [17] Kerson Huang. *Quarks, Leptons and Gauge Fields*. World Scientific, 2nd edition, 1992.
- [18] Prof. Edmund Klatt and Dietrich Dr. Roy. *Langenscheidt Wörterbuch Englisch*. Langenscheidt KG, 1983.
- [19] Edward W. Kolb and Michael Turner. *The Early Universe*. Addison-Wesley, 1990.
- [20] Edward W. Kolb and Stephen Wolfram. Baryon number generation in the early universe. *Nucl. Phys.*, B172:224, 1980. Erratum-ibid.B195:542,1982.
- [21] L.D. Landau and E.M. Lifshitz. *Statistical Physics*, volume I. Butterworth-Heinemann, 3rd edition, 1980.
- [22] Jiang Liu and Gino Segre. Reexamination of generation of baryon and lepton number asymmetries by heavy particle decay. *Phys. Rev.*, D48:4609–4612, 1993.
- [23] Rabindra N. Mohapatra. *Unification and Supersymmetry: The Frontiers of Quark-Lepton Physics*. Springer-Verlag, 3rd edition, 2003.
- [24] Rabindra N. Mohapatra and Palash B. Pal. *Massive Neutrinos in Physics and Astrophysics*. World Scientific Publishing Co.Pte.Ltd., 1991.
- [25] Keith A. Olive. Big bang nucleosynthesis: in review of particle physics (rpp 2000). *Eur. Phys. J.*, C15:133–135, 2000.
- [26] Jogesh C. Pati and Abdus Salam. Lepton number as the fourth color. *Phys. Rev.*, D10:275–289, 1974.
- [27] Michael E. Peskin and Daniel V. Schroeder. *An Introduction to Quantum Field Theory*. Addison-Wesley, 1995.
- [28] Michael Ratz. Neutrinogenese, 1999. Diplomarbeit, Technische Universität München, Physik-Department, Institut für Theoretische Physik T30.
- [29] Lewis H. Ryder. *Quantum Field Theory*. Cambridge Univ. Press, 2nd edition, 1996.
- [30] Varun Sahni and Alexei A. Starobinsky. The case for a positive cosmological lambda-term. *Int. J. Mod. Phys.*, D9:373–444, 2000.
- [31] A. D. Sakharov. Violation of cp invariance, c asymmetry, and baryon asymmetry of the universe. *JETP Letters*, 5:24, 1967.

- [32] R. Slansky. Group theory for unified model building. *Phys. Rept.*, 79:1–128, 1981.
- [33] Steven Weinberg. *Gravitation and Cosmology : Principles and Applications of the General Theory of Relativity*. Wiley, 1972.
- [34] Steven Weinberg. *The Quantum Theory of Fields*, volume I. Cambridge Univ. Press, 1995.
- [35] Steven Weinberg. *The Quantum Theory of Fields*, volume II. Cambridge Univ. Press, 1996.
- [36] Ivaylo Zlatev, Li-Min Wang, and Paul J. Steinhardt. Quintessence, cosmic coincidence, and the cosmological constant. *Phys. Rev. Lett.*, 82:896–899, 1999.

Danksagung

An dieser Stelle möchte ich einigen Menschen danken, die, jeder auf seine Art, einen Teil zu dieser Diplomarbeit beigetragen haben:

- Manfred Lindner, der mich nicht nur an seinem Lehrstuhl meine Diplomarbeit schreiben ließ, sondern sich auch dafür einsetzte, dass mich die Universität Stuttgart meine Diplomarbeit an der TU-München schreiben ließ. Zudem dafür, dass er es mir ermöglicht hat an weiteren Aktivitäten, wie der Sommerschule in Italien und dem Workshop auf Schloss Ringberg teilzunehmen. Zu guter letzt natürlich auch für die Zeit, die er sich immer wieder in physikalischen Diskussionen für mich nahm, welche mir oft weiterhalfen.
- Professor Dr. Ulrich Kneißl (im Ruhestand) dafür, dass er mir weiterhalf, beim Versuch meine Diplomarbeit extern zu schreiben, und Professor Dr. Ulrich Weiß, dass er einverstanden war, als Mitberichter bei meiner Diplomarbeit aufzutreten,
- Michael Ratz, dessen Diplomarbeit eine Grundlage dieser Arbeit war, für gute Ratschläge und Diskussionen,
- Stefan Antusch, der mein erster Zimmernachbar war, und der mir oft bei Fragen weiterhelfen konnte,
- Claudia Hagedorn für viele nützliche Diskussionen,
- Mathias Garny für seine Hilfe bei der Behandlung von Quintessenzfeldern,
- Patrick Huber, Michael Schmidt, Thomas Schwetz, Gerhart Seidl und Walter Winter für ihren Anteil an der angenehmen Stimmung innerhalb unserer Gruppe, insbesondere für interessante Diskussionen beim Kaffee,
- Florian Bauer und Markus Michael Müller unter anderem dafür, dass ich nicht achtzehn Stunden am Stück autofahren musste,
- Jörn Kersten für seine Beharrlichkeit immer wieder Treffen von Teilen der Gruppe am Abend oder am Wochenende zu organisieren, die wir anderen gerne in Anspruch nahmen, aber immer zu faul waren selbst etwas dafür zu tun,

- Mark Rolinec, Klemens Rottler, Felix Schwab, Michael Spranger und Elmar Wyszomirski für das Korrekturlesen von Teilen dieser Diplomarbeit, kritische Einwände und Vorschläge für Formulierungen, insbesondere Michael Spranger für die Aufbereitung des Uni-Stuttgart Logos auf der Titelseite,
- Klemens Rottler, Michael Spranger und Elmar Wyszomirski für die gemeinsamen Nachtschichten,
- Mark Rolinec und Felix Schwab dafür, dass sie mich von weiteren David Lynch Filmen verschont ließen,
- Klemens Rottler ohne dessen Vorräte ich dem Hungertod ein gutes Stück näher gewesen wäre,
- Mark Rolinec für unzählige Filmzitat E-mails,
- Bill Watterson, für einen fröhlichen Start in den Tag.

In die Zeit meiner Diplomarbeit fielen neben guten auch persönlich schwierige Zeiten. In diesen habe ich Rückhalt bei meinen Freunden Christopher, Clemens und Mathias erfahren, denen ich an dieser Stelle dafür danken will.

Mein größter Dank gilt natürlich meiner Familie: Julia, Guido und insbesondere meinen Eltern. Sie alle haben mich nicht nur während meiner Diplomarbeit, sondern während des gesamten Studiums und auch der Zeit davor auf jede nur erdenkliche Weise unterstützt.¹

¹Auch Aiku soll nicht ganz unerwähnt bleiben.

Erklärung

Ich erkläre hiermit, diese Arbeit selbstständig verfasst und keine anderen als die angegebenen Quellen und Hilfsmittel benutzt zu haben.

Marc-Thomas Eisele, Garching bei München, 8. Mai, 2004.